GENETIC MONITORING OF CUCURBIT DOWNY MILDEW IN MICHIGAN

By

Julian Camilo Bello Rodriguez

A DISSERTATION

Submitted to
Michigan State University
in partial fulfillment for the requirements
for the degree of

Plant Pathology – Doctor of Philosophy

2020

ABSTRACT

GENETIC MONITORING OF CUCURBIT DOWNY MILDEW IN MICHIGAN

By

Julian Camilo Bello Rodriguez

Cucurbit downy mildew (CDM) caused by the oomycete obligate pathogen, *Pseudoperonospora cubensis*, incites foliar blighting of several cucurbit genera worldwide. In 2004, the pathogen re-emerged in the U.S. infecting historically resistant cucumber cultivars and requiring the adoption of an intensive fungicide program. Due to an influx of aerially dispersed sporangia from overwinter sources, CDM occurs annually in cucumber growing regions of northern U.S. The genetic monitoring of incoming *P. cubensis* populations is essential for growers to make informed decisions regarding CDM management strategies. However, the scale and resolution of genetic studies of downy mildews (*Peronosporaceae*) remains limited due to the logistical constraints involved in the genotyping of these species (e.g. obtaining DNA of sufficient quantity and quality). To gain an evolutionary and ecological perspective of *P. cubensis*, we describe a targeted enrichment (TE) protocol able to genotype environmental samples of *Pseudoperonospora* spp. using less than 50 ng of DNA for library preparation. Using the TE protocol, we were able to enrich 736 target genes across 101 samples and identified 2,978 high quality SNP variants. This SNPs resolved the population structure of *P. cubensis* in Michigan and detected significant (AMOVA, P=0.01) genetic differentiation among the *P. cubensis* populations from squash (clade I) and cucumber (clade II). No evidence of location-based differentiation was detected within the *P. cubensis* (clade II) subpopulation of Michigan.

Timely alerts of an influx of airborne inoculum of two distinct host-adapted clades of *P. cubensis* can assist Michigan growers in assessing the need to initiate fungicide sprays. However, the inability to distinguish between the morphologically identical sporangia of *P. humuli* and *P. cubensis* has been a significant shortcoming. Using spore traps and qPCR assays, an improved methodology for the aerial monitoring of each *Pseudoperonospora* taxa was identified. A highly specific qPCR assay differentiated *Pseudoperonospora humuli*, the causal agent of downy mildew on hop, and the two host-adapted clades of *P. cubensis* (clade I and II) on spore trap samples. After two years of monitoring, *P. cubensis* clade II DNA was detected in spore trap samples >2 days before CDM symptoms were first observed in commercial cucumber fields (August), while *P. humuli* DNA was only detected early in the growing season (May and June). *P. cubensis* clade I DNA was not detected in air samples before or after the disease onset in cucumber fields. Additionally, the probability for *P. cubensis* detection in Burkard spore trap samples was higher compared to impaction spore trap samples with approximately the same number of sporangia, suggesting that the efficiency of recovery of sporangia by Burkard spore traps exceeds the recovery of impaction spore traps. The methodology described in this study to monitor the airborne concentrations of *Pseudoperonospora spp.* sporangia could be used as part of a CDM risk advisory system to time fungicide applications that protect cucurbit crops in Michigan.

ACKNOWLEDGMENTS

I would like to thank my co-advisor, Dr. Mary Hausbeck, for taking me as her student and for the work-related support she provided to me over the years. It was an honor to be part of her program and I'm thankful for your patience with my stubbornness. I would also like to thank my co-advisor Dr. Monique Sakalidis, for her guidance and questions, they challenged me and encourage me to continue in the graduate program. In addition, Dr. Andy Jarosz and Dr. Timothy Miles, for their invaluable advice as members of my committee.

I could not have achieved my degree without the assistance of the technical staff and graduate students of the Hausbeck and Sakalidis Labs. Special thanks to Doug Higgins, my program fellow, for the countless hours of discussions after 5 p.m. Your insights, critics, and suggestions were essential to complete my objectives.

I thank my parents for investing in my undergraduate program and for being there for me under any circumstances. I love you both. I also thank my sisters and brother; I made it to this program because you are always challenging me. And last, but not least, I would like to thank my good friends, Marcela Tabares, Oscar Benitez, and Clarissa Strieder, for their emotional support during the hardest times of my time far from home, you guys help me build the best version of myself.

TABLE OF CONTENTS

LIST OF TABLES

LIST OF FIGURES

CHAPTER I: LITERATURE REVIEW - *PSEUDOPERONOSPORA CUBENSIS* THE CAUSAL AGENT OF CUCURBIT DOWNY MILDEW

INTRODUCTION

Pseudoperonospora cubensis (Berk. & M. A. Curtis) Rostovzev, the causal agent of cucurbit downy mildew (CDM), is a highly destructive pathogen recognized as one of the greatest contemporary disease threats to cucumber production worldwide (Brzozowski et al., 2016). In the U.S., two distinct evolutionary clades of *P. cubensis* (clade I and II) affect the production of cucurbit species including agronomically important crops such as cucumber, pumpkin, watermelon, and squash (Wallace et al., 2020). The disease only affects foliage creating small, irregular to angular chlorotic areas, and in most cases, sporulation on the lower leaf surface (Cohen et al., 2015). Leaf lesions coalesce and become necrotic leading to leaf blighting and premature defoliation which results in stunted plants and yield reduction, especially in cucumber (*Cucumis sativus L.*) and squash (*Cucurbita moschata*) (Reuveni et al., 1980; Adams et al., 2019; Hausbeck et al., 2019; Perla et al., 2019).

In the U.S., the disease was only of minor concern prior to 2004 due to the deployment of resistant cucumber cultivars starting in 1960 (Thomas et al., 2017c). However, in 2004, a highly virulent strain of *P. cubensis* was introduced into U.S. that overcame this host resistance and stunned the cucumber industry (Holmes et al., 2014; Thomas et al., 2017a). In the absence of fully resistant cucurbit cultivars, chemical control is currently the most effective strategy to control CDM (Hausbeck and Goldenhar, 2017) but the evolution of resistant *P. cubensis* isolates to multiple fungicides has created an urgent need for alternative disease management strategies (Thomas et al., 2017).

Public breeding programs have made progress in the development of new cultivars to respond to the rising virulence of CDM, and have released slicing cucumbers with good levels of resistance (Brzozowski et al., 2016). However, the resistance of these varieties to the downy mildew pathogen has not yet been incorporated into processing (pickling) cucumbers that represent a significant portion of the cucurbit crops grown in the country. The U.S. is the seventh-largest producer of cucumber in the world (Keinath et al., 2017) and in 2019, 756,000 metric tons of fresh market (20%) and pickling cucumbers (80%) were grown on 42000 ha for a combined value of $279 million (USDA, 2020). Michigan is the second-largest producer of cucumbers in the country where approximately half of the national production of cucumbers (300,000 metric tons fresh and pickling) is harvested every year (USDA, 2020). Similarly, Michigan is also a big producer of other susceptible crops to CDM such as squash and pumpkin. In 2019, 85,600 and 41,200 metric tons of squash and pumpkins, respectively, were grown on a combined area of 5700 ha (USDA, 2020).

P. cubensis clade II is especially destructive on cucumbers (Holmes et al., 2014). The pathogen cannot overwinter in northern regions of the U.S. that experience frost, but the disease reoccurs yearly due to the influx of airborne sporangia from overwintering sites with mild winters (Ojiambo and Holmes, 2010; Quesada-Ocampo et al., 2012). CDM has changed the way cucumber growers manage their fields in Northern states such as Michigan. The pickling cucumber growers of Michigan apply fungicides frequently to limit CDM, with an estimated cost of more than $6 million annually (Goldenhar and Hausbeck, 2019). Oxathiapiprolin (FRAC 49), ethaboxam (FRAC 22), fluazinam (FRAC group 29), cyazofamid (FRAC 21),

ametoctradin/dimethomorph (FRAC 45/40), and the broad-spectrum fungicides mancozeb (FRAC M03) and chlorothalonil (FRAC M05) are among the best fungicide alternatives for CDM control in different regions of the U.S. (Goldenhar and Hausbeck, 2019; Adams et al., 2020; Dutta, 2020; Miller et al., 2020).

Application timing of fungicides is crucial when weather conditions are especially favorable for CDM and to reduce the risk of the pathogen developing resistance, fungicides must be applied preventively (Hollomon, 2007). To optimize application timing, the airborne concentration of *P. cubensis* sporangia can be monitored to coordinate the initiation of fungicide applications with the arrival of the pathogen into cucumber production fields (Granke et al., 2013; Goldenhar and Hausbeck, 2019). The accurate detection and quantification of sporangia can enable a more efficient application timing of fungicides and possibly, delay the development of pathogen resistant isolates to fungicides.

Spore trapping can provide quantitative data on airborne spore numbers (Dung et al., 2018); however, the processing and microscopic examination of spore trap samples is time consuming and can result in misidentification due to morphological similarities between *Pseudoperonospora* taxa (e.g. *P. cubensis* and *P. humuli*). The combination of spore traps and PCR technologies is an ongoing area of investigation that seeks to improve and accelerate the detection of *P. cubensis* sporangia from air samples. Next generation sequencing technologies have recently facilitated the identification of new diagnostics markers for pathogen detection (Withers et al., 2016; Rahman et al., 2019) and the development of qPCR assays that could improve the monitoring of airborne *P. cubensis* sporangia (Summers et al., 2015a).

Similarly, these technologies have also facilitated the implementation of new tools to monitor CDM populations (Summers et al., 2015; Wallace & Quesada-Ocampo, 2017; Withers et al., 2016). This important progress has made possible the execution of more comprehensive genetic studies to better understand the epidemiology of CDM in the U.S. (Summers et al., 2015; Thomas et al., 2017). This review briefly summarizes our current understanding of *P. cubensis* biology including taxonomy, dispersal, management, fungicide resistance and population genetics. Additionally, we also elaborate on future directions for the effective control of CDM including plant breeding and early pathogen detection

TAXONOMY AND DISEASE CYCLE

Pseudoperonospora cubensis (Berk. & Curt.) Rost., the causal agent of cucurbit downy mildew (CDM), is an oomycete plant pathogen belonging to the family *Peronosporaceae* (Oomycota, Oomycetes, Peronosporales). This family is made up of an extensive number of plant pathogens that threaten natural and managed ecosystems including all downy mildews (DM) and other genera such as *Phytopythium spp*., *Halophytophthora* spp. and *Phytophthora* spp. (Thines and Choi, 2015). All DM are considered obligate biotrophic plant parasites and as such, they can only grow in association with living host tissue (Thines, 2014). *Phytophthora* spp., on the other hand, are hemibiotrophic or necrotrophic and only a small group of species are obligate biotrophs (Thines, 2014; Bourret et al., 2018).

So far, 19 downy mildew genera have been described that contain more than 700 species (Thines and Choi, 2015). Most DM genera are present in three major monophyletic groups: 1) downy mildews with colored conidia (*Peronospora* and

Pseudoperonospora), 2) downy mildews with pyriform haustoria (*Basidiophora*, *Benua*, *Bremia*, *Novotelnova*, *Paraperonospora*, *Plasmopara*, *Plasmoverna*, and *Protobremia*), and the brassicolous downy mildews (*Hyaloperonospora* and *Perofascia*). Apart from these three groups, several grass-parasitic downy mildew genera have been described, of which the graminicolous downy mildews with lasting sporangiophores (*Graminivora*, *Poakatesthia*, and *Viennotia*) seem to be monophyletic (Thines, 2014; Thines and Choi, 2015; Bourret et al., 2018). DM were thought to form a single monophyletic group, however, a recent multigene phylogenetic analysis showed that Graminicolous downy mildews (GDM), brassicolous downy mildews (BDM) and downy mildews with colored conidia (DMCC) form a monophyletic clade with the *Phytophthora* taxon totara; while downy mildews with pyriform haustoria (DMPH) were placed in their own clade (Bourret et al., 2018).

The genus *Pseudoperonospora* has been place alongside *Peronospora* in the group of downy mildews with colored conidia. Six species have been described within the *Peronosporaceae* genus, including two economically important species: *P. cubensis* and *P. humuli* (causal agent of hop downy mildew). *P. cubensis* causes disease on approximately 20 cucurbits genera (approximately 40 – 60 different species) including cucumber (*Cucumis sativus*), cantaloupe (*C. melo*), pumpkin (*Cucurbita maxima*), watermelon (*Citrullus lanatus*), squash (*Cucurbita pepo*), gourd (*C. moschata*), and wild cucurbit species such as balsam apple (*Momordica balsamina*), bitter melon (*M. charantia*) and Buffalo Gourd (*Cucurbita foetidissima*) (Quesada-Ocampo et al., 2012; Savory et al., 2011; Wallace et al., 2014; Wallace et al., 2015).

P. cubensis requires a living host to complete its life cycle which begins when sporangia (2n) land on the adaxial surface of susceptible host. Under the right environmental conditions (15-20 °C, 1-5h of leaf wetness), sporangia release zoospores (2n) capable of swimming and encysting in host stomata (Granke et al., 2013; Cohen et al., 2015). From the encysted zoospore, a germ tube forms, penetrating the host tissue through an appressorium. Hyphae (2n) grow into the intracellular space where nutrient acquisition occurs. Sporangiophores form clonally from the intracellular growing hyphae holding sporangia produced mitotically in their tips (2n). Sporangia dislodge from Sporangiophores by a twisting mechanism that occurs when relative humidity (RH) decreases, and then fly through the air until they reach a new susceptible host re-initiating the cycle.

Several oomycete pathogens reproduce in a mixed mode (asexual and sexual reproduction), however, it is not clear if *P. cubensis* undergoes a sexual phase in U.S. fields. The formation of oospores by *P. cubensis* seems to be rare but it has been reported several times in other countries such as China, Israel and India (Cohen et al., 2003; Savory et al., 2011; Zhang et al., 2012). A recent study confirmed the presence of two different mating types in the U.S. (A1 and A2) as well as its ability to produce viable oospores in vitro. (Thomas, A. Carbone, I. Ojiambo, 2013). This suggests that *P. cubensis* could potentially reproduce sexually in cucurbits within U.S. but the actual frequency of oospore formation could be very low due to the strict association of each mating type to a particular host (i.e. the A1 mating type isolates were uniquely found in cucumbers while the A2 mating type was mainly found in squash) (Thomas et al., 2016; Cohen et al, 2011; Cohen et al., 2015). The incidence of sexual reproduction and the

formation of oospores could have an important role in the epidemiology of CDM in the country. Monitoring of sexual reproduction in U.S. fields is key to identify new sources of genetic variation.

SURVIVAL AND DISPERSAL OF *P. CUBENSIS*

P. cubensis sporangia do not survive for a long time on non-living or necrotic tissue and its ability to infect cucumbers is reduced greatly under dry conditions, surviving only for 22 hours at temperature between 35 and 40 Celsius degrees (Cohen and Rotem, 1971). Additionally, overwintering-sexual structures such as oospores have not been detected in soil or host tissue in the U.S., and are not considered a source of inoculum (Naegele et al., 2016). Thus, *P. cubensis* survival in the U.S. depends on the availability of susceptible hosts (Savory et al., 2011) and the pathogen cannot survive in fields of regions where cucurbits cannot be grown year-round due to long winters with frost. In northern U.S., CDM reoccurs yearly due to the influx of sporangia that originated from warm weather plantings along the eastern seaboard and/or greenhouses in colder locales where the pathogen can survive on living host tissue (Ojiambo and Holmes, 2010; Quesada-Ocampo et al., 2012). CDM outbreaks in the great lakes region of the U.S. and Ontario, Canada are thought to result from the arrival of sporangia from southern states (e.g. Florida) that migrate north by wind currents using plantings of susceptible crops (Ojiambo et al., 2015). However, migration inferences made at a genetic level suggest a more restricted movement of sporangia in the country (Quesada-Ocampo et al., 2012).

Although *P. cubensis* sporangia can travel up to 1,000 kilometers via air currents and migrate between fields in different states (Ojiambo and Holmes, 2010; Ojiambo et

al., 2015; Naegele et al., 2016), the CDM population from southern U.S. (i.e. Florida, Georgia, North Carolina) are highly dissimilar to the pathogen population in the Upper Midwest (Quesada-Ocampo et al., 2012). Evidence has been found that support the exchange of migrants among states in the upper Midwest and Canada (Naegele et al., 2016) but evidence of the movement of sporangia between northern and southern states has not yet been found.

The progressive movement of the pathogen between states depends mainly on three factors: the asexual production of sporangia, its passive atmospheric transportation and the availability of new susceptible host (Ojiambo & Holmes, 2010). These factors in combination with environmental variables are correlated with the occurrence of CDM (Granke et al., 2013) and provide the basis of the CDM forecasting system (CDM ipmPIPE) that estimates the risk of outbreaks at any particular area (Ojiambo et al., 2015). Under field conditions, airborne sporangial concentrations, time post-planting, temperature, and leaf wetness are positively associated with disease occurrence, while solar radiation is the only factor negatively associated with disease (Granke and Hausbeck, 2011; Granke et al., 2013).

Recent studies indicate that the *P. cubensis* can also be transmitted by seeds (Cohen et al., 2014) and infect wild cucurbits (Wallace et al., 2014; Wallace et al., 2015; Wallace and Quesada-Ocampo, 2016). CDM symptoms and sporulation have been observed on the leaves of wild species such as Balsam apple (*Momordica balsamina*), bitter melon (*Momordica charantia*), buffalo gourd (*Cucurbita foetidissima*), and bottle gourd (*Lagenaria siceraria*) (Wallace and Quesada-Ocampo, 2016), however, it is still unknown if the pathogen can overwinter in the dormant tissue of these species (Wallace

et al., 2014; Wallace et al., 2015). Further research is needed to establish the role of non-commercial cucurbits in the yearly CDM epidemic, which will aid the efforts of the CDM ipmPIPE to predict disease outbreaks.

GENETIC STRUCTURE

Research on *P. cubensis* populations from Europe and the U.S. have identified 6 distinct genetic clusters among 465 samples (Quesada-Ocampo et al., 2012; Kitner et al., 2015). Some clusters were more frequently associated with particular geographical regions, however, all of them were detected in Europe and in the U.S. This suggests that some genotypes are persistent and widely dispersed and/or have migrated from one population to others (Quesada-Ocampo et al., 2012). Initial studies may have underestimated the diversity of the populations due to the low number of markers used (Quesada-Ocampo et al., 2012; Kitner et al., 2015), however, the general structure patterns have also been observed in analyses using larger numbers of genetic markers (Summers et al., 2015b; Thomas et al., 2017a; Wallace and Quesada-Ocampo, 2017).

At the genetic and phenotypic level (i.e. host preference), *P. cubensis* is structured by host in the U.S. (Thomas et al., 2017a; Wallace et al., 2020). In fact, it was recently shown that *P. cubensis* in the U.S. can be divided into two host-specific clades (Wallace et al., 2020). Further genetic studies have confirmed that these two clades are host-adapted at the cucurbit species level (Summers et al., 2015b; Thomas et al., 2017a; Wallace et al., 2020), with clade I isolates recovered more frequently from commercial varieties of *Cucurbita pepo, C. moschata, C. maxima,* and *Citrullus lanatus* and clade II isolates associated more frequently with commercial varieties of the *Cucumis sativus* and *Cucumis melo* (Wallace et al., 2020). Additionally, clade II isolates

were also found infecting the wild cucurbit species *Lagenaria siceraria* while clade I was also isolated from the wild species *Momordica balsamina and Momordica charantia* (Thomas, A. Carbone, I. Ojiambo, 2013; Wallace et al., 2020). Both clades were only found with low frequency in *Cucumis melo* and *Cucurbita foetidissima* (Wallace et al., 2020).

It is still unclear if sexual reproduction occurs under field conditions within the *P. cubensis* population of the U.S. However, signs of recombination were found using genetic markers in clade I consistent with a sexually reproducing population, while no evidence of random mating was found for clade II (Wallace et al., 2020). This suggests that only clade I could be heterothallic while clade II may only reproduce clonally. Thomas et al., (2017) confirmed the presence of two mating types (A1 and A2) in the U.S. able to form oospores *in vitro* but information on the clade membership of the isolates used is not available. The existence of two different mating types within each clade has not been confirmed and it is unknown if recombination between isolates of different clades can occur. However, both clades are rarely detected within a single host (*Cucumis melo*) suggesting the possibility of two different mating-types from each clade encountering each other is low.

As well as clustering by host, clustering between *P. cubensis* isolates by geographic location has also been reported in the U.S. (Quesada-Ocampo et al., 2012; Naegele et al., 2016) but it is unclear if this geographic structure is real or is an artifact of the population differentiation driven by the host or a temporal effect of the sampling. Population studies of *P. cubensis* have are limited by the sporadic occurrence of the disease due to the obligate nature of the pathogen. This makes the collection of isolates

highly dependent on the availability of susceptible hosts, whose production is regionally and temporally affected. The cucurbit growing season along the states in the eastern seaboard of the U.S has minimal overlap making comparisons among *P. cubensis* populations from northern and southern states difficult without considering a temporal factor. In Northern U.S., cucurbits are mainly grown during the summer while southern states such as Florida and Georgia produce cucurbits only during the spring and fall (Aerts and Mossler, 2003). Thus, the genetic differentiation in space (e.g. region, state) detected previously (Quesada-Ocampo et al., 2012) might be an artifact of the host driven structure and/or a biased sampling. A population study performed in Czech Republic over two years of sampling revealed no clustering based on geographical origin (Kitner et al., 2015).

PATHOGENIC VARIATION

The change in the host range of CDM that occurred in Europe in 2009, when *P. cubensis* became a significant problem for species like *Cucurbita moschata*, *C. pepo*, *C. maxima* and *Citrullus lanatus*, was attributed to a significant change in the structure of pathogen population (Kitner et al., 2015). Pre-epidemic samples were different significantly from samples collected after 2009 and they clustered in completely different clades. Only a limited number of heterozygous samples collected after 2009 clustered in the pre-epidemic clade, suggesting the occurrence of rare recombination events between populations (Cohen et al., 2015).

In the same way, the emergence of new pathotypes (physiological races) has been proposed as an explanation for the breaking of host resistance in the United States. However, this hypothesis has not yet been proved due to the small number of

samples collected before 2004, and the limited resolution of the studies performed so far (Quesada-Ocampo et al., 2012). A better understanding of *P. cubensis* populations at the local level is key to control and prevent the emergence of more virulent pathogen populations with additional levels of fungicide resistance.

FUNGICIDE RESISTANCE

In the absence of fully resistant cucumber varieties, fungicide use is currently the most effective method to control CDM (Hausbeck and Goldenhar, 2017). However, *P. cubensis* is a high-risk pathogen in terms of evolving fungicide resistance both because of its shorth generation time on the genetically uniform monocultures of its hosts and the huge population size during outbreaks that offer many opportunities for mutations (Kitner et al., 2015). In fact, *P. cubensis*, was the first pathogen to be reported as resistant to the phenylamide fungicide mefenoxam (FRAC 4), a widely used fungicide against most of the oomycete plant pathogens (Reuveni et al., 1980). Over 17 different fungicides (representing 15 FRAC codes) are registered to control CDM (Table 1-1), however, complete resistance or reduction in the sensitivity to multiple fungicides has been reported within *P. cubensis* populations (Urban and Lebeda, 2006; Goldenhar and Hausbeck, 2019).

Complete resistance of *P. cubensis* to fungicides in the FRAC groups 4 (phenylamides), 11 (quinone outside inhibitors), and 40 (carboxylic acid amides) (Gisi and Sierotzki, 2015; Ojiambo et al., 2015) has been documented. In the U.S., single-site fungicides including mefenoxam (FRAC 4) and azoxystrobin (FRAC 11) were ineffective when the pathogen reemerged in 2004 (Ernest et al., 2005; Gevens and Hausbeck, 2005; Thornton et al., 2006). Since that time, *P. cubensis* resistance to dimethomorph

(FRAC 40) (Zhu et al., 2007) and mandipropamid (FRAC 40) (Hausbeck and Cortright, 2010; Blum et al., 2011) has been reported in the U.S. (Holmes et al., 2014; Keinath, 2015). Similarly, reduced efficacy of fluopicolide and cymoxanil (FRAC 43) against CDM has been observed in field trials in Michigan (Hausbeck and Linderman, 2014; Goldenhar and Hausbeck, 2019), Georgia (Langston and Sanders, 2013), and North Carolina (Adams and Quesada-Ocampo, 2014; Keinath, 2015). Propamomcarb (FRAC 28) was effective against CDM for several years, but in 2013 its efficacy was compromised in field trials in North Carolina (Keinath, 2015; Thomas et al., 2018), Pennsylvania (Gugino and Grove, 2016), and Michigan (Hausbeck and Linderman, 2014; Hausbeck et al., 2017).

The number of effective fungicides against CDM is limited, and fungicide efficacy can vary between years (Goldenhar and Hausbeck, 2019) due to changes in environmental conditions and the pathogen population. However, oxathiapiprolin (FRAC 49), ethaboxam (FRAC 22), fluazinam (FRAC group 29), cyazofamid (FRAC 21), ametoctradin/dimethomorph (FRAC 45/40), and the broad-spectrum fungicides mancozeb (FRAC M03) and chlorothalonil (FRAC M05) have shown a good control levels of CDM in field trials in Ohio (Miller et al., 2020), Georgia (Dutta, 2020), North Carolina (Adams et al., 2020) and Michigan (Goldenhar and Hausbeck, 2019; Hausbeck et al., 2019)

Oxathiapiprolin is a relatively new active ingredient with proven efficacy against *P. cubensis* (Cohen 2015; Goldenhar and Hausbeck 2016). However, it is a single site fungicide inhibitor and as such, it is considered at high risk of pathogen resistance (Cohen 2015; FRAC 2018). Similarly, ethaboxam had demonstrated efficacy against

CDM (Quesada-Ocampo and Adams, 2014; Gugino and Grove, T.L., 2020) and was classified as a fungicide for which the development of resistance is at low to medium risk (FRAC, 2020); still, in 2017 its efficacy was compromised in field trials in Michigan (Goldenhar and Hausbeck, 2019). Fluazinam, cyazofamid and ametoctradin/dimethomorph have shown consistent good control of CDM (Adams and Quesada-Ocampo, 2014; Keinath, 2015; Goldenhar and Hausbeck, 2019) and only Fluazinam is not widely used by cucurbit growers due to its high cost (Neufeld et al., 2017). Resistance to broad spectrum fungicide is rare in *P. cubensis* populations, but metalaxyl-resistant isolates found in Israel also exhibited moderate levels of resistance against active ingredients such as mancozeb (Reuveni et al., 1980)

It seems inevitable to avoid hastening the emergence of resistance given the limited amount of options against CDM and the high rates at which fungicides are applied (every 7 to 10 days). Thus, resistance management is key to maintaining the efficacy of single-site fungicides, and growers are encouraged to rotate among fungicides from different FRAC groups (FRAC, 2020). The continuous monitoring of fungicide efficiency at the local level is essential to provide the best recommendations to cucumber growers in the U.S. and ensure that *P. cubensis* is effectively managed.

Table 1-1. **List of fungicides registered for the control of cucumber downy mildew in the U.S.**

Active ingredient	Product name	Registrant	FRAC code	[a] Reduce efficacy	FRAC chemical group	Target site
Metalaxyl/ mefenoxam	Ridomil	Syngenta	4	Yes	PhenylAmides (PA) - fungicides	RNA polymerase I
Chlorothalonil	Bravo Weather Stik	Syngenta	M05	No	Chloronitrites	Multi-site contact activity
Fluopicolide	Presidio	Valent	43	Yes	Benzamides	Delocalization of spectrin-like proteins
Propamomcarb	Previcur Flex	Bayer	28	Yes	Carbamates	Cell membrane permeability, fatty acids (proposed)
Cyazofamid	Ranman	FMC	21	No	Quinone inside inhibitor (Qil) - fungicides	Complex III: cytochrome bc1 at Qi site
Zoxamide/ mancozeb	Gavel	Gowan	22/M03	No	Dithio-carbamates (M03) / thiazole carboxamide (22)	Multi-site contact activity (M03) / B-tubulin assembly in mitosis (22)
Mancozeb	Dithane	BASF	M03	No		
Cymoxanil	Curzate	DuPont	27	Yes	Cyanoacetamide-oxime	Unknown
Fluazinam	Omega	Syngenta	29	No	Unestablished	Uncouplers of oxidative phosphorylation

[a]Reduce efficacy or completed resistance reported in the U.S.

Table 1-1. **(cont'd)**

Active ingredient	Product name	Registrant	FRAC code	[a] Reduce efficacy	FRAC chemical group	Target site
Mandipropamid	Revus	Syngenta	40	Yes	Carboxylic Acid Amides (CAA) - fungicides (40)	Cellulose synthase (40)/ complex III: cytochrome bc1 (45)
Dimethomorph	Forum	BASF	40	Yes		
Ametoctradin/ dimethomorph	Zampro	BASF	45/40	No		
Fluxapyroxad/ pyraclostrobin	Priaxor	BASF	11/7.	Yes	Quinone outside Inhibitors (QoI) - fungicides (11)	Complex III: cytochrome bc1 at Qo site (11)
Pyraclostrobin	Cabrio	BASF	11	Yes		
Famoxadone/ cymoxanil	Tanos	DuPont	11/27.	Yes		
Oxathiapiprolin	Orondis	Syngenta	49	No	OSBPI oxysterol binding protein homologue inhibition	Lipid homeostasis and transfer/storage
Ethaboxam	Elumin	Valent	22	No	Thiazole carboxamide	ß-tubulin assembly in mitosis

[a]Reduce efficacy or completed resistance reported in the U.S

BREEDING EFFORTS

Cucumber (*Cucumis aestivus*) is a widely cultivated plant of the Cucurbitaceae family, with annual production above 71 million tons globally (FAO, 2013). The U.S. is the fifth largest producer of cucumber, and in 2019, 756,000 metric tons of fresh market and pickling cucumbers were grown on approximately 42000 ha for a combined value of $279 million (USDA, 2020). Several diseases affect cucumber production including target spot, powdery mildew and Phytophthora crown and root rot (Tuttle McGrath, 2004; Keinath et al., 2017), however, cucurbit downy mildew (CDM) caused by the oomycete, *Pseudoperonospora cubensis* is probably the most important disease of cucumber in the country (Thomas et al., 2017a). CDM is a highly destructive foliar disease able to cause 50% reduction in cucumber yield even after fungicides are applied one-week post-symptom appearance (Cohen et al., 2015).

Currently no cultivar has robust resistance to the disease, but for decades, downy mildew on cucumbers was effectively managed with genetic host resistance. (Sitterly, 1972). The introgression of the *dm-1* gene from PI 197087 into the cultivars ‘Polaris’, ‘Poinsett’, ‘Pixie’, and ‘Chipper’ provided cucumber growers with genetic control of downy mildew for more than 40 years (Call et al., 2012a; Cohen et al., 2015; Thomas et al., 2017a). From 1961 to 2003, downy mildew was only a moderate problem in North America and was easily controlled with fungicides (Cohen et al., 2015). However, the resistance of commercial cultivars in the U.S. was defeated in 2004 when a highly virulent strain of *P. cubensis* was introduced in the country (Thomas et al., 2017a). Since then, *P. cubensis* has reoccurred yearly in cucumber production areas of

eastern U.S., costing cucumber growers millions annually in fungicide sprays to protect their crop (Granke and Hausbeck, 2011; Savory et al., 2011).

Over the last ten years, a number of new downy mildew-resistant cucumber lines have been released by public and private breeding programs including the slicing varieties SV3462CS, SV4719CS, and Bristol, and the pickling varieties Citadel and Peacemaker from Seminis (Holdsworth et al., 2014; Brzozowski et al., 2016). These varieties have shown an intermediate level of resistance to *P. cubensis* and reached comparable yields to commercial standards (e.g. Vlaspik) but still required the utilization of fungicides to provide full disease control (Hausbeck and Goldenhar, 2017). The Cornell breeding program have made significant progress in the development of new cultivars to control CDM releasing slicing cucumbers with exceptional levels of resistance (Brzozowski et al., 2016). The released line “DMR-NY401” retained the disease resistance of its predecessor line “DMR-NY264” while showing significantly higher fruit length, yield, and earliness of initial harvest (Brzozowski et al., 2016). However, the resistance of these varieties has not yet been incorporated in pickling cucumber varieties which are highly important in the country.

Race-specific R gene breeding: Plant pathogens such as *P. cubensis* secrete effector proteins during infection that modulate host innate immunity (Goss et al., 2013). Many of these effectors function only as virulence factors, but others can be recognized by plant R proteins resulting in the activation of effector triggered immunity. In such cases, the effectors are known as avirulence (AVR) factors (Brzozowski et al., 2016). In most cases, the response induced by AVR factors involves the hypersensitive response (HR) followed by restriction of the invading pathogen (Vleeshouwers et al., 2008).

Virulence factor can be identified throughout the phenotypic characterization of the *P. cubensis* population and can then be functionally profiled on cucurbit species to detect cognate R genes. R genes have been successfully identified using virulence factors in the model system *P. infestans*-potato plant and other fungal species such as *Cryptococcus neoformans* (Vleeshouwers et al., 2008; Desjardins et al., 2017). However, the identification of R genes in the cucurbit downy-mildew system using this strategy faces two important obstacles. First, as an obligate biotroph, *P. cubensis* requires a living host tissue for reproduction and dispersal, complicating the maintenance, identification and phenotyping of isolates. Secondly, the specific spectrum of novel CDM R-genes cannot be assessed in the absence of a diverse panel of isolates or pathotypes (isolates with the same pathogenicity). Due to these difficulties almost every phenotypic or genotypic study performed so far includes only a limited number of isolates.

An effort to identify diagnostic pathotypes of *P. cubensis* was recently performed by Thomas, et al. (2017). In this study, thirteen different pathotypes were identified based on a set of 15 different cucurbit species. The authors suggest the existence of 10 different avirulence factors (Avr genes), assuming that disease resistance is only expressed when an R gene product in the host can recognize the pathogen's corresponding effector. Interestingly, specific pathotypes form subgroups according to mating type which suggests the association between virulence and mating type (Thomas et al., 2017c).

The ways in which virulence factors evolve will be highly valuable in breeding of specific R genes and the designing of effective management strategies in agricultural

systems. Unfortunately, these concepts are poorly understood for obligate plant pathogen (Thomas et al., 2017c). In order to understand the evolution of Avr genes, particularly in the cucurbit downy-mildew system, substantial efforts need to be made to identify virulence factors and their genes. This could help to survey the temporal and spatial distribution of virulence factors and race structure of the *P. cubensis* population.

EARLY DETECTION OF *P. CUBENSIS*

In the absence of fully resistant cucurbit cultivars, chemical control is currently the most effective method for controlling CDM (Wu et al., 2016). However, the risk for the evolution of resistance by *P. cubensis* is high due to its fast mode of reproduction, and the low abundance of multi-site inhibitors to control the disease. It seems inevitable to avoid hastening the emergence of resistant *P. cubensis* isolates given the limited amount of options for CDM control. Therefore, the reduction of fungicide use and the alternation between fungicides in different FRAC groups is key to maintaining the efficacy of single-site inhibitors (Goldenhar and Hausbeck, 2019).

Application timing is crucial to optimize fungicide utilization and preventive application of fungicides can reduce the risk of the pathogen developing resistance (Hollomon, 2007). Thus, coordinating the initiation of fungicide applications with the arrival of pathogens into production fields could result in more efficient fungicide use. In California, measurements of aerial spore loads obtained from spore traps have been used to schedule the timing of fungicide applications against the lettuce pathogen, *Bremia lactucae*. This strategy resulted in the reduction of sprays without a significant increase in disease incidence (Dhar et al., 2019).

Monitoring the airborne concentration of *P. cubensis* sporangia using spore traps could also help to improve the scheduling of fungicides applications to control CDM in regions where disease occurrence depends on the influx of *P. cubensis* sporangia (Granke and Hausbeck, 2011; Granke et al., 2013; Dung et al., 2018). However, the processing and examination of spore trap samples need improvement to reduce the processing time and avoid misidentification. The screening of spore trap samples using qPCR can significantly improve the detection of airborne plant pathogens. qPCR has significantly improve the sensitivity and specificity for the detection of *Peronospora effusa* (Klosterman et al., 2014)*, Bremia lactucae* (Kunjeti et al., 2016)*,* and *Botrytis cinerea* (Kunjeti et al., 2016) in spore trap samples.

The use of molecular markers to differentiate between *P. cubensis* and *P. humuli* sporangia could aid to improve the airborne monitoring of CDM. Previous PCR assays have been used to monitor airborne *Pseudoperonospora humuli* sporangia near hop yards to inform the timing of fungicide sprays, but since this assay also detects *P. cubensis,* its accuracy decreases in areas where hops and cucurbits are grown in close proximity (Gent et al., 2009). The specificity for the detection of *P. cubensis* was improved with the development of a qPCR assay able to differentiate between *P. cubensis* and *P. humuli* based on the recognition of a single SNP in the *cox2* gene (Summers et al., 2015a). However, this assay is unable to differentiated between the two host adapted clades of *P. cubensis* and its specificity was compromise in samples containing samples from both species (*P. cubensis* and *P. humuli).* A new multiplex qPCR assay has been designed based on the recognition of a more polymorphic mitochondrial loci that also allow the differentiation between *P. cubensis* and *P. humuli*

(Crandall, 2020). These loci have less similarity between species and also allow the differentiation between two distinct clades of *P. cubensis* (clade I and II) (Thomas et al., 2017a; Wallace et al., 2020).

In northern regions of the U.S., CDM occurs annually due to an influx of airborne sporangia from overwinter sources. Burkard spore traps couple with light microscopy have been used to monitor the influx of *Pseudoperonospora* spp. sporangia and inform growers that the disease is likely to occur. Burkard spore traps collect spores by vacuuming air into a collection chamber that contains a reel mounted in a clockwork mechanism were spores and other particles are impacted onto a greased tape that covers the reel (Burkard Manufacturing Co. Ltd., U.K.). Burkard spore traps can continuously collect data for up to 7 days and the collecting tape can be split at different intervals allowing the precise quantification of spores per unit of time. Although Burkard spore traps are the most common devices used to monitor the air concentration of plant pathogens, the impaction spore traps have become popular in the last decade (Jackson and Bayliss, 2011). These devices possess rods coated with adhesive material, which spin at a standard rate to impact and collect the airborne inoculum (TSE Systems, Chesterfield, MO), however, impaction traps require constant monitoring to allow accurate estimations per unit of time (i.e. an hour or day). Burkard spore traps are robust and highly autonomous but impaction spore traps can be more cost-effective and easier to use by growers (Jackson and Bayliss, 2011; Choudhury et al., 2016a).

There are numerous comparative studies investigating the efficiency of these two spore traps, and in most cases, Burkard spore traps perform better than impaction spore traps. However, impaction spore traps have been used successfully for airborne

detection of pathogens such as *Bremia lactucae, Peronospora effusa* and *Peronospora schachtii* (Jenkyn, 1974; Li and Lin, 1999; Evenhuis et al., 2003), and could also be used for early detection *P. cubensis* sporangia in cucumber growing regions.

LITERATURE CITED

LITERATURE CITED

Aerts, M., Mossler, M. (2003). Crop profile for cucumbers in Florida. In the National IPM Database [Data file]. Available from https://ipmdata.ipmcenters.org/documents/cropprofiles/FLcucumber2003.pdf

Adams, M. L., and Quesada-Ocampo, L. M. (2014) Evaluation of fungicides for control of downy mildew on cucumber. Kinston 2013. Plant Dis Manag Rep 8: V240

Adams, M., Collins, H., Quesada-Ocampo, L.M. (2020) Evaluation of fungicides and cultivars for control of downy mildew on cucumber, Kinston, NC 2019. Plant Dis Manag Rep Report 14: V107

Adams, M., D'Arcangelo, K, Collins, H, Quesada-Ocampo, L (2019) Evaluation of cultivars for control of downy mildew on squash, Kinston 2018. Plant Dis Manag Reports 13: V124

Ali, S., Gautier, A., Leconte, M., Enjalbert, J., de Vallavieille-Pope, C. (2011) A rapid genotyping method for an obligate fungal pathogen, *Puccinia striiformis f.sp. tritici*, based on DNA extraction from infected leaf and multiplex PCR genotyping. BMC Res Notes 4: 240

Billard, A., Laval, V., Fillinger, S., Leroux, P., Lachaise, H., Beffa, R., and Debieu, D. (2012) The allele-specific probe and primer amplification assay, a new real-time PCR method for fine quantification of single-nucleotide polymorphisms in pooled DNA. Appl Environ Microbiol 78: 1063–1068

Blum, M., Waldner, M., Olaya, G., Cohen, Y., Gisi, U., and Sierotzki, H. (2011) Resistance mechanism to carboxylic acid amide fungicides in the cucurbit downy mildew pathogen *Pseudoperonospora cubensis*. Pest Manag Sci 67: 1211–1214

Bolger, A.M., Lohse, M., Usadel, B. (2014) Trimmomatic: a flexible trimmer for Illumina sequence data. Bioinformatics 30: 2114–2120

Bourret, T.B., Choudhury, R.A., Mehl, H.K., Blomquist, C.L., McRoberts, N., Rizzo, D.M. (2018) Multiple origins of downy mildews and mito-nuclear discordance within the paraphyletic genus *Phytophthora*. PLoS One 13: e0192502

Brown, A.H.D., Feldman, M.W., Nevo, E. (1980) Multilocus structure of natural populations of *Hordeum spontaneum*. Genetics 96: 523-536.

Brzozowski, L., Holdsworth, W., Mazourek, M. (2016) 'DMR-NY401': A new downy mildew–resistant slicing cucumber. HortScience 51: 1294–1296

Burkhardt, A., Buchanan, A., Cumbie, J.S, Savory, E.A., Chang, J.H., Day, B. (2014) Alternative splicing in the obligate biotrophic oomycete pathogen *Pseudoperonospora cubensis*. Mol Plant-Microbe Interact 28: 298–309

Burkhardt, A., Day, B. (2016) Transcriptome and small RNAome dynamics during a resistant and susceptible interaction between cucumber and downy mildew. The Plant Genome: 9:1-19.

Bustin, S. A., Benes, V., Garson, J.A., Hellemans, J., Huggett, J., Kubista, M., Mueller, R., Nolan, T., Pfaffl, M.W., Shipley, G.L., Vandesompele, J., and Wittwer, C. T (2009) The MIQE guidelines: minimum information for publication of quantitative real-time PCR experiments. Clin Chem 55: 611–622

Call, A.D., Criswell, A.D., Wehner, T.C., Ando, K., Grumet, R. (2012a) Resistance of cucumber cultivars to a new strain of cucurbit downy mildew. HortScience 47: 171–178

Call, A.D., Criswell, A.D., Wehner, T.C., Klosinska, U., Kozik, E.U. (2012b) Screening cucumber for resistance to downy mildew caused by *Pseudoperonospora cubensis* (Berk. and Curt.) Rostov. Crop Sci 52: 577–592

Carisse, O., McNealis, V., Kriss, A. (2017) Association between weather variables, airborne inoculum concentration, and raspberry fruit rot caused by *Botrytis cinerea*. Phytopathology 108: 70–82

Carisse, O., Tremblay, D.M., Lévesque, C.A., Gindro, K., Ward, P., and Houde, A. (2009) Development of a Taqman real-time PCR assay for quantification of airborne conidia of *Botrytis squamosa* and management of Botrytis leaf blight of onion. Phytopathology 99: 1273–1280

Carleson NC, Fieland VJ, Scagel CF, Weiland JE, Grünwald NJ (2019) Population structure of *Phytophthora plurivora* on *Rhododendron* in Oregon nurseries. Plant Dis 103: 1923–1930

Chee, H.Y., Nelson, M.E., Grov,e G.G., Eastwell, K.C., Kenny, S.T., Klein, R.E. (2006) Population biology of *Pseudoperonospora humuli* in Oregon and Washington. Plant Dis 90: 1283–1286

Choi, Y-J., Hong, S-B., Shin, H-D. (2005) A re-consideration of *Pseudoperonospora cubensis* and *P. humuli* based on molecular and morphological data. Mycol Res 109: 841–848

Choi, Y-J., Thines, M. (2015) Host jumps and radiation, not co-divergence drives diversification of obligate pathogens. a case study in downy mildews and *Asteraceae*. PLoS One 10: e0133655

Choudhury, R.A., Koike, S.T., Fox, A.D., Anchieta, A., Subbarao, K.V., Klosterman, S.J., McRoberts, N. (2016b) Spatiotemporal patterns in the airborne dispersal of spinach downy mildew. Phytopathology 107: 50–58

Clark, M.J., Chen, R, Lam, H.Y.K., Karczewski, K.J., Chen, R., Euskirchen, G., Butte, A.J., Snyder, M. (2011) Performance comparison of exome DNA sequencing technologies. Nat Biotechnol 29: 908–914

Cohen, Y., Van den Langenberg, K.M., Wehner, T.C, Ojiambo, P.S., Hausbeck, M, Quesada-Ocampo, L.M., Lebeda, A., Sierotzki, H., and Gisi, U. (2015) Resurgence of *Pseudoperonospora cubensis*: the causal agent of cucurbit downy mildew. Phytopathology 105: 998–1012

Cohen, Y., Meron, I., Mor, N., Zuriel, S. (2003) A new pathotype of *Pseudoperonospora cubensis* causing downy mildew in cucurbits in Israel. Phytoparasitica 31: 458–466

Cohen, Y., and Rotem, J. (1971) Dispersal and viability of sporangia of *Pseudoperonospora cubensis*. Trans Br Mycol Soc 57: 67–74

Cohen, Y., Rubin, A.E., Galperin, M. (2011) Formation and Infectivity of oospores of *Pseudoperonospora cubensis*, the causal agent of downy mildew in cucurbits. Plant Dis 95: 874

Cohen, Y., Rubin, A.E., Galperin, M, Ploch, S., Runge, F., Thines, M. (2014) Seed transmission of *Pseudoperonospora cubensis*. PLoS One 9: e109766

Cohen, Y., Samoucha, Y. (1983) Cross-resistance to four systemic fungicides in metalaxyl-resistant strains of *Phytophthora infestans* and *Pseudoperonospora cubensis*. Plant Dis 68: 137-139.

Coley-Smith, J.R. (1962) Overwintering of hop downy mildew *Pseudoperonospora humuli* (Miy. and Tak.) Wilson. Ann Appl Biol 50: 235–243

Cruz-Dávalos, D.I., Llamas, B., Gaunitz, C., Fages, A., Gamba, C., Soubrier, J., Librado, P., Seguin-Orlando, A., Pruvost, M., Alfarhan, A.H., et al (2017) Experimental conditions improving in-solution target enrichment for ancient DNA. Mol Ecol Resour 17: 508–522

Cui, C., Herlihy, J.H., Bombarely, A., McDowell, J.M., Haak, D.C. (2019) Draft assembly of *Phytophthora capsici* from long-read sequencing uncovers complexity. Mol Plant-Microbe Interact 32: 1559–1563

Desjardins, C.A., Giamberardino, C., Sykes, S.M., Yu, C-H., Tenor, J.L., Chen, Y., Yang, T., Jones, A.M., Sun, S., Haverkamp, M.R., et al (2017) Population genomics and the evolution of virulence in the fungal pathogen *Cryptococcus neoformans*. Genome Res 27: 1207-1219

Dhar, N., Mamo, B.E., Subbarao, K., Koike, S., Fox, A., Anchieta, A., and Klosterman, S.J. (2019) Measurements of aerial spore load by qPCR facilitates lettuce downy mildew risk advisement. Plant Dis 104: 82–93

Dung, J.K.S, Scott, J.C., Cheng, Q., Alderman, S.C., Kaur, N., Walenta, D.L., Frost, K.E., and Hamm, P.B. (2018) Detection and quantification of airborne *Claviceps purpurea* sensu lato ascospores from Hirst-type spore traps using real-time quantitative PCR. Plant Dis 102: 2487–2493

Dutta, B. (2020) Evaluation of individual fungicides for downy mildew control in cucumber in Tift County, Georgia, 2019. Plant Dis Manag Rep Report 14: V086

Ernest, E.G., Kee, W.E., and Everts, K.L. (2005) Evaluation of fungicides for control of downy mildew on pickling cucumber, Trial 2, 2005. Plant Dis Manag Rep 2: V066

Evenhuis, A., Verdam, B., Zadoks, J.C. (2003) Splash dispersal of conidia of *Mycocentrospora acerina* in the field. Plant Pathol 46: 459–469

Faircloth, B.C., Branstetter, M.G., White, N.D., Brady, S.G. (2015) Target enrichment of ultraconserved elements from arthropods provides a genomic perspective on relationships among Hymenoptera. Mol Ecol Resour 15: 489–501

Fletcher, K., Gil, J., Bertier, L.D., Kenefick, A., Wood, K.J., Zhang, L., Reyes-Chin-Wo, S., Cavanaugh, K., Tsuchida, C., Wong, J., et al (2019) Genomic signatures of heterokaryosis in the oomycete pathogen *Bremia lactucae*. Nat Commun 10: 2645

Fungicide Resistance Action Committee (FRAC) (2018) ode List 2018: Fungicides sorted by mode of action (including FRAC Code numbering).

Gent, D.H., Adair, N., Knaus, B.J., Grünwald, N.J. (2019) Genotyping-by-sequencing reveals fine-scale population differentiation in populations of *Pseudoperonospora humuli*. Phytopathology. doi: 10.1094/PHYTO-12-18-0485-R

Gent, D.H., Nelson, M.E., Farnsworth, J.L., Grove, G.G. (2009) PCR detection of *Pseudoperonospora humuli* in air samples from hop yards. Plant Pathol 58: 1081–1091

Gent, D.H., Ocamb, C.M. (2009) Predicting Infection Risk of Hop by *Pseudoperonspora humuli*. Phytopathology 99: 1190–1198

Gent DH, Ocamb CM, Farnsworth JL (2010) Forecasting and Management of hop downy mildew. Plant Dis 94: 425–431

Gevens, A.J., and Hausbeck, M.K. (2005) Control of downy mildew of cucumbers with fungicides, 2005. Plant Dis Manag Rep 2: V066

Gisi U, Sierotzki H (2015) Oomycete fungicides: phenylamides, quinone outside inhibitors, and carboxylic acid amide. In H Ishii, DW Hollomon (eds) Fungicide resistance in plant pathogens: Principles and a guide to practical management. Springer Japan, Tokyo, pp 145–174

Gisi, U., Sierotzki, H. (2008) Fungicide modes of action and resistance in downy mildews. Eur J Plant Pathol 122: 157–167

Gnirke, A., Melnikov, A., Maguire, J., Rogov, P., LeProust., E.M., Brockman, W., Fennell, T., Giannoukos, G., Fisher, S., Russ, C., et al (2009) Solution hybrid selection with ultra-long oligonucleotides for massively parallel targeted sequencing. Nat Biotechnol 27: 182–189

Goldenhar, K.E., Hausbeck, M.K. (2019) Fungicides for control of downy mildew on pickling cucumber in Michigan. Plant Heal Prog 20: 165–169

Goss, E.M., Press, C.M., Grünwald, N.J. (2013) Evolution of RXLR-class effectors in the oomycete plant pathogen *Phytophthora ramorum*. PLoS One 8: e79347

Goudet, J. (2005) hierfstat, a package for r to compute and test hierarchical F-statistics. Mol Ecol Notes 5: 184–186

Granke, L.L., and Hausbeck, M.K. (2011) Dynamics of *Pseudoperonospora cubensis* sporangia in commercial cucurbit fields in Michigan. Plant Dis 95: 1392–1400

Granke, L.L., Morrice, J.J., and Hausbeck, M.K. (2013) Relationships between airborne *Pseudoperonospora cubensis* sporangia, environmental conditions, and cucumber downy mildew severity. Plant Dis 98: 674–681

Grünwald, N.J., Everhart, S.E., Knaus, B.J., Kamvar, Z.N. (2017) Best practices for population genetic analyses. Phytopathology 107: 1000–1010

Grünwald, N.J., McDonald, B.A., Milgroom, M.G. (2016) Population genomics of fungal and oomycete pathogens. Annu Rev Phytopathol 54: 323–346

Gugino, B.K., Grove, T.L. (2020) Evaluation of select fungicides and fungicide programs for managing downy mildew of cucumber, 2019. Plant Dis Manag Rep Report 14: V005

Gugino, B.K., and Grove, T.L. (2016) Evaluation of selected fungicides and fungicide programs for managing downy mildew of cucumber, 2015. Plant Dis. Manag. Rep. 10:V072:

Hartl, D., Clark, A. (1997) Principles of population genetics. Sinauer Associates, Inc, Sunderland, Massachusetts

Hausbeck, M. K., and Linderman, S.D. (2014) Evaluation of fungicides for control of downy mildew of cucumber, 2013. Plant Dis Manag Rep 8: V304

Hausbeck, M., Brisco-McCann, E., Goldenhar, K., and Cook, A. (2017) Evaluation of fungicide programs for control of downy mildew of cucumber, 2016. Plant Dis Manag Reports 11: V063
Hausbeck, M., Goldenhar, K. (2017) Downy mildew recommendations for cucumbers. MSU Ext.,
https://www.canr.msu.edu/news/downy_mildew_recommendations_for_cucumbers

Hausbeck, M.K., and Cortright, B. (2010) Evaluation of fungicides and application methods for control of downy mildew of cucumber, 2010. Plant Dis. Manag. Rep. V6:

Hausbeck, M.K., Perla, D.E., and Cook, A.J. (2019) Evaluation of single fungicide products for control of downy mildew of cucumber, 2018. Plant Dis Manag Reports 139: V13

Holdsworth, W.L., Summers, C.F., Glos, M., Smart, C.D., Mazourek, M. (2014) Development of downy mildew-resistant cucumbers for late-season production in the Northeastern United States. HortScience horts 49: 10–17

Hollomon, B. (2007) Fungicide resistance in crop pathogens: How can it be managed?. 2nd ed. FRAC, Brussels

Holmes, G.J., Ojiambo, P.S., Hausbeck, M.K., Quesada-Ocampo, L., and Keinath, A.P. (2014) Resurgence of cucurbit downy mildew in the United States: a watershed event for research and extension. Plant Dis 99: 428–441

Jackson, S.L., Bayliss, K.L. (2011) Spore traps need improvement to fulfil plant biosecurity requirements. Plant Pathol 60: 801–810

Jenkyn, J. (1974) A comparison of seasonal changes in deposition of spores of *Erysiphe graminis* on different trapping surfaces. Ann Appl Biol 76: 257–267

Johnson, D.A, Alldredge, J.R, Allen, J.R, Allwine, R. (1991) Spatial pattern of downy mildew in hop yards during severe and mild disease epidemics. Phytopathology 81: 1369–1374

Jombart, T., and Ahmed, I. (2011) adegenet 1.3-1: new tools for the analysis of genome-wide SNP data. Bioinformatics 27: 3070–3071

Jones, L., Riaz, S., Morales-Cruz, A., Amrine, K.C.H., McGuire, B., Gubler, W.D., Walker, M.A., Cantu, D. (2014) Adaptive genomic structural variation in the grape powdery mildew pathogen, *Erysiphe necator*. BMC Genomics 15: 1081

Kamvar, Z.N., Brooks, J.C., Grünwald, N.J. (2015) Novel R tools for analysis of genome-wide population genetic data with emphasis on clonality. Front Genet 6: 208

Kamvar, Z.N., Tabima, J.F., Grünwald, N.J. (2014) Poppr: an R package for genetic analysis of populations with clonal, partially clonal, and/or sexual reproduction. PeerJ 2: e281

Kanetis, L., Holmes, G.J, and Ojiambo, P.S. (2010) Survival of *Pseudoperonospora cubensis* sporangia exposed to solar radiation. Plant Pathol 59: 313–323

Kanetis, L., Vasiliou, A., Neophytou, G., Samouel, S., Tsaltas, D. (2013) First report of downy mildew caused by *Peronospora belbahrii* on sweet basil (*Ocimum basilicum*) in Cyprus. Plant Dis 98: 283

Keinath, A. P. (2015) Utility of a cucumber plant bioassay to assess fungicide efficacy against *Pseudoperonospora cubensis*. Plant Dis 100: 490–499

Keinath, A.P., Wintermantel WM, Zitter TA, eds (2017) Compendium of cucurbit diseases and pests, 2nd ed. St. Paul, Minnesota, USA

Kitner, M., Lebeda, A., Sharma, R., Runge, F., Dvořák, P., Tahir, A., Choi, Y-J., Sedláková, B., Thines, M. (2015) Coincidence of virulence shifts and population genetic changes of *Pseudoperonospora cubensis* in the Czech Republic. Plant Pathol 64: 1461–1470

Klosterman, S.J., Anchieta, A., McRoberts, N., Koike, S.T., Subbarao, K. V., Voglmayr, H., Choi, Y-J., Thines, M., and Martin, F.N. (2014) Coupling spore traps and quantitative PCR assays for detection of the downy mildew pathogens of spinach (*Peronospora effusa*) and beet (*P. schachtii*). Phytopathology 104: 1349–1359

Knaus, B.J., Grünwald, N.J. (2017) vcfr: a package to manipulate and visualize variant call format data in R. Mol Ecol Resour 17: 44–53

Kozarewa, I., Armisen, J., Gardner, A.F., Slatko, B.E., Hendrickson, C.L. (2015) Overview of target enrichment strategies. Curr Protoc Mol Biol 112: 7.21.1-7.21.23

Kunjeti, S.G., Anchieta, A., Martin ,F.N., Choi, Y-J., Thines, M., Michelmore, R.W., Koike, S.T., Tsuchida, C., Mahaffee, W., Subbarao, K. V., Klosterman, S. J. (2016) Detection and quantification of *Bremia lactucae* by spore trapping and quantitative PCR. Phytopathology 106: 1426–1437

Lane, C.R., Beales, P.A., O'Neill, T.M., McPherson, G.M., Finlay, A.R., David, J., Constantinescu, O., Henricot, B. (2005) First report of Impatiens downy mildew (*Plasmopara obducens*) in the UK. Plant Pathol 54: 243

Langston, D., Sanders, F.H. (2013) Evaluation of fungicides for control of downy mildew on cucumber in Georgia I, 2012. Plant Dis. Manag. Rep. 7: V108.

Lebeda, A., Urban, J. (2010) Screening for resistance to cucurbit downy mildew (*Pseudoperonospora cubensis*). MASS Screen. Tech. Sel. Crop. Resist. TO Dis. International Atomic Energy Agency, Viena, pp 284–295

Li, C-S., Lin, Y-C. (1999) Sampling performance of impactors for fungal spores and yeast cells. Aerosol Sci Technol 31: 226–230

Li, H., Durbin, R. (2009) Fast and accurate short read alignment with Burrows-Wheeler transform. Bioinformatics. doi: 10.1093/bioinformatics/btp324

Li, H., Handsaker, B., Wysoker, A., Fennell, T., Ruan J., Homer, N., Marth, G., Abecasis, G., Durbin, R., Subgroup 1000 Genome Project Data Processing (2009) The sequence alignment/map format and SAMtools. Bioinformatics 25: 2078–2079

Lim, H.C., Braun, M.J. (2016) High-throughput SNP genotyping of historical and modern samples of five bird species via sequence capture of ultraconserved elements. Mol Ecol Resour 16: 1204–1223

Lizotte, E., and Miles, T.D. (2020) Hop disease management in Michigan for 2020. MSU Ext., https://www.canr.msu.edu/news/managing-hop-downy-mildew-in-michigan

Ma, X., Shao, Y., Tian, L., Flasch, D.A., Mulder, H.L., Edmonson, M.N., Liu, Y., Chen, X., Newman, S., Nakitandwe, J., et al (2019) Analysis of error profiles in deep next-generation sequencing data. Genome Biol 20: 50

McCormack JE, Tsai WLE, Faircloth BC (2016) Sequence capture of ultraconserved elements from bird museum specimens. Mol Ecol Resour 16: 1189–1203

Michigan Department of Agriculture & Rural Development (2018) Michigan Agriculture Facts & Figures.
https://www.michigan.gov/documents/mdard/MI_Ag_Facts__Figures_474011_7.pdf

Milgroom, M.G. (2015) Population biology of plant pathogens: genetics, ecology, and evolution. The American Phytopathological Society, St. Paul, Minnesota

Milgroom, M.G. (1996) Recombination and the multilocus structure of fungal populations. Annu Rev Phytopathol 34: 457–477

Miller SA, Vargas A, Amrhein J (2020) Bioassay for sensitivity of *Pseudoperonospora cubensis* to fungicides in OH, 2019. Plant Dis Manag Rep Report 14: V024

Mitchell, M.N., Ocamb, C.M., Grünwald, N.J., Mancino, L.E., and Gent, D.H. (2011) Genetic and pathogenic relatedness of *Pseudoperonospora cubensis* and *P. humuli*. Phytopathology 101: 805–818

Naegele, R. P., Quesada-Ocampo, L. M. , Kurjan, J. D., Saude, C., and Hausbeck, M. K. (2016) Regional and temporal population structure of *Pseudoperonospora cubensis* in Michigan and Ontario. Phytopathology 106: 372–379

Nei, M (1972) Genetic distance between populations. Am Nat 106: 283–292
Neufeld, K.N., Keinath, A.P., Ojiambo, P.S. (2017) Evaluation of a model for predicting the infection risk of squash and cantaloupe by *Pseudoperonospora cubensis*. Plant Dis 102: 855–862

Ojiambo, P.S., Gent, D.H., Quesada-Ocampo, L.M., Hausbeck, M.K., and Holmes, G.J. (2015) Epidemiology and population biology of *Pseudoperonospora cubensis*: a model system for management of downy mildews. Annu Rev Phytopathol 53: 223–246

Ojiambo, P.S., and Holmes, G.J. (2010) Spatiotemporal spread of cucurbit downy mildew in the Eastern United States. Phytopathology 101: 451–461

Ojiambo, P.S., Holmes, G.J., Britton, W., Babadoost, M., Bost, S.C., Boyles, R., Brooks, M., Damicone, J., Draper, M.A., Egel, D.S., et al (2011) Cucurbit Downy Mildew ipmPIPE: A next generation web-based interactive tool for disease management and extension outreach. Plant Heal Prog 12: 26

Oyola, S.O., Gu, Y., Manske, M., Otto, T.D., O'Brien, J., Alcock, D., MacInnis, B., Berriman, M., Newbold, C.I., Kwiatkowski, D.P, et al (2013) Efficient depletion of host DNA contamination in malaria clinical sequencing. J Clin Microbiol 51: 745 LP – 751

Perea, C., De La Hoz, J.F., Cruz, D.F., Lobaton, J.D., Izquierdo, P., Quintero, J.C., Raatz, B., Duitama, J. (2016) Bioinformatic analysis of genotype by sequencing (GBS) data with NGSEP. BMC Genomics 17: 498

Perla, D., Hausbeck, M.K., Cook, A. (2019) Evaluation of fungicide programs for control of downy mildew of cucumber, 2018. Plant Dis Manag Reports 147: V13

Potapov, V., Ong, J.L. (2017) Examining sources of error in PCR by single-molecule sequencing. PLoS One 12: e0169774

Quesada-Ocampo L.M., Granke, L.L., Olsen, J., Gutting, H.C., Runge, F., Thines, M., Lebeda, A., and Hausbeck, M.K. (2012) The genetic structure of *Pseudoperonospora cubensis* populations. Plant Dis 96: 1459–1470

Quinlan, AR, Hall, IM (2010) BEDTools: a flexible suite of utilities for comparing genomic features. Bioinformatics 26: 841–842

Rahman, A., Góngora-Castillo, E., Bowman, M.J., Childs, K.L., Gent, D.H., Martin, F.N., Quesada-Ocampo, L.M. (2019) Genome sequencing and transcriptome analysis of the hop downy mildew pathogen *Pseudoperonospora humuli* reveal species-specific genes for molecular detection. Phytopathology 109: 1354–1366

Reuveni, M., Eyal, H., Cohen, Y. (1980) Development of resistance to metalaxyl in *Pseudoperonospora cubensis.* Plant Dis 64: 1108–1109

Rivera, Y., Salgado-Salazar, C., Gulya, T.J., Crouch, J.A. (2016) Newly emerged populations of *Plasmopara halstedii* infecting rudbeckia exhibit unique genotypic profiles and are distinct from sunflower-infecting strains. Phytopathology 106: 752–761

Rogers, S.L., Atkins, S.D., and West, J.S. (2009) Detection and quantification of airborne inoculum of *Sclerotinia sclerotiorum* using quantitative PCR. Plant Pathol 58: 324–331

Royle, D.J. (1973) Quantitative relationships between infection by the hop downy mildew pathogen, *Pseudoperonospora hutnuli*, and weather and inoculum factors. Ann Appl Biol 73: 19–30

Runge, F., and Thines, M. (2011) Reevaluation of host specificity of the closely related species *Pseudoperonospora humuli* and *P. cubensis*. Plant Dis 96: 55–61

Savory, E.A., Adhikari, B.N., Hamilton, J.P., Vaillancourt, B., Buell, C.R., Day, B. (2012a) mRNA-Seq analysis of the *Pseudoperonospora cubensis* transcriptome during cucumber (*Cucumis sativus L.*) infection. PLoS One 7: e35796

Savory, E.A., Granke, L.L., Quesada-Ocampo, L.M., Varbanova, M., Hausbeck, M.K., Day, B. (2011) The cucurbit downy mildew pathogen *Pseudoperonospora cubensis*. Mol Plant Pathol 12: 217–26

Savory, E.A., Zou, C., Adhikari, B.N., Hamilton, J.P., Buell, C.R., Shiu, S-H., Day, B. (2012b) Alternative splicing of a multi-drug transporter from *Pseudoperonospora cubensis* generates an RXLR effector protein that elicits a rapid cell death. PLoS One 7: e34701

Sharma, R., Xia, X., Cano, L.M., Evangelisti, E., Kemen, E., Judelson, H., Oome, S., Sambles, C., van den Hoogen, D.J., Kitner, M., et al (2015) Genome analyses of the sunflower pathogen *Plasmopara halstedii* provide insights into effector evolution in downy mildews and *Phytophthora*. BMC Genomics 16: 741

Sitterly, W.R. (1972) Breeding for disease resistance in cucurbits. Annu Rev Phytopathol 10: 471–490

Starrett, J., Derkarabetian, S., Hedin, M., Bryson, Jr. R.W., McCormack, J.E., Faircloth, B.C. (2017) High phylogenetic utility of an ultraconserved element probe set designed for Arachnida. Mol Ecol Resour 17: 812–823

Stassen, J., Seidl, M., Vergeer, P., Nijman, I., Snel, B., Cuppen, E., Van den ackerveken, G. (2012) Effector identification in the lettuce downy mildew *Bremia lactucae* by massively parallel transcriptome sequencing. Mol Plant Pathol 13: 719–731

Summers, C., Adair, N., Gent, D., Mcgrath, M., and Smart, C. (2015a) *Pseudoperonospora cubensis* and *P. humuli* detection using species-specific probes and high definition melt curve analysis. Can J Plant Pathol 37: 150605144651006

Summers C.F., Gulliford C.M., Carlson C.H., Lillis J.A., Carlson M.O., Cadle-Davidson L., Gent, D.H., Smart, C.D. (2015b) Identification of genetic variation between obligate plant pathogens *Pseudoperonospora cubensis* and *P. humuli* using RNA sequencing and genotyping-by-sequencing. PLoS One 10: e0143665

Tabima, J.F., Coffey, M.D., Zazada, I.A., Grünwald, N.J. (2018) Populations of *Phytophthora rubi* show little differentiation and high rates of migration among states in the western United States. Mol Plant-Microbe Interact 31: 614–622

Thines, M. (2014) Phylogeny and evolution of plant pathogenic oomycetes—a global overview. Eur J Plant Pathol 138: 431–447

Thines, M., Choi, Y-J. (2015) Evolution, Diversity, and Taxonomy of the Peronosporaceae, with Focus on the Genus Peronospora. Phytopathology 106: 6–18

Thomas, A., Carbone, I., Ojiambo, P. (2013) Comparative genomic analysis of *Pseudoperonospora cubensis* to elucidate the genetic basis of host specialization. Phytopathology 103: S2.145

Thomas, A., Carbone, I., Choe, K., Quesada-Ocampo, L.M., and Ojiambo, P.S. (2017a) Resurgence of cucurbit downy mildew in the United States: Insights from comparative genomic analysis of *Pseudoperonospora cubensis*. Ecol Evol 7: 6231–6246

Thomas, A., Carbone, I., Cohen, Y., Ojiambo, P.S. (2017b) Occurrence and Distribution of Mating Types of *Pseudoperonospora cubensis* in the United States. Phytopathology 107: 313–321

Thomas, A., Carbone, I., Lebeda, A., Ojiambo, P.S. (2017c) Virulence structure within populations of *Pseudoperonospora cubensis* in the United States. Phytopathology 107: 777–785

Thomas, A., Neufeld, K.N., Seebold, K.W., Braun, C.A., Schwarz, M.R., and Ojiambo, P.S. (2018) Resistance to fluopicolide and propamocarb and baseline sensitivity to

ethaboxam among isolates of *Pseudoperonospora cubensis* from the Eastern United States. Plant Dis 102: 1619–1626

Thornton, A.C, Adams, M.L., and Holmes, G.J. (2006) Evaluation of fungicides for control of downy mildew of cucumber I, 2006. Plant Dis Manag Rep 1: V122

McGrath, M (2004) Diseases of cucurbits and their management BT - Diseases of fruits and vegetables volume I: diagnosis and management. *In* SAMH Naqvi (ed) Springer Netherlands, Dordrecht, pp 455–510
Urban, J., Lebeda, A. (2006) Fungicide resistance in cucurbit downy mildew – methodological, biological and population aspects. Ann Appl Biol 149: 63–75

USDA (2020) United States Department of Agriculture. 2019. Vegetables Annual Summary. https://usda-library-cornell-edu.proxy1.cl.msu.edu/concern/publications/02870v86p?locale=en

Vleeshouwers, V.G., Rietman, H, Krenek, P., Champouret, N., Young, C., Oh, S-K., Wang, M., Bouwmeester, K., Vosman, B., Visser, R.G.F., et al (2008) Effector genomics accelerates discovery and functional profiling of potato disease resistance and *Phytophthora Infestans* avirulence genes. PLoS One 3: e2875

Wallace, E., Adams, M., Ivors, K., Ojiambo, P.S., Quesada-Ocampo, L.M. (2014) First report of *Pseudoperonospora cubensis* causing downy mildew on *Momordica balsamina* and *M. charantia* in North Carolina. Plant Dis 98: 1279

Wallace, E., Adams, M., Quesada-Ocampo, L.M. (2015) First report of downy mildew on buffalo gourd (*Cucurbita foetidissima*) caused by *Pseudoperonospora cubensis* in North Carolina. Plant Dis 99: 1861

Wallace, E., Quesada-Ocampo, L. (2016) *Pseudoperonospora cubensis* on commercial and non-commercial cucurbits in North Carolina: Population structure determined by simple sequence repeats. Phythopathology 106: (Suppl) S412

Wallace, E.C., D'Arcangelo, K.N., Quesada-Ocampo, L.M. (2020) Population analyses reveal two host-adapted clades of *Pseudoperonospora cubensis*, the causal agent of cucurbit downy mildew, on commercial and wild cucurbits. Phytopathology. doi: 10.1094/PHYTO-01-20-0009-R

Wallace, E.C., Quesada-Ocampo, L.M. (2017) Analysis of microsatellites from the transcriptome of downy mildew pathogens and their application for characterization of *Pseudoperonospora* populations. PeerJ 5: e3266

Withers, S., Gongora-Castillo, E., Gent, D., Thomas, A., Ojiambo, P.S., and Quesada-Ocampo, L.M. (2016) Using Next-Generation sequencing to develop molecular diagnostics for *Pseudoperonospora cubensis*, the cucurbit downy mildew pathogen. Phytopathology 106: 1105–1116

Wong, F.P, and Wilcox, W.F (2001) Comparative physical modes of action of azoxystrobin, mancozeb, and metalaxyl gainst *Plasmopara viticola* (grapevine downy mildew). Plant Dis 85: 649–656

Wu, E-J., Yang, L-N., Zhu, W., Chen, X-M., Shang, L-P., Zhan, J. (2016) Diverse mechanisms shape the evolution of virulence factors in the potato late blight pathogen *Phytophthora infestans* sampled from China. Sci Rep 6: V26182

Zhang, Y., Pu, Z., Qin, Z., Zhou, X., Liu, D., Dai, L., Wang, W. (2012) A study on the overwintering of cucumber downy mildew oospores in China. J Phytopathol 160: 469–474

Zhu, S.S., Liu, X.L., Wang, Y., Wu, X.H., Liu, P.F., Li, J.Q., Yuan, S.K., and Si, N.G. (2007) Resistance of *Pseudoperonospora cubensis* to flumorph on cucumber in plastic houses. Plant Pathol 56: 967–975

CHAPTER II: DETECTION OF AIRBORNE SPORANGIA OF *PSEUDOPERONOSPORA CUBENSIS* AND *P. HUMULI* IN MICHIGAN USING BURKARD SPORE TRAPS COUPLED TO QPCR

ABSTRACT

Cucurbit downy mildew (CDM), caused by the oomycete pathogen *Pseudoperonospora cubensis*, is a devastating foliar disease on cucumber resulting in reduced yields. In 2004, the pathogen re-emerged in the U.S., infecting historically resistant cucumber cultivars and requiring the adoption of an intensive fungicide program. The pathogen cannot overwinter in Michigan fields but due to an influx of airborne sporangia cucurbit downy mildew occurs annually. In Michigan, spore traps are used to monitor the presence of airborne *P. cubensis* sporangia in cucumber growing regions to guide the initiation of a fungicide program. However, *Pseudoperonospora humuli* sporangia, the causal agent of downy mildew on hop, are morphologically indistinguishable from *P. cubensis* sporangia. This morphological similarity reduces the ability to accurately detect *P. cubensis* from spore trap samples when examined with the aid of light microscopy. To improve *P. cubensis* detection, we adapted a qPCR-based assay to allow the differentiation between *P. cubensis* and *P. humuli* on Burkard spore trap samples collected in the field. Specifically, we evaluated the specificity and sensitivity of *P. cubensis* detection on Burkard spore trap tapes using a morphological based and qPCR-based identification assay and determined whether sporangia of *P. cubensis* and *P. humuli* on Burkard samples could be distinguished using qPCR. We found that the qPCR assay was able to detect a single sporangium of each species on spore trap samples collected in the field with C_q values below 35.5. The qPCR assay also allowed the detection of *P. cubensis* and *P. humuli* in samples containing sporangia from both species. However, the number of sporangia quantified using light microscopy explained only 54% and 10% of the variation in the C_q values of *P. cubensis*

and *P. humuli,* respectively, suggesting a limited capacity of the qPCR assay for the absolute quantification of sporangia in field samples. After two years of monitoring using Burkard spore traps coupled with the qPCR in cucumber fields, *P. humuli* sporangia were detected more frequently than *P. cubensis* early in the growing season (May and June). *P. cubensis* sporangia were detected approximately 5 -10 days before cucurbit downy mildew symptoms were first observed in cucumber fields during both years. This research describes an improved sporangial detection system that is key for the monitoring and management of *P. cubensis* in Michigan.

INTRODUCTION

Pseudoperonospora cubensis (Berk. & M. A. Curtis) Rostovzev, the causal agent of cucurbit downy mildew (CDM), infects approximately 20 cucurbit genera including the economically important crops of cucumber, cantaloupe, squash, watermelon and pumpkin (Cohen et al., 2015; Lebeda and Cohen, 2011). CDM symptoms include angular, chlorotic lesions that coalesce and become necrotic, resulting in leaf blight and death; pathogen sporulation occurs on the abaxial side of the leaf (Salcedo et al., 2020). In cucumber, foliar blighting resulting from CDM can result in yield reduction (Hausbeck et al., 2019; Perla et al., 2019; Reuveni et al., 1980).

In the U.S., Michigan is the largest producer of pickling cucumber and the second-largest producer of cucumber for the fresh market, with approximately 4.1 million cwt of cucumbers sold in 2018 (USDA, 2020). For nearly 40 years, resistant cucumber cultivars had been used successfully to mitigate CDM (Brzozowski et al., 2016). In 2004, a highly virulent strain of *P. cubensis* emerged in the U.S. overcoming this host resistance (Thomas et al., 2017) and since then fungicides have been relied on

for control (Blum et al., 2011; Holmes et al., 2014). However, fungicide-resistant *P. cubensis* isolates have presented crop protection challenges. Single-site fungicides including mefenoxam and azoxystrobin were ineffective when the pathogen emerged in 2004 (Ernest et al., 2005; Gevens and Hausbeck, 2005; Thornton et al., 2006). Since that time, *P. cubensis* resistance to dimethomorph (Zhu et al., 2007) and mandipropamid (Hausbeck and Cortright, 2010; Blum et al., 2011) has been reported in the U.S. (Holmes et al., 2014; Keinath, 2015). Similarly, reduced efficacy of fluopicolide against CDM has been observed in field trials in Michigan (Hausbeck and Linderman, 2014), Georgia (Langston and Sanders, 2013), and North Carolina (Adams and Quesada-Ocampo, 2014). While propamomcarb was effective against CDM for several years, since 2013 its efficacy appeared to be compromised in field trials in North Carolina (Keinath, 2015; Thomas et al., 2018), Pennsylvania (Gugino and Grove, 2016), and Michigan (Hausbeck and Linderman, 2014; Hausbeck et al., 2017).

P. cubensis is an obligate pathogen and its survival depends on the availability of susceptible hosts (Cohen et al., 2015). The pathogen does not survive in regions that experience frost, instead its sporangia are dispersed to northern latitudes from overwintering sites (Ojiambo and Holmes, 2010; Quesada-Ocampo et al., 2012). Airborne sporangia concentrations influence CDM onset (Granke et al., 2013) and under conducive weather conditions, *P. cubensis* sporangia can spread rapidly within and between fields (Ojiambo et al, 2015). Airborne concentrations of *P. cubensis* sporangia in Michigan's cucumber fields have been monitored using Burkard spore traps (Burkard Manufacturing Co Ltd, U.K.) with light microscopy used to identify and enumerate the pathogen sporangia based on morphology (Granke and Hausbeck,

2011; Granke et al., 2013). *Pseudoperonospora humuli*, the causal agent of hop downy mildew (HDM) is nearly identical *to P. cubensis* morphologically (Runge and Thines, 2011) but rarely infects cucurbits in the U.S. (Mitchell et al., 2011). Approximately 400 ha of hops are planted in Michigan (Michigan Department of Agriculture & Rural Development, 2018) and *P. humuli* is prevalent (Lizotte et al., 2020). Thus, relying on morphological identification, alone, to monitor airborne sporangial concentrations of *P. cubensis* could result in inaccurate estimations of the pathogen's presence and concentration.

PCR-based methods have been used successfully to detect and quantify airborne plant pathogens such as *Peronospora effusa* (Klosterman et al., 2014), *Peronospora schachtii* (Klosterman et al., 2014) *Claviceps purpurea* (Dung et al., 2018) and *P. humuli*, infecting spinach, beet, grass-seed and hop (Gent et al., 2009), respectively. A qPCR assay was developed that differentiates between *P. cubensis* and *P. humuli* sporangia (Summers et al., 2015). This assay, with or without microscopic visualization of spore trap tapes, could accelerate the speed and accuracy of *P. cubensis* detection and inform the initiation of fungicide sprays. The objective of our study was to improve the detection of airborne concentrations of *P. cubensis* sporangia by adapting a qPCR-based assay (Summers et al., 2015) that distinguishes between *P. cubensis* and *P. humuli* using Burkard spore trap samples collected in the field.

MATERIALS AND METHODS

In vitro evaluations to assess the sensitivity of the qPCR-based assay were performed using isolates of *P. cubensis* (CDM23) and *P. humuli* (HDM19) obtained in 2017 using methods similar to those described by Thomas et al. (2017). Briefly,

diseased tissue was placed in a moist chamber overnight to induce sporulation. Sporangia from a single cucumber leaf lesion or an infected hop basal shoots (spike) were suspended in 1 ml of distilled water and the resulting inoculum (1,000-10,000 sporangia/ml) applied to the abaxial side of detached leaves of 'Vlaspik' cucumber or 'Centennial' hop, respectively, contained in Petri dishes (100 X 15 mm). Inoculated leaves were then incubated in a growth chamber at 18°C under a 12/12-hr light/dark cycle. Seven to 10 days post inoculation, sporangia were gently rinsed from infected leaves using a Preval spray power unit (Preval, Chicago) filled with distilled water. A new set of leaves were inoculated with the resulting sporangia.

Collection of sporangia and extraction of genomic DNA. *P. cubensis* (CDM23) and *P. humuli* sporangia (HDM19) were gently rinsed from host tissue into centrifuge tubes (50 ml) using a Preval spray power unit filled with distilled water. The sporangial suspension was concentrated by centrifugation (5424R centrifuge, Eppendorf) at 14,000 rpm for 5 min and homogenized in impact-resistant 2mL tubes (Lysing Matrix H, MP Biomedicals) using a TissueLyser II (Qiagen, Valencia, CA) for 4min at 30 Hz. DNA was extracted using a NucleoSpin Plant II isolation kit (Macherey-Nagel, Bethlehem, PA) following manufacturer's instructions and DNA concentration was determined using the Qubit double-stranded DNA High Sensitivity Assay Kit (Life Technologies, Carlsbad, CA).

Competitive qPCR internal control. A competitive internal positive control (IC) was designed in this study and incorporated into every qPCR reaction to monitor for the presence of PCR inhibitors in each sample. The IC consisted of a single-stranded linear synthetic DNA that utilizes the same primers of the target mitochondrial *cox2* gene, and

an additional fluorogenic probe (ICprobeJ2: /5CYS/A+GCATTATT+GTTTAT+CATATATACA/3IABkFQ/) for amplification and detection. The sequence of the internal control (Table 2-1) showed no significant nucleotide identity to any known naturally occurring PCR-amplifiable nucleotide sequences reported in the NCBI database.

qPCR protocol with purified DNA. All qPCR experiments were conducted using a modified version of the protocol described by Summers et al. (2015) in accordance with the Minimum Information for Publication of Quantitative Real-Time Experiments (MIQE) guidelines (Bustin et al., 2009). The Summers et al. (2015) assay was modified by changing the commercial master mix IQ Supermix (Bio-rad, Hercules, CA) to the Prime-Time Gene Expression Master Mix (IDT, Skokie, IL). This new master mix reduced the variation between technical replicates and increased the amplification efficiency of qPCR reactions. Additionally, we also added an internal-positive control to identify any alterations in amplification efficiency in field air samples. qPCR reactions with a final volume of 20 μl were manually assembled in 96-well white plates (Bio-rad MLL9651) containing 10 μl of the Prime-Time Gene Expression Master Mix, 2 μl of template DNA, 600 nM of each primer (RT33F and RT182R), 500 nM of the LNA probe HUMprobeSNP105, 250 nM of the LNA probe CUBprobeSNP105, 250 nM of the LNA probe ICprobeJ2, and 7.5 $x10^{-10}$ nM (0.75 aM) of our internal positive control (IC) (Table 2-1). The IC was set to this concentration to obtain a C_q value of 29 without affecting the sensitivity or specificity of the other probes. Negative control reactions lacking the DNA template were included in every plate run. The qPCR protocol run on a CFX 96 Touch qPCR system (Bio-rad) and included an initial denaturation step at 95°C for 3 min

followed by 38 cycles of 95°C for 10 s and 65°C for 45 s. Two technical replicates of each sample were run and the average C_q and standard deviation were calculated using Bio-rad CFX Manager software (version 3.1) (Bio-rad 1845000).

Sensitivity and specificity of qPCR with LNA probes. The Burkard spore traps use a vacuum pump to draw air (approximately 10 liters/min) into a collection chamber containing a reel, covered with a melinex tape; the reel was mounted on a clockwork mechanism (Hirst, 1952). The melinex tape (Burkard Manufacturing Co. Ltd., U.K.) was coated with an adhesive of petroleum jelly and paraffin (9:1 wt/wt) dissolved in sufficient toluene to provide adequate coverage of tape at the desired thickness (Granke et al., 2013).

The sensitivity and specificity of the qPCR assay was evaluated using three different experiments; the first generated a standard curve using pure DNA of *P. humuli and P. cubensis,* the second used samples that contained a mixture of *P. humuli* and *P. cubensis* DNA and the third used samples of *P. cubensis* sporangia that also contained the melinex tape and the adhesive used on the Burkard spore trap tapes. The first procedure included ten-fold dilutions of genomic DNA from two independent DNA extractions from each pathogen isolate (CDM23 and HDM19) which were used to generate standard curves ranging from 10 to 100,000 fg. Three technical replicates of each sample dilution were tested using qPCR and the average C_q values with the standard deviation were calculated using the Bio-rad CFX Manager software (Bio-rad).

Mean C_q values were plotted against the $\log_{10}$ of template DNA concentrations and used to generate standard curves. The second procedure included the evaluation of mixed-DNA samples to assess the specificity of the qPCR assay. An *in vitro*

assessment was used to determine whether the assay could detect *P. cubensis and P. humuli* in mixed samples containing DNA from both pathogens. Ten-fold dilutions of genomic DNA from each species were made from 100 to 100,000 fg and used as templates, both separately and mixed in varying concentrations (Table 2-2), for the qPCR assay described above. Three technical replicates of each concentration and mixture were run and the average C_q and standard deviations were calculated using Bio-rad CFX Manager software. The third procedure included five independent extractions from solutions containing 10, 100, or 1000 sporangia of *P. cubensis* prepared using a hemocytometer counting cell chamber. Sporangia were homogenized in impact-resistant 2 mL tubes using a TissueLyser (4 min at 30 Hz) and DNA was extracted using the NucleoSpin Plant II isolation kit (Macherey-Nagel, Bethlehem, PA). Subsequently, 2 μl of the extraction product were evaluated using qPCR. Finally, 9 x 48 mm sections (representing a 24 h-sampling period) of melinex tape with adhesive were spiked with 10, 20, 50, 100 or 300 *P. cubensis* sporangia. DNA was extracted and evaluated using qPCR as previously described. Three technical replicates of an average of four independent extractions of each sample dilution were tested and the average C_q values with standard deviation were calculated using the Bio-rad CFX Manager software.

Collection of field samples for screening using qPCR. Airborne sporangial concentrations were monitored during the cucumber growing season (May to September) in 2018 and 2019 using Burkard spore traps. Each year, a spore trap was placed 20 m from a commercial cucumber field located in Muskegon County in northwest Michigan and a cucumber research plot at the Michigan State University

(MSU) Plant Pathology Farm located in Ingham County in southcentral Michigan. The MSU cucumber research plot (0.25 ha) was direct seeded during the last week of July and was located 200 m from an abandoned hop research yard (0.25 ha) where systemically infected basal shoots (spikes) were observed beginning in late April 2019. An additional Burkard spore trap was placed in a commercial hop yard in Berrien County in 2019.

The reel in each Burkard trap was covered with a melinex tape coated with an adhesive as described previously. The tape was removed weekly and cut longitudinally along the center line into two subsections of 9 x 336 mm each (Rogers et al., 2009). The first section was then cut into 48-mm lengths (equivalent to a monitoring period of 24 h), scored at hourly intervals (2 mm) and stained to facilitate counting according to the protocol described by Granke et al. (2013). The second section was also cut into 48-mm lengths, placed into impact-resistant 2mL tubes (Lysing Matrix H, MP Biomedicals) and subjected to DNA extraction as previously described using a NucleoSpin Plant II isolation kit (Macherey-Nagel, Bethlehem, PA). Subsequently, 2 μl of the extraction product was evaluated using qPCR. Fields were scouted weekly for signs and/or symptoms of *P. cubensis*. Leaf samples with lesions resembling CDM symptoms and signs of the pathogen were returned to the laboratory and examined using light microscopy to verify the presence of sporangia. .

RESULTS

Sensitivity and specificity of qPCR. Using 10-fold dilutions of *P. cubensis* and *P. humuli* DNA, the qPCR assay exhibited a significant linear response with an efficiency of 93.6% (R^2=0.99) and 90.7% (R^2=1), respectively (Figs. 2-1A, 2-1C). Both

species-specific LNA probes detected each pathogen within total DNA template amounts ranging between 100 to 100,000 fg per reaction (Figs. 2-1A, 2-1C). The average C_q values for samples containing 100 fg of *P. humuli* and *P. cubensis* DNA was < 35.5. Most samples with concentrations below 100 fg were either not detected or detected without reasonable certainty (<95% of the times tested); thus, 100 fg of template DNA was considered as the lower limit of detection (LOD) of the qPCR assay for both species. Although the LNA probes were specifically designed to detect either *P. humuli* or *P. cubensis* based on the recognition of a SNP at the 105-base of the *cox2* gene (Summers et al., 2015), the HEX-labelled LNA probe CUBprobeSNP105 for *P. cubensis* detection showed nonspecific amplification of *P. humuli* DNA. However, the amplification curves of *P. humuli* DNA with this probe did not show the same shape as those generated using the *P. cubensis* DNA (Fig. 2-1B). *P. cubensis* samples were classified as positive based on the shape of the amplification curve using the probe CUBprobeSNP105 and no amplification of the FAM-labelled LNA probe HUMprobeSNP105. This probe (HUMprobeSNP105) designed to recognize *P. humuli* was highly specific and no background signal was observed when *P. cubensis* DNA was analyzed (Figs. 2-2D).

Additionally, when mixed-samples containing DNA from both species were assessed using the qPCR assay, no significant changes were observed in the Cq values of the samples containing *P. cubensis* or *P. humuli* DNA in a 1:1 ratio (Table 2-2). However, when 10,000 fg of *P. cubensis* DNA was mixed with 100 fg of *P. humuli* DNA, no detection of *P. humuli* DNA was observed (Table 2-2). Detection of *P. cubensis* occurred in all mixtures, but when 10,000 fg of *P. humuli* DNA was mixed with

1,000 or 100 fg *of P. cubensis* DNA, the detection of *P. cubensis* occurred at significant lower C_q values than in reactions including only *P. cubensis* DNA (Table 2-2). Mixed-samples containing DNA from both species generated amplification curves with both probes (CUBprobeSNP105 and HUMprobeSNP105). This clearly differentiated them from samples containing only *P. cubensis* DNA for which there was only amplification with the CUBprobeSNP105 probe (Supplementary Fig. 2-S1 A, C). Although the samples containing only *P. humuli* DNA also generated amplification curves with both probes (Supplementary Fig. 2-S1 B), the amplification curves generated with the CUBprobeSNP105 probe for mixed samples showed faster growth in the exponential phase of the curves. This was the case for mixed-samples containing DNA from both species in a 1:1 ratio and samples containing *P. cubensis* and *P. humuli* DNA in 10:1 ratio (Supplementary Fig. 2-S1 C, D). Only the amplification curves of the samples containing *P. cubensis* and *P. humuli* DNA in 1:10 and 1:100 ratio were not clearly differentiated from the amplification curves containing only *P. humuli* DNA (Supplementary Fig. 2-S1 B, E).

Both LNA probes detected DNA from extractions containing 10, 100 or 1000 sporangia of *P. cubensis and P. humuli*. Upon regression analysis, a linear relationship between C_q values and DNA extracted from purified sporangia was observed for both species (*P. cubensis*, R^2= 0.99, P_{value} = 0.03 and *P. humuli*, R^2= 0.98, P_{value} = 0.084) (Fig. 2-2A). The average C_q value for detecting 10 *P. cubensis* sporangia was < 35.5 (Fig. 2-2A) and samples with less than 10 sporangia could not be detected with reasonable certainty (>95% of the times tested). C_q values ≤ 35.5 were classified as

specific to *P. humuli* and *P. cubensis* and were used as a threshold to evaluate field samples.

The sensitivity of the assay to detect *P. cubensis* was minimally affected by the adhesive applied to the melinex tape (Fig. 2-2B). DNA was detected from extractions of tapes spiked with 20, 50,100, or 300 sporangia and a reduced number of samples (4/10) containing 10 sporangia had average C_q values below 35.5. All the extractions showed C_q values that were significantly different from the background signal observed in the negative controls. The relationship between sporangial numbers and C_q values was significant ($p = 0.003$) and the assay exhibited a linear response with a R^2 value of 0.99 (Fig. 2-2B). The average C_q values of the different sporangial dilutions were within the 95% confidence interval. However, a high standard error of the mean was observed among biological replicates of extractions with the same number of sporangia (Fig. 2-2B) indicating that the extraction affects the precision of quantifying sporangia using the qPCR-based assay.

Assessment of field samples using light microscopy and qPCR. A total of 560 samples collected from May to August in 2018 and 2019 were assessed using qPCR. *P. cubensis* or *P. humuli* DNA was detected using qPCR on field samples with fewer than 10 sporangia (Fig. 2-2C). Approximately 90% of all samples that tested positive for either pathogen using qPCR (204 out of 227) had one or more sporangia on the corresponding half of the tape analyzed using light microscopy. The average C_q value of the IC remained relatively constant and had an average of 28.8 ± 1.7 (SD) among all the field samples evaluated. Regression analysis indicated that the number of sporangia on the second half of the tape of the samples (quantified using light

microscopy) explained 54% (R^2 = 0.54) and 10% (R^2 = 0.10) of the variation in the C_q values of *P. cubensis* and *P. humuli*, respectively (Fig. 2-2C).

Using light microscopy, *Pseudoperonospora* spp. sporangia were first detected in 2018 during May (Muskegon Co. commercial field, 15 May) and June (Ingham Co. research field, June 13) (Fig. 2-3). From May to July at the research field, fewer than 5 sporangia/day were observed via light microscopy with *P. cubensis* DNA confirmed using qPCR on 13 June and 10, 23 July; while *P. humuli* was confirmed on 19 June and 7 July (Fig. 2-3A). At the commercial field, fewer than 10 sporangia/day were detected using light microscopy from May to July, except for 21 June (Fig. 2-3B). Using qPCR, we confirmed the presence of *P. humuli* DNA on 29 May to 4 June and 21 to 26 June (Fig. 2-3B) while *P. cubensis* DNA was detected on 5 and 13 June (Fig. 2-3B). Airborne sporangial concentrations increased during the first week of August and reached the maximum during the third week of the month in both locations monitored in 2018 (Figs. 2-3A, 2-3B). CDM symptoms were observed at the research field on 15 August, a peak of 16 sporangia was observed via light microscopy 10 days prior (5 August) and *P. cubensis* DNA was confirmed by qPCR on 1 to 6 August and 10 August (Fig. 2-3A). After CDM symptoms were observed in the research field, daily sporangial counts via light microscopy exceeded 10 sporangia/day with *P. cubensis* DNA detected nearly every day using qPCR (Figs. 2-3A, 2-3B). CDM symptoms were observed at the commercial field on 7 August, a peak of 22 sporangia was observed via light microscopy four days prior (3 August) and *P. cubensis* DNA was confirmed by qPCR on 3, 5 August, and 28, 30, and 31 July (Fig. 2-3B). The day following the detection of

CDM symptoms, more than 80 sporangia/day were captured by the spore traps and *P. cubensis* DNA was detected every day using qPCR (Fig. 2-3B).

In 2019, *Pseudoperonospora* spp. sporangia were first detected in May across all locations using light microscopy (Fig. 2-4). During May and June, concentrations of airborne sporangia exceeded 10 sporangia/day in the commercial hop yard (Fig. 2-4A) and the research field (Fig. 2-4B). Using qPCR, *P. humuli* DNA was detected several times in the commercial hop yard from May through August while *P. cubensis* DNA was only detected on 12, 14, and 18 August (Fig. 2-4A). Based on data from light microscopy, the research field which was in proximity to a non-treated hop yard, had more than 10 sporangia/day during the last week of May, the first and fourth week of June and the first week of July (Fig. 2-4B). At this location, *P. humuli* DNA was detected from May to July using qPCR (Fig. 2-4B). During August, fewer than 10 sporangia/day were observed at the research field. CDM symptoms were confirmed at this site on 21 August and *P. cubensis* DNA was verified by qPCR on 11, 19, and 20 August. Following CDM symptoms, *P. cubensis* DNA was detected from 22 to 31 August (Fig. 2-4B). In the commercial cucumber field, fewer than 10 sporangia/day were observed using light microscopy from May through July with the exception of 18, 21 and 23 June (Fig. 2-4C). *P. humuli* DNA was confirmed with qPCR on 22 and 23 June (Fig. 2-4C). At this location, the sporangial counts increased from the third to the last week of August. CDM symptoms were confirmed on 16 August and *P. cubensis* DNA was detected using qPCR in air samples every day from 12 to 31 August (Fig. 2-4C).

DISCUSSION

The ability to detect and differentiate between *P. cubensis* and *P. humuli* in field air samples using qPCR represents an important advance for CDM monitoring and management. The qPCR detection of airborne sporangia could be used as a decision-making tool to initiate fungicide sprays (Dhar et al., 2019) or as a complementary variable to forecast the risk (Carisse et al., 2009) of CDM outbreaks in Michigan. Early and specific detection of *P. cubensis* sporangia could ensure timely crop protection and avoid unnecessary fungicide applications. *P. cubensis* does not overwinter in Michigan and for disease to occur, the pathogen must be introduced into the state's growing regions annually (Naegele et al., 2016). Burkard spore traps coupled with light microscopy have been used since 2007 to alert Michigan growers to an influx of *P. cubensis* sporangia into their growing region. However, HDM is prevalent in the state (Lizotte et al., 2020) where approximately 400 ha of hops have been planted (Hop Growers of America, 2019). Using a qPCR assay, we were able to distinguish between the morphologically similar sporangia of *P. cubensis* and *P. humuli* collected from Burkard spore traps. During the two years of monitoring using Burkard spore traps coupled with the qPCR assay in cucumber fields, *P. cubensis* sporangia were detected approximately 5-10 days before CDM symptoms were observed in monitored cucumber fields.

We adapted the qPCR assay developed by Summers et al. (2015) to a high degree of sensitivity for use with the Burkard spore trap samples. Using DNA extracted from purified sporangial suspensions of *P. cubensis* and *P. humuli,* we were able to

detect DNA concentrations ranging from 100 fg to 100,000 fg. This sensitivity was validated with the detection of the two downy mildew pathogens in field samples containing less than 10 sporangia (Cq <35.5). We split the tape of Burkard spore traps to facilitate the comparison between light microscopy and qPCR and observed that the number of sporangia deposited onto one half of the tape was linearly correlated with the Cq values obtained after the assessment of the other half using qPCR. However, the change in the number of sporangia on field samples quantified using light microscopy explained only 54% and 10% of the variation in the C_q values of *P. cubensis* and *P. humuli,* respectively, suggesting a limited capacity of the qPCR assay for the absolute quantification of sporangia in field samples.

The low correlation between Cq values and sporangial numbers of field samples may be explained by the high variation in the yield of DNA extraction among samples (Summers et al., 2015), inaccurate visual quantification, the low specificity of one of our probes, and possibly, the multicopy nature of the target sequence (Klosterman et al., 2014; Kunjeti et al., 2016; Dung et al., 2018). Similarly, the yield variation of DNA extractions among samples may also explain the variation observed in the Cq values of samples with the same number of sporangia *in vitro*. This variation is introduced in all the samples collected in the field and may reduce the precision for the quantification of sporangia using the extraction protocol and qPCR assay described in this study. However, assessing the first half of the spore trap tape using qPCR could reduce the number of samples that require microscopic analysis for spore quantification, accelerating the turn-around time associated with monitoring airborne *P. cubensis* sporangia. The reduction of variation in the yield of DNA extractions and the utilization

of a qPCR assay based on a single-copy marker may be more appropriate for quantification (Rahman et al., 2020) but may result in a system with reduced sensitivity when compared to the multi-copy system that we used.

The nonspecific amplification of *P. humuli* DNA affected the quantification capacity of the assay when both species were present in the same reaction. However, the inclusion of a second probe ensured that the detection of each species was possible even when *P. cubensis* and *P. humuli* were present in the same sample. The nonspecific amplification of *P. humuli* did not occur under the conditions described by Summers et al. (2015) and was a consequence of the change in the commercial master mix used for the qPCR reactions (Supplementary Fig. 2-S2). The master mix used in this study reduced the variation among technical replicates (data not shown) and increased the amplification efficiency of the qPCR reactions (exponential phase) but affected the specificity of the assay. Different qPCR master mixes influences how oligonucleotides (primers and probes) bind to target regions (Morinha et al., 2020), thus the suitability of new reagents must be carefully evaluated as they may condition the results of the qPCR. The detection of both species using our qPCR assay was hindered only in samples with a significantly higher amount of *P. humuli* compared to *P. cubensis* (i.e. samples containing *P. cubensis* and *P. humuli* DNA in 1:10 and 1:100 ratio). In these cases, or in locations where a higher number of *P. humuli* sporangia relative to the number of *P. cubensis* sporangia is expected (e.g. hop yards) the use of the IQ Supermix (Bio-rad, Hercules, CA) as described by Summers et al. (2015) for qPCR reactions should allow a more accurate evaluation of the samples.

During two years of monitoring in commercial cucumber fields, we did not detect any periods when both pathogens were detected simultaneously, however, overlapping periods may have occurred at the commercial hop yard during late August. The identification of genetic regions with a higher number of polymorphisms has allowed the design of more specific primer and probes for *P. cubensis* detection (Rahman et al., 2020). Using this new set of primers and probes in combination with the probe HUMprobeSNP105 (for detection of *P. humuli*) could ensure both specific detection and quantification of *P. cubensis* and *P. humuli* sporangia using qPCR even during periods when both species are present.

Despite the limitations of the qPCR assay described in this study, we were able to detect low atmospheric concentrations of *P. cubensis* and *P. humuli* (<10 sporangia/day). Detection of *P. cubensis* before symptoms developed in the field was linked to a sporangial concentration below 10 sporangia/day as estimated using light microscopy. In other crops including lettuce and onion, measurements of aerial spore load (sporangia/day) have been used to guide fungicide application to control *Bremia lactucae* (Dhar et al., 2019) and *Botrytis squamosa* (Carisse et al., 2009), respectively. In these systems, fungicide applications began once spore loads reached a critical level between 300-500 spores/day (10 sporangia/m^3). In the cucumber fields monitored in 2018, CDM symptoms were observed after airborne *P. cubensis* sporangial concentrations were greater than 15 sporangia/day as determined via light microscopy, suggesting that the critical concentration for CDM could be close to this number depending on the coincident environmental conditions. Using the qPCR assay, *P. cubensis* sporangia were detected before concentrations reached >15 sporangia/day.

More than 15 sporangia/day were also observed one month before CDM was detected in the cucumber fields (June 2018 and 2019), however, these sporangia were identified as *P. humuli* using qPCR. In Michigan, information on the airborne concentration of sporangia is used to provide an early warning for growers that CDM is likely to occur (Hausbeck, 2020) and prompt the application of fungicides. Using light microscopy only, *P. humuli* sporangia could have triggered unnecessary fungicide applications, highlighting the importance of a qPCR assay system that reliably distinguishes between *P. cubensis* and *P. humuli.*

Using light microscopy and qPCR, differences in the airborne sporangial concentrations of *P. humuli* and *P. cubensis* were detected between the two years of monitoring. From June to August 2018 at the commercial cucumber field, we detected higher airborne sporangial concentrations of *P. cubensis* compared to 2019. A relatively cold and rainy spring delayed the planting of cucumbers for pickling in 2019 (USDA, 2020). This reduced host availability may have also resulted in reduced infection and *P. cubensis* sporangia production. Similarly, from May to July 2018, low concentrations of *P. humuli* (<10 sporangia/day) were detected in the two monitored fields whereas a higher concentration (>10 sporangia/day) was observed at the three locations monitored in 2019. *P. humuli* overwinters in dormant hop buds or crowns, growing into expanding basal shoots in spring and early summer (Coley-Smith, 1962). Extended periods of wetness, high RH, and temperatures below 20°C (Royle, 1973; Gent and Ocamb, 2009) occurred during the cold and rainy spring of 2019 (NOAA, 2019) and may have favored the pathogen's reproduction and infection.

These results suggest that the qPCR-based assay allowed for precise monitoring of airborne *P. cubensis* and *P. humuli* sporangia over two different years; the specific detection of these two species was not possible using light microscopy only. Cucumber growers in Michigan desire to know when sporangia of *P. cubensis* have arrived in their production region/field so that scouting efforts can be intensified, and costly fungicide programs initiated. The information on *P. cubensis* detection derived from spore traps coupled with qPCR could be used by growers to make informed decisions regarding fungicide usage leading to increased efficiency. Judicious use of fungicides may slow the development of pathogen resistance and decrease the cost associated with CDM control. The deployment of a broader network of spore traps and the evaluation of air samples using qPCR could also improve the risk assessment of CDM epidemics. Future evaluation of more cost-effective spore traps such as impaction traps for the monitoring of *P. cubensis* is essential to increase the geographic coverage of the spore trapping network in Michigan. The use of more spore traps at a local level could make the monitoring more geographically precise and trigger the execution of disease management practices only in fields at high risk of infection based on the qPCR detection of *P. cubensis* and the local environmental conditions.

APPENDIX

APPENDIX

Table 2-1. *Primers and locked nucleic acids (LNA) probes for the qPCR assay differentiating Pseudoperonospora cubensis and P. humuli using the 105 SNP in the mitochondrial Cox2 gene.*

	Code name	[Conc][a]	Sequence 5'->3'
Primer	RT33F[b]	600 nM	AACTCCCGTTATGGAAGGTATT
Primer	RT182R[b]	600 nM	CCATGTACAACAGTAGCTGGA
Probe	CUBprobeSNP105[b]	250 nM	HEX/A+C+AAA+C+G+AATA+CT/BHQ [c]
Probe	HUMprobeSNP105[b]	500 nM	FAM/AA+C+AAA+C+A+AATA+CTG/BHQ [c]
Probe	ICprobeJ2	250 nM	CYS/A+GCATTATT+GTTTAT+CATATATACA/BHQ[c]
Internal Control	IC	7.5×10^{-10} nM (0.75 aM[d])	AACTCCCGTTATGGAAGGTATTATCATTAATCAT GATTTGTATATATGATAAACAATAATGCTATAAC ATAGAGTCTCTTTCATGAATAATCCAGCTACTGT TGTACATGG

[a]Concentrations used in a 20 μl qPCR reaction.
[b]Primers and LNA probes were adapted from Summers et al. (2015).
[c]Locked nucleic acids in the probes are followed by a plus (+) sign
[d]Attomole (aM) = 10^{-18} moles per liter

***Table 2-2*. Threshold cycle (C_q) values of the qPCR assays using LNA probes and varying concentrations of genomic DNA.**

	DNA		Probe			
			CUBprobeSNP105		HUMprobeSNP105	
	P. cubensis	*P. humuli*	C_q-HEX	SD	C_q-FAM	SD
	10,000 fg	--	28.39[a]	0.10	NA	NA
	1,000 fg	--	32.12[b]	0.21	NA	NA
Un-	100 fg	--	35.49[c]	0.74	NA	NA
mixed	--	10,000 fg	29.88[nc]	0.34	28.29[d]	0.08
	--	1,000 fg	32.96[nc]	0.17	31.70[e]	0.30
	--	100 fg	NA	NA	36.61[f]	0.14
	10,000 fg	10,000 fg	28.67[a]	0.23	28.52[d]	0.60
	1,000 fg	1,000 fg	31.44[b]	0.37	32.42[e]	0.08
	100 fg	100 fg	35.32[c]	0.98	35.11[f]	0.59
Mixed	10,000 fg	1,000 fg	28.37[a]	0.15	32.07[e]	0.33
	10,000 fg	100 fg	28.39[a]	0.26	NA[z]	NA
	1,000 fg	10,000 fg	29.78[x]	0.37	27.96[d]	0.34
	100 fg	10,000 fg	30.58[y]	0.24	24.99[d]	5.91

The HEX-labelled probe (CUBprobeSNP105) was designed to detect only DNA from *P. cubensis* and the FAM-labelled probe (HUMprobeSNP105) was designed to detect only DNA from *P. humuli.* Cq values with the same letter are not significantly different (t-Test; P=0.05). --: not DNA added. NC: not used for comparison in the t-Test. NA: not defined.

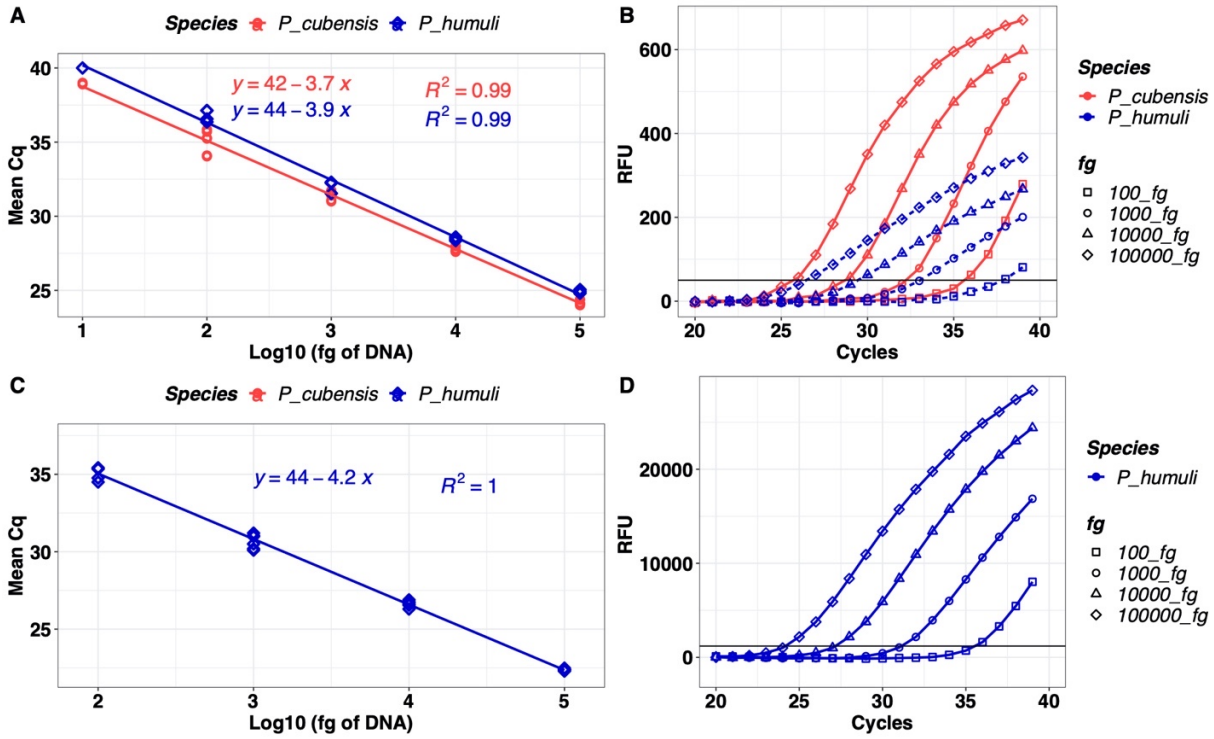

Figure 2-1. **Regression and amplification curves of *Pseudoperonospora cubensis* and *P. humuli* DNA using qPCR.**

A. Standard curve for the quantification of *P. cubensis* and *P. humuli* DNA using the LNA probe CUBprobeSNP105. The log10 of DNA (100fg, 1,000fg, 10,000fg, and 100,000fg) is plotted against the quantification cycle (C_q) values. Each curve was plotted separately using DNA from each pathogen. The data points below 100fg were not included in the regression analysis. **B**. Amplification curves of *P. cubensis* and *P. humuli* DNA with different concentrations using the LNA probe CUBprobeSNP105. Each curve was plotted separately using DNA from each pathogen **C.** Standard curve for the quantification of *P. cubensis* and *P. humuli* DNA using the LNA probe HUMprobeSNP105. The log10 of DNA (100fg, 1,000fg, 10,000fg, and 100,000fg) is plotted against the quantification cycle (C_q) values. Each curve was plotted separately using DNA from each pathogen. **D**. Amplification curves of *P. cubensis* and *P. humuli* DNA with different concentrations using the LNA probe HUMprobeSNP105. Each curve was plotted separately using DNA from each pathogen

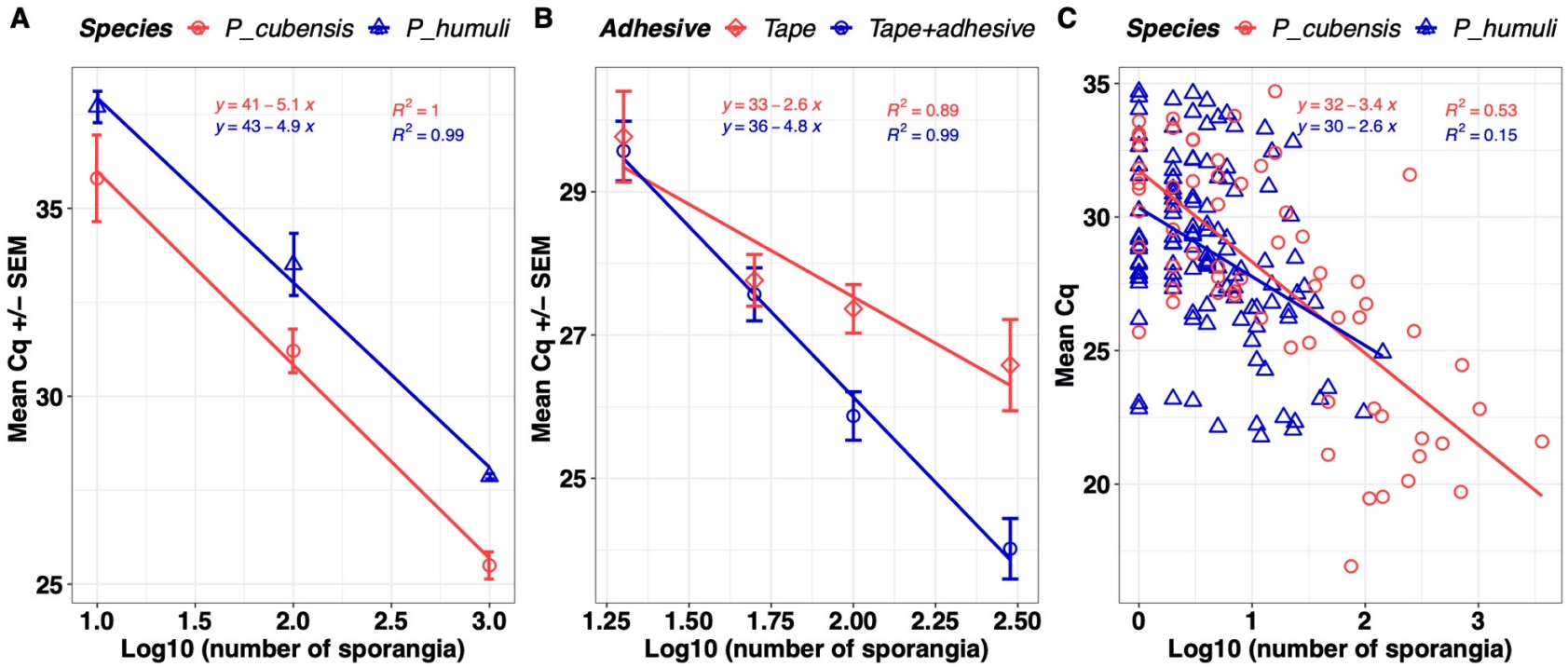

Figure 2-2. **Standard curves for the quantification of *Pseudoperonospora cubensis* and *P. humuli* sporangia using qPCR**.

A. The log10 of the number of sporangia is plotted against the quantification cycle values (C_q). The centerline represents the line of fit and error bars represent standard error of the mean. Each curve was plotted separately using the LNA probes specific to each pathogen. Data points represent three technical replicates from two DNA extractions. **B.** Standard curves based on the qPCR assays of DNA extractions from *P. cubensis* sporangia (20, 50, 100 and 300) in the presence and absence of the adhesive mix used on the melinex tape. All data points are from three technical replicates from 4 independent DNA extractions. **C.** Linear regression of *Pseudoperonospora* spp. sporangia counted using light microscopy against corresponding mean C_q values. All the samples used in this regression were collected using spore traps in the field.

A. Cucumber research plot - Ingham (2018)

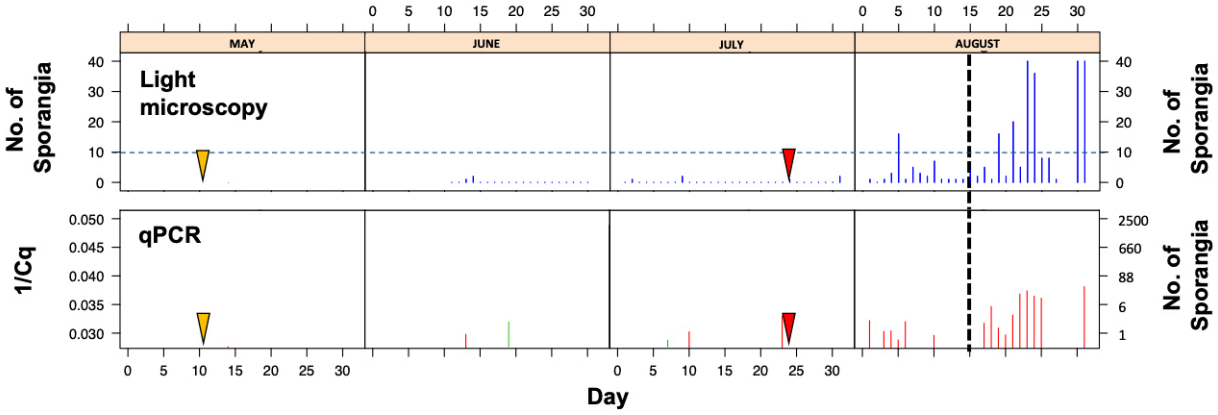

B. Commercial cucumber field - Muskegon (2018)

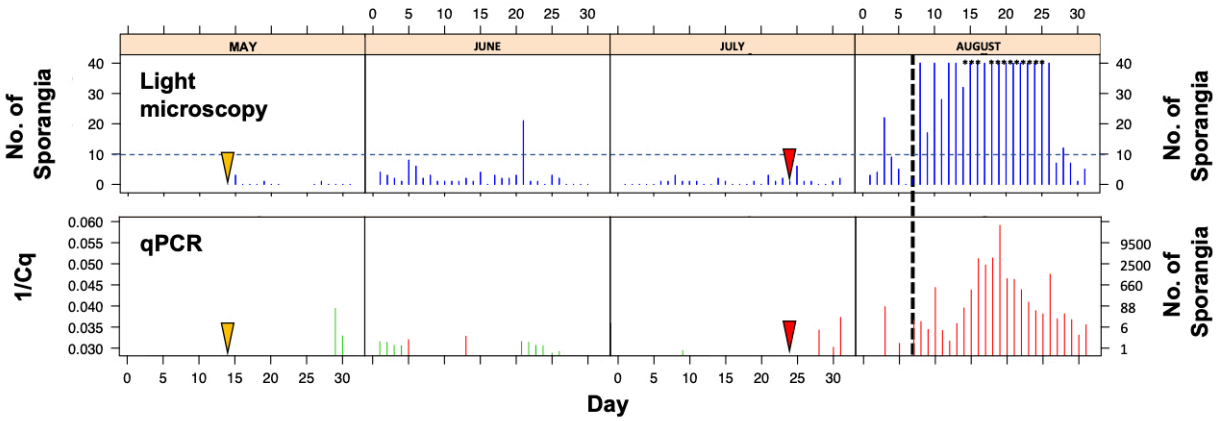

Figure 2-3. **Monitoring of *Pseudoperonospora cubensis* and *P. humuli* sporangia using Burkard spore traps in Ingham (A) and Muskegon (B) in 2018.**

The data from each county was divided into two panels. **The first top panel** represents the daily sporangia numbers estimated through the analysis of Burkard spore trap samples using light microscopy (blue bars). The y-axis was trimmed to 40 sporangia to facilitate the visualization of low counts. **The middle panel** represents the qPCR results for the detection of *P. cubensis* (red bars) and *P. humuli* (green bars) in the tape of Burkard spore traps. Yellow triangles denote the monitoring starting date. Red triangles denote the first confirmed report of cucurbit downy mildew in the state. The dashed line denotes the date of cucurbit downy mildew detection in the field. Scouting efforts to detect CDM symptoms in growing cucumber regions are intensified once sporangial loads exceed 10 sporangia/day.

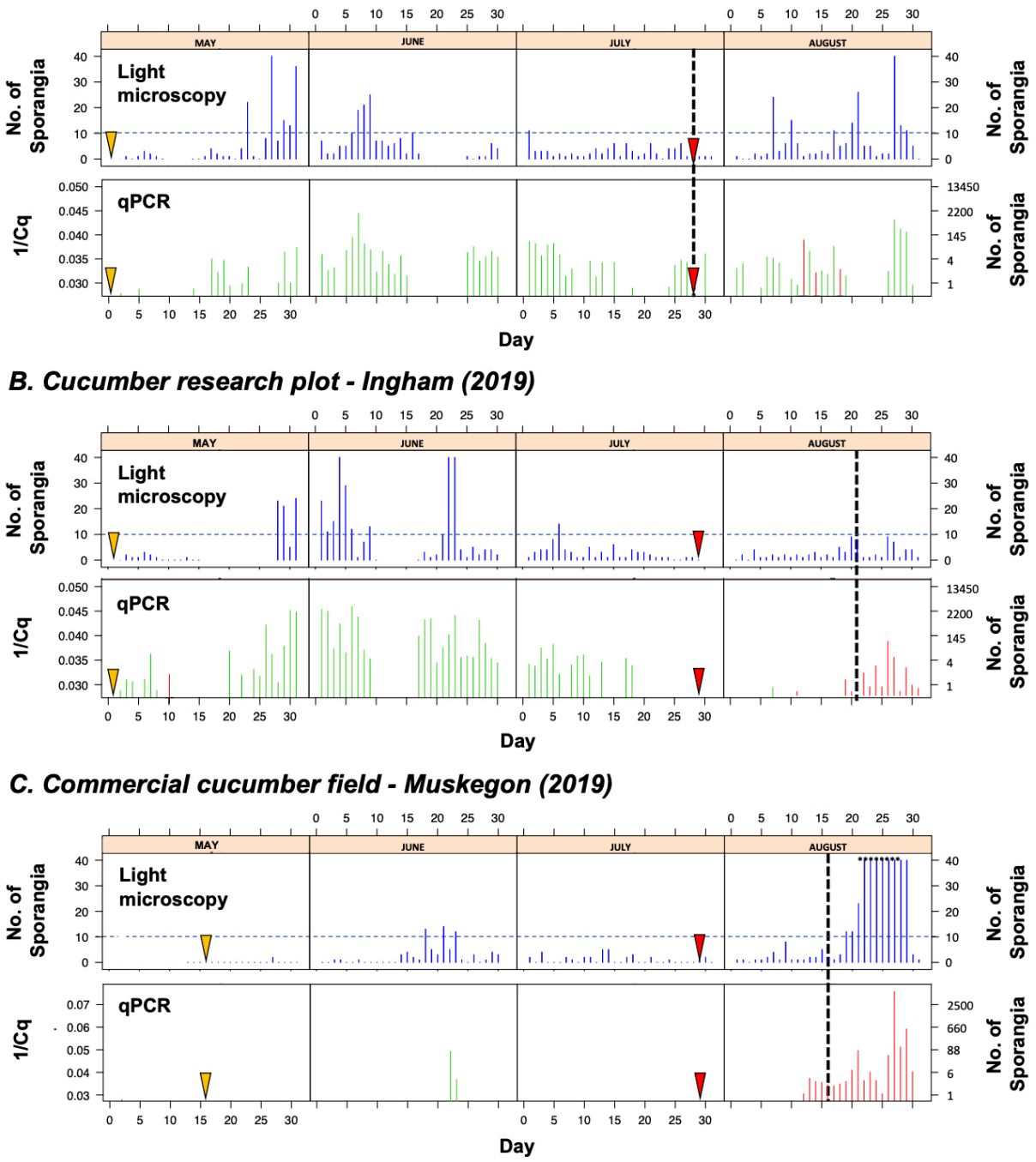

Figure 2-4. **Monitoring of *Pseudoperonospora cubensis* and *P. humuli* sporangia using Burkard spore traps in Berrien (A), Ingham (B) and Muskegon (C) in 2019.**

The data from each county was divided into two panels. **The first top panel** represents the daily sporangia numbers estimated through the analysis of Burkard spore trap samples using light microscopy (blue bars). The y-axis was trimmed to 40 sporangia to

Figure 2-4. (cont'd)

facilitate the visualization of low counts. **The middle panel** represents the qPCR results for the detection of *P. cubensis* (red bars) and *P. humuli* (green bars) in the tape of Burkard spore traps. Yellow triangles denote the monitoring starting date. Red triangles denote the first confirmed report of cucurbit downy mildew in the state. The dashed line denotes the date of cucurbit downy mildew detection in the field. Scouting efforts to detect CDM symptoms in growing cucumber regions are intensified once sporangial loads exceed 10 sporangia/day.

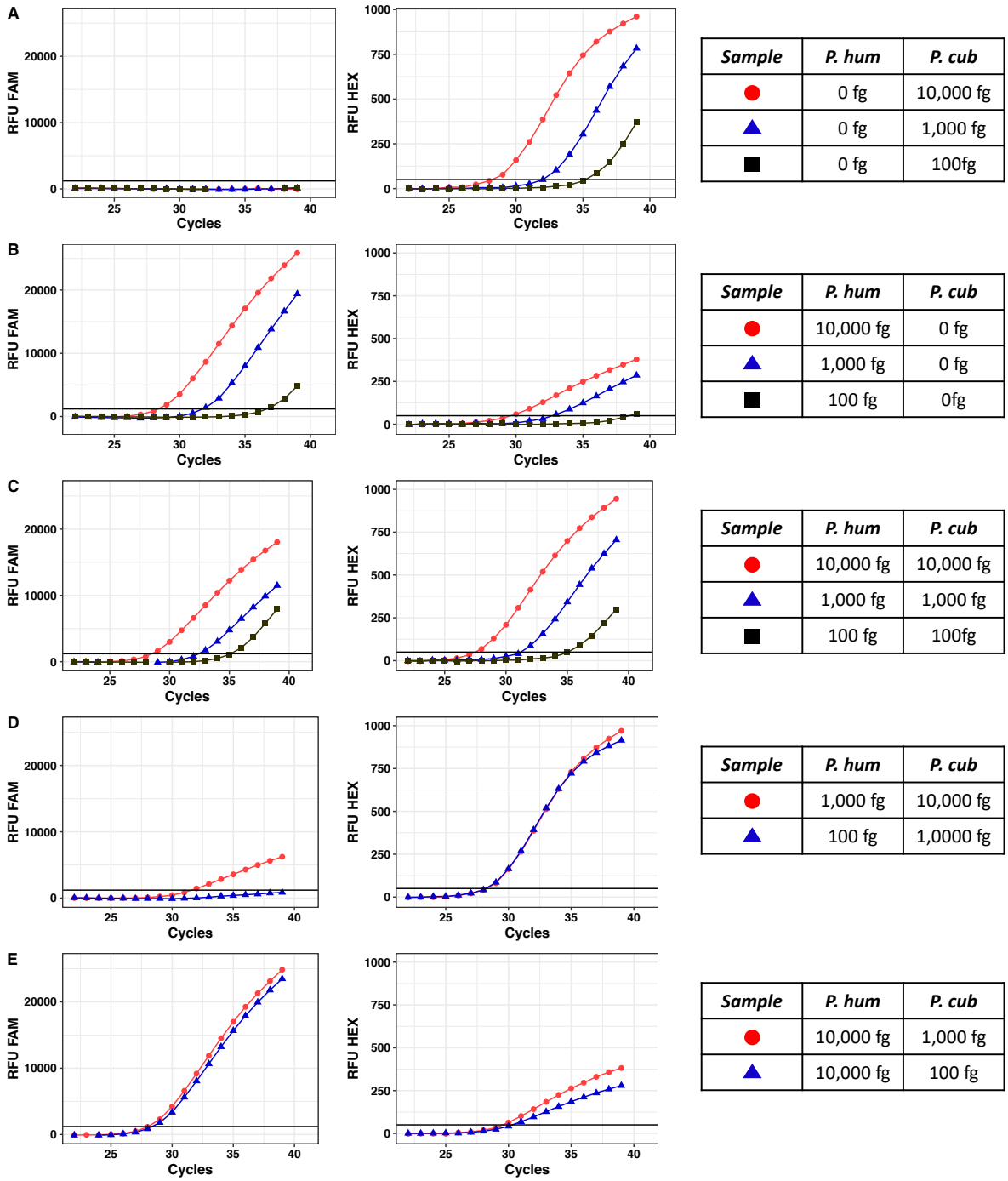

Sample	P. hum	P. cub
●	0 fg	10,000 fg
▲	0 fg	1,000 fg
■	0 fg	100fg

Sample	P. hum	P. cub
●	10,000 fg	0 fg
▲	1,000 fg	0 fg
■	100 fg	0fg

Sample	P. hum	P. cub
●	10,000 fg	10,000 fg
▲	1,000 fg	1,000 fg
■	100 fg	100fg

Sample	P. hum	P. cub
●	1,000 fg	10,000 fg
▲	100 fg	1,0000 fg

Sample	P. hum	P. cub
●	10,000 fg	1,000 fg
▲	10,000 fg	100 fg

Supplementary Figure 2-S1. Amplification curves of *Pseudoperonospora cubensis (Pcu)* and *P. humuli (Phu)* DNA using qPCR. **A**. Amplification curves of *P. cubensis* DNA with different concentrations using the LNA probes HUMprobeSNP105 (left, FAM) and CUBprobeSNP105 (right. HEX). **B.** Amplification curves of *P. humuli* DNA with different concentrations using the LNA probes HUMprobeSNP105 (left, FAM) and CUBprobeSNP105 (right, HEX).

Supplementary Figure 2-S1*. (cont'd)*

C. Amplification curves of *P. humuli and P. cubensis* DNA mix in a 1:1 ratio using the LNA probes HUMprobeSNP105 (left, FAM) and CUBprobeSNP105 (right, HEX). **D.** Amplification curves of *P. humuli and P. cubensis* DNA mix in a 1:10 and 1:100 ratio using the LNA probes HUMprobeSNP105 (left, FAM) and CUBprobeSNP105 (right, HEX). **E.** Amplification curves of *P. cubensis and P. humuli* DNA mix in a 1:10 and 1:100 ratio using the LNA probes HUMprobeSNP105 (left, FAM) and CUBprobeSNP105 (right, HEX)

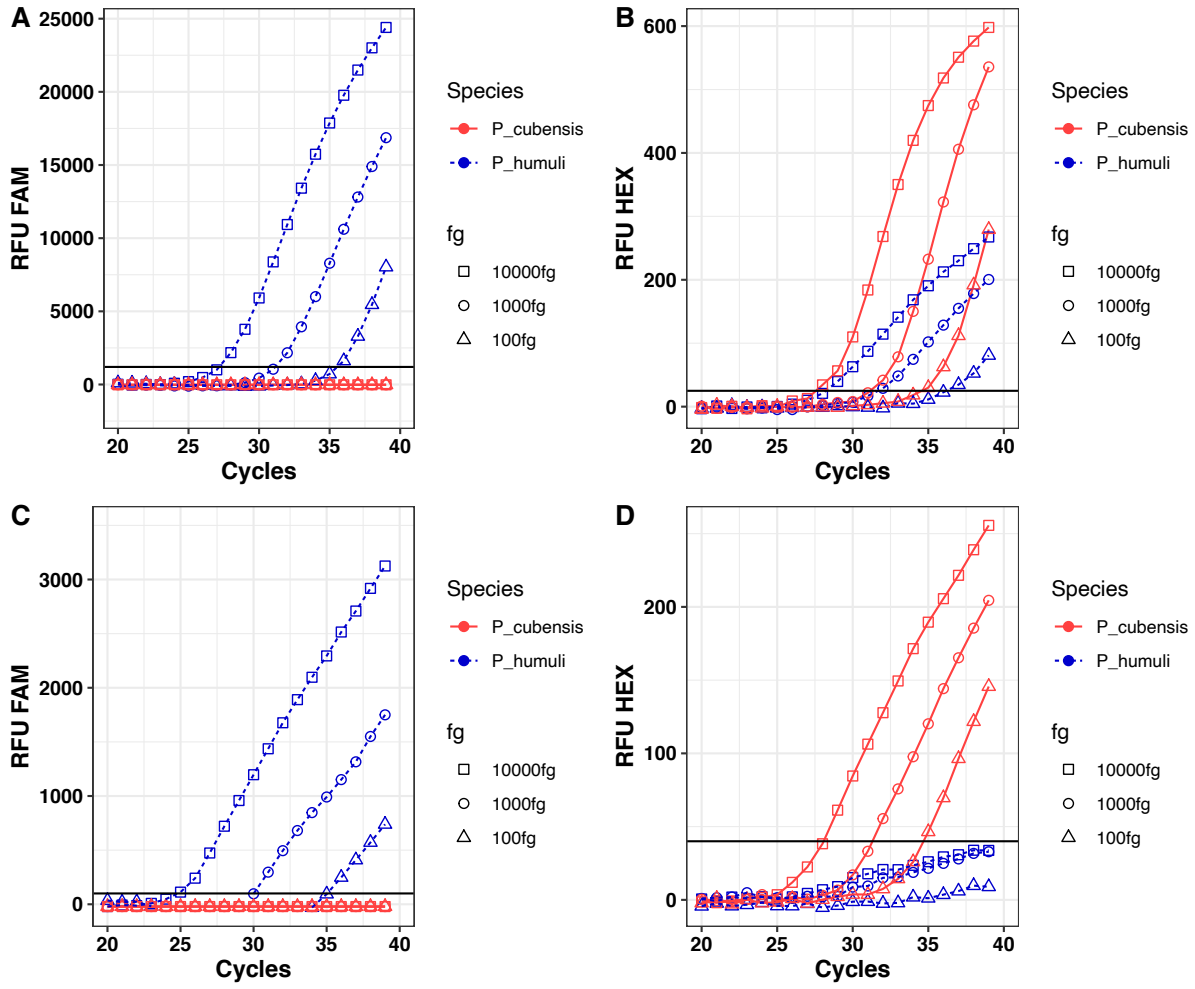

Supplementary Figure 2-S2. Amplification curves of *Pseudoperonospora cubensis* and *P. humuli* DNA using qPCR. **A.** Amplification curves of *P. cubensis* and *P. humuli* DNA with different concentrations using the LNA probe HUMprobeSNP105 and the Prime-Time Gene Expression Master Mix (IDT, Skokie, IL). **B.** Amplification curves of *P. cubensis* and *P. humuli* DNA with different concentrations using the LNA probe CUBprobeSNP105 and the Prime-Time Gene Expression Master Mix. **C.** Amplification curves of *P. cubensis* and *P. humuli* DNA with different concentrations using the LNA probe HUMprobeSNP105 and the IQ Supermix (Bio-rad, Hercules, CA). **D.** Amplification curves of *P. cubensis* and *P. humuli* DNA with different concentrations using the LNA probe CUBprobeSNP105 and the IQ Supermix.

LITERATURE CITED

LITERATURE CITED

Adams, M. L., and Quesada-Ocampo, L. M. (2014) Evaluation of fungicides for control of downy mildew on cucumber. Kinston 2013. Plant Dis Manag Rep 8: V240

Blum, M., Waldner, M., Olaya, G., Cohen, Y., Gisi, U., and Sierotzki, H. (2011) Resistance mechanism to carboxylic acid amide fungicides in the cucurbit downy mildew pathogen *Pseudoperonospora cubensis*. Pest Manag Sci 67: 1211–1214

Brzozowski, L., Holdsworth, W., and Mazourek, M. (2016) 'DMR-NY401': A new downy mildew–resistant slicing cucumber. HortScience 51: 1294–1296

Bustin, S. A., Benes, V., Garson, J.A., Hellemans, J., Huggett, J., Kubista, M., Mueller, R., Nolan, T., Pfaffl, M.W., Shipley, G.L., Vandesompele, J., and Wittwer, C. T (2009) The MIQE guidelines: minimum information for publication of quantitative real-time PCR experiments. Clin Chem 55: 611–622

Carisse, O., Tremblay, D.M., Lévesque, C.A., Gindro, K., Ward, P., and Houde, A. (2009) Development of a Taqman real-time PCR assay for quantification of airborne conidia of *Botrytis squamosa* and management of Botrytis leaf blight of onion. Phytopathology 99: 1273–1280

Cohen, Y., Van den Langenberg, K.M., Wehner, T.C, Ojiambo, P.S., Hausbeck, M, Quesada-Ocampo, L.M., Lebeda, A., Sierotzki, H., and Gisi, U. (2015) Resurgence of *Pseudoperonospora cubensis*: the causal agent of cucurbit downy mildew. Phytopathology 105: 998–1012

Cohen, Y., and Rotem, J. (1971) Dispersal and viability of sporangia of *Pseudoperonospora cubensis*. Trans Br Mycol Soc **57**: 67–74

Coley-Smith, J.R. (1962) Overwintering of hop downy mildew *Pseudoperonospora humuli* (Miy. and Tak.) Wilson. Ann Appl Biol 50: 235–243

Dhar, N., Mamo, B.E., Subbarao, K., Koike, S., Fox, A., Anchieta, A., and Klosterman, S.J. (2019) Measurements of aerial spore load by qPCR facilitates lettuce downy mildew risk advisement. Plant Dis 104: 82–93

Dung, J.K.S, Scott, J.C., Cheng, Q., Alderman, S.C., Kaur, N., Walenta, D.L., Frost, K.E., and Hamm, P.B. (2018) Detection and quantification of airborne *Claviceps purpurea* sensu lato ascospores from Hirst-type spore traps using real-time quantitative PCR. Plant Dis 102: 2487–2493

Ernest, E.G., Kee, W.E., and Everts, K.L. (2005) Evaluation of fungicides for control of downy mildew on pickling cucumber, Trial 2, 2005. Plant Dis Manag Rep 2: V066

Gent, D.H., Ocamb, C.M. (2009) Predicting infection risk of hop by *Pseudoperonospora humuli*. PhytopathologyTM 99: 1190–1198

Gent, D.H., Nelson, M.E., Farnsworth, J.L. and Grove, G.G. (2009), PCR detection of *Pseudoperonospora humuli* in air samples from hop yards. Plant Pathology, 58: 1081-1091.

Gevens, A.J., and Hausbeck, M.K. (2005) Control of downy mildew of cucumbers with fungicides, 2005. Plant Dis Manag Rep 2: V066

Granke, L.L., and Hausbeck, M.K. (2011) Dynamics of *Pseudoperonospora cubensis* sporangia in commercial cucurbit fields in Michigan. Plant Dis 95: 1392–1400

Granke, L.L., Morrice, J.J., and Hausbeck, M.K. (2013) Relationships between airborne *Pseudoperonospora cubensis* sporangia, environmental conditions, and cucumber downy mildew severity. Plant Dis 98: 674–681

Gugino, B.K., and Grove, T.L. (2016) Evaluation of selected fungicides and fungicide programs for managing downy mildew of cucumber, 2015. Plant Dis. Manag. Rep. 10: V072:

Hausbeck, M. K., and Linderman, S.D. (2014) Evaluation of fungicides for control of downy mildew of cucumber, 2013. Plant Dis Manag Rep 8: V304

Hausbeck, M., Brisco-McCann, E., Goldenhar, K., and Cook, A. (2017) Evaluation of fungicide programs for control of downy mildew of cucumber, 2016. Plant Dis Manag Reports 11: V063

Hausbeck, M.K., and Cortright, B. (2010) Evaluation of fungicides and application methods for control of downy mildew of cucumber, 2010. Plant Dis. Manag. Rep. V6:

Hausbeck, M.K., Perla, D.E., and Cook, A.J. (2019) Evaluation of single fungicide products for control of downy mildew of cucumber, 2018. Plant Dis Manag Reports 139: V13

Hausbeck, M.K. (2020) First cucumber downy mildew outbreak of 2020 confirmed in Berrien County. MSU Ext., https://www.canr.msu.edu/news/cucumber-downy-mildew-outbreak-of-2020

Hirst, J.M. (1952) An automatic volumetric spore trap. Annals of Applied Biology, 39, 259–265.

Holmes, G.J., Ojiambo, P.S., Hausbeck, M.K., Quesada-Ocampo, L., and Keinath, A.P. (2014) Resurgence of cucurbit downy mildew in the united states: a watershed event for research and extension. Plant Dis 99: 428–441

Hop growers of America (2019) 2018 Statistical report - hops. HGA Stat. Pack. - Revis., https://www.usahops.org/img/blog_pdf/168.pdf

Kanetis, L., Holmes, G.J, and Ojiambo, P.S. (2010) Survival of *Pseudoperonospora cubensis* sporangia exposed to solar radiation. Plant Pathol 59: 313–323

Keinath, A. P (2015) Utility of a cucumber plant bioassay to assess fungicide efficacy against *Pseudoperonospora cubensis*. Plant Dis 100: 490–499

Klosterman, S.J., Anchieta, A., McRoberts, N., Koike, S.T., Subbarao, K. V., Voglmayr, H., Choi, Y-J., Thines, M., and Martin, F.N. (2014) Coupling spore traps and quantitative PCR assays for detection of the downy mildew pathogens of spinach (*Peronospora effusa*) and beet (*P. schachtii*). Phytopathology 104: 1349–1359

Kunjeti, S.G., Anchieta, A., Martin, F.N., Choi, Y-J., Thines, M., Michelmore, R.W., Koike, S.T., Tsuchida, C., Mahaffee, W., Subbarao, K. V., Klosterman, S. J. (2016) Detection and quantification of *Bremia lactucae* by spore trapping and quantitative PCR. Phytopathology 106: 1426–1437

Lebeda, A., Cohen, Y. (2011) Cucurbit downy mildew (*Pseudoperonospora cubensis*)—biology, ecology, epidemiology, host-pathogen interaction and control. Eur J Plant Pathol 129, 157–192

Langston, D., Sanders, F.H. (2013) Evaluation of fungicides for control of downy mildew on cucumber in Georgia I, 2012. Plant Dis. Manag. Rep. 7: V108.

Lizotte, E., and Miles, T.D. (2020) Hop disease management in Michigan for 2020. MSU Ext., https://www.canr.msu.edu/news/managing-hop-downy-mildew-in-michigan

Michigan Department of Agriculture & Rural Development (2018) Michigan Agriculture Facts & Figures.
https://www.michigan.gov/documents/mdard/MI_Ag_Facts__Figures_474011_7.pdf

Mitchell, M.N., Ocamb, C.M., Grünwald, N.J., Mancino, L.E., and Gent, D.H. (2011) Genetic and pathogenic relatedness of Pseudoperonospora cubensis and P. humuli. Phytopathology 101: 805–818

Morinha, F., Magalhães, P. and Blanco, G. (2020), Different qPCR master mixes influence telomere primer binding within and between bird species. J Avian Biol, 51: doi:10.1111/jav.02352

Naegele, R. P., Quesada-Ocampo, L. M., Kurjan, J. D., Saude, C., and Hausbeck, M. K. (2016) Regional and temporal population structure of Pseudoperonospora cubensis in Michigan and Ontario. Phytopathology 106: 372–379

NOAA (2019) National Climate Report - May to August 2019.
https://www.ncdc.noaa.gov/sotc/national/201905

Ojiambo, P.S., Gent, D.H., Quesada-Ocampo, L.M., Hausbeck, M.K., and Holmes, G.J. (2015) Epidemiology and Population Biology of *Pseudoperonospora cubensis*: A Model System for Management of Downy Mildews. Annu Rev Phytopathol 53: 223–246

Ojiambo, P.S., and Holmes, G.J. (2010) Spatiotemporal spread of cucurbit downy mildew in the Eastern United States. Phytopathology 101: 451–461

Perla, D., Hausbeck, M.K., Cook, A. (2019) Evaluation of fungicide programs for control of downy mildew of cucumber, 2018. Plant Dis Manag Reports 147: V13

Quesada-Ocampo L.M., Granke, L.L., Olsen, J., Gutting, H.C., Runge, F., Thines, M., Lebeda, A., and Hausbeck, M.K. (2012) The genetic structure of *Pseudoperonospora cubensis* populations. Plant Dis 96: 1459–1470

Rahman, A., Standish, J., D'Arcangelo, K.N., Quesada-Ocampo, L.M. (2020) Clade-specific biosurveillance of *Pseudoperonospora cubensis* using spore traps for precision disease management of cucurbit downy mildew. Phytopathology. doi: 10.1094/PHYTO-06-20-0231-R

Reuveni, M., Eyal, H., Cohen, Y. (1980) Development of resistance to metalaxyl in *Pseudoperonospora cubensis.* Plant Dis 64: 1108–1109

Rogers, S.L., Atkins, S.D., and West, J.S. (2009) Detection and quantification of airborne inoculum of *Sclerotinia sclerotiorum* using quantitative PCR. Plant Pathol 58: 324–331

Royle, D.J. (1973) Quantitative relationships between infection by the hop downy mildew pathogen, *Pseudoperonospora hutnuli*, and weather and inoculum factors. Ann Appl Biol 73: 19–30

Runge, F., and Thines, M. (2011) Reevaluation of host specificity of the closely related species *Pseudoperonospora humuli* and *P. cubensis*. Plant Dis 96: 55–61

Salcedo, A., Hausbeck, M., Pigg, S., Quesada-Ocampo, L.M. (2020) Diagnostic Guide for Cucurbit Downy Mildew. Plant Heal Prog 21: 166–172

Summers, C., Adair, N., Gent, D., Mcgrath, M., and Smart, C. (2015) *Pseudoperonospora cubensis* and *P. humuli* detection using species-specific probes and high definition melt curve analysis. Can J Plant Pathol 37: 150605144651006

Thomas, A., Carbone, I., Choe, K., Quesada-Ocampo, L.M., and Ojiambo, P.S. (2017) Resurgence of cucurbit downy mildew in the United States: Insights from comparative genomic analysis of *Pseudoperonospora cubensis*. Ecol Evol 7: 6231–6246

Thomas, A., Neufeld, K.N., Seebold, K.W., Braun, C.A., Schwarz, M.R., and Ojiambo, P.S. (2018) Resistance to Fluopicolide and Propamocarb and baseline sensitivity to

Ethaboxam among isolates of *Pseudoperonospora cubensis* from the Eastern United States. Plant Dis 102: 1619–1626

Thornton, A.C, Adams, M.L., and Holmes, G.J. (2006) Evaluation of fungicides for control of downy mildew of cucumber I, 2006. Plant Dis Manag Rep 1: V122

USDA (2020) United States Department of Agriculture. 2019. Vegetables Annual Summary. https://usda-library-cornell-edu.proxy1.cl.msu.edu/concern/publications/02870v86p?locale=en

Withers, S., Gongora-Castillo, E., Gent, D., Thomas, A., Ojiambo, P.S., and Quesada-Ocampo, L.M. (2016) Using Next-Generation sequencing to develop molecular diagnostics for *Pseudoperonospora cubensis*, the cucurbit downy mildew pathogen. Phytopathology 106: 1105–1116

Zhu, S.S., Liu, X.L., Wang, Y., Wu, X.H., Liu, P.F., Li, J.Q., Yuan, S.K., and Si, N.G. (2007) Resistance of *Pseudoperonospora cubensis* to flumorph on cucumber in plastic houses. Plant Pathol 56: 967–975

CHAPTER III: OPTIMIZING SPORE TRAPS AND QUANTITATIVE PCR ASSAYS FOR THE MONITORING OF CUCURBIT DOWNY MILDEW.

ABSTRACT

Current management of *Pseudoperonospora cubensis*, the causal agent of cucurbit downy mildew (CDM), relies on an intensive fungicide program. In Michigan, CDM occurs annually due to an influx of airborne sporangia; timely alerts of airborne inoculum can assist growers in assessing the need to initiate fungicide sprays. The main objective of our research was to improve the detection and quantification of airborne concentrations of *P*. *cubensis* sporangia by adapting two qPCR-based assays to distinguish between *P. cubensis* clade I and II and *P. humuli* in spore trap samples. We also aim to evaluate the efficiency of Burkard and impaction spore traps for the detection airborne concentrations of *P. cubensis* sporangia. A new qPCR assay improved the specificity of *P. cubensis* detection and resulted in a better linear correlation between the number of sporangia observed using light microscopy and Cq values obtained from Burkard spore traps (R^2=0.6; p = 0.01). After two years of monitoring, *P. cubensis* clade II and *P. humuli* DNA were detected in air samples collected in commercial cucumber fields, while *P. cubensis* clade I DNA was not detected. *P. cubensis* clade II DNA was detected in spore trap samples >2 days before CDM symptoms were first observed in cucumber fields (August), while *P. humuli* DNA was only detected early in the growing season (May and June). *P. cubensis* clade I DNA was not detected in air samples before or after the disease onset in cucumber fields. Additionally, the probability for *P. cubensis* detection in Burkard spore trap samples was higher compared to impaction spore trap samples with approximately the same number of sporangia, suggesting that the efficiency of recovery of sporangia by Burkard spore traps exceeds the recovery of impaction spore traps. Our study identified

an improved methodology to monitor the airborne concentrations of *Pseudoperonospora spp.* sporangia using spore traps coupled with qPCR. This methodology could be used as part of a CDM risk advisory system to time fungicide applications that protect cucurbit crops in Michigan.

INTRODUCTION

Cucurbit downy mildew (CDM), caused by the obligate oomycete *Pseudoperonospora cubensis*, incites foliar blighting of several Cucurbitaceae species worldwide (Mitchell et al., 2011). Symptoms include irregular to angular chlorotic leaf lesions and pathogen sporulation on the lower leaf surface (Cohen et al., 2015) leading to premature defoliation, stunted plants and reduced yield, especially in cucumber (Reuveni et al., 1980; Adams et al., 2019; Hausbeck et al., 2019; Perla et al., 2019). In the U.S., *P. cubensis* overwinters on living hosts in regions that do not experience a frost or in heated greenhouses (Ojiambo et al., 2011; Naegele et al., 2016). The pathogen's airborne sporangia disperse to northern U.S. growing regions annually from overwintering sources (Ojiambo & Holmes, 2010; Ojiambo et al., 2015).

Michigan is the number one producer of pickling cucumbers and squash in the U.S. (USDA, 2020), but since 2005 CDM has threatened cucumber production annually in the state. In the absence of CDM resistant cucumber cultivars, growers rely on intensive fungicide spray programs to limit disease at a significant cost (Savory et al., 2011), however, *P. cubensis* has developed resistance to key fungicides (Zhu et al., 2007; Blum et al., 2011; Holmes et al., 2014; Keinath, 2015). For more than 10 years, information on the sporangial concentrations of *P. cubensis* derived from Burkard spore

traps has been used in Michigan as a decision-making tool to initiate fungicide sprays to control CDM (Granke and Hausbeck, 2011; Granke et al., 2013).

Burkard and impaction spore traps are the most widely used devices for atmospheric sampling in plant pathology (Frenz, 1999). The Burkard spore trap has been used in aerobiological studies for over 60 years (West and Kimber, 2015) and operates by drawing air into a collection chamber containing a reel mounted onto a clockwork mechanism. Spores and other air-borne particles are impacted onto a greased tape covering the reel (Burkard Manufacturing Co. Ltd., U.K.) that rotates past the intake orifice at 2 mm/hr for 7 days. The impaction spore trap, also known as a rotating-arm spore sampler or rotorod spore trap, has become popular for the early detection of airborne plant pathogens (Jackson and Bayliss, 2011; Klosterman et al., 2014; Fall et al., 2015; Choudhury et al., 2016a; Kunjeti et al., 2016). This device includes rods coated with adhesive material which spin at a standard rate in a rotating arm, impacting and collecting airborne particles (TSE Systems, Chesterfield, MO). However, frequent monitoring is required to obtain accurate estimations of inoculum per unit of time (i.e. an hour or day). Although Burkard spore traps are robust and highly autonomous, impaction spore traps can be more cost-effective and grower friendly (i.e. easier to use) (Jackson and Bayliss, 2011; Choudhury et al., 2016a). The efficiency of impaction spore traps to monitor *P. cubensis* sporangia in comparison to Burkard spore traps has not yet been assessed under field conditions.

While the spore traps provide quantitative data on airborne sporangial concentrations, the processing and microscopic examination of the tapes and/or rods is time consuming and can result in misidentification due to the morphological similarities between species (Dung et al., 2018). A qPCR assay was designed for molecular

differentiation of the morphologically identical sporangia of *P. cubensis* and *Pseudoperonospora humuli*, the causal agent of hop downy mildew (HDM) (Summers et al., 2015a). The detection of each species is based on the recognition of a conserved single nucleotide polymorphism (SNP) in the cytochrome oxidase subunit II (*cox2*) gene. However, quantification of sporangia using this assay was compromised in spore trap samples containing DNA from both species due to the high similarities between them in the region targeted (Bello et al., 2020).

To further improve the specificity and facilitate the quantification of *P. cubensis* and *P. humuli* sporangia, a new qPCR assay targeting unique sequences in the pathogens' mitochondrial genome was developed that also enables detection and differentiation of both species in a single reaction (Crandall, 2020). This assay can also differentiate between *P. cubensis* clades I and II. Isolates belonging to these two clades are host-adapted at the cucurbit species level (Summers et al., 2015b; Thomas et al., 2017a; Wallace et al., 2020). Clade I isolates are recovered more frequently from commercial varieties of *Cucurbita pepo, C. moschata, C. maxima,* and *Citrullus lanatus* and clade II isolates are associated more frequently with commercial varieties within the *Cucumis* genus (Wallace et al., 2020). Accurate identification of airborne sporangia of *P. humuli* and *P. cubensis* (clades I and II) is critical to monitor the pathogen's arrival into Michigan's growing regions so as to inform fungicide applications. This new multiplex qPCR assay has the potential to improve quantification of airborne sporangia in spore trap samples without sacrificing accuracy.

The main objective of our research was to improve the detection and quantification of airborne concentrations of *Pseudoperonospora* spp. sporangia by adapting two qPCR-based assays to distinguish between *P. cubensis* and *P. humuli* in

spore trap samples collected in the field. The specific detection and monitoring of sporangia from each clade of *P. cubensis* (clade I and II) in commercial cucumber fields was of particular interest. Additionally, we also aimed to evaluate Burkard and impaction spore traps for their efficiency in detecting airborne concentrations of *P. cubensis* sporangia.

MATERIALS AND METHODS

***Pseudoperonospora* isolates.** To perform *in vitro* evaluations, a single-lesion isolate of *P. cubensis* clade II (CDM23 cucumber) and clade I (CDM-YUM squash), and a single-spike isolate of *P. humuli* (isolate HDM19) were maintained as described by Bello et al. (2020). Sporangia from each isolate were rinsed from the host tissue into falcon tube with distilled water and the sporangial suspensions were concentrated by centrifugation (5424R centrifuge, Eppendorf, New York, NY) at 14.000 rpm for 5 min. The resulting pellet was homogenized in impact-resistant 2mL tubes (Lysing Matrix H, MP Biomedicals, Irvine, CA) using a TissueLyser II (Qiagen, Valencia, CA) for 4 min at 30 Hz. DNA was extracted using a NucleoSpin Plant II isolation kit (Macherey-Nagel, Bethlehem, PA) following manufacturer's instructions and the DNA concentration was determined using the Qubit double-stranded DNA High Sensitivity Assay Kit (Life Technologies, Carlsbad, CA).

Multiplexing of qPCR assays. All qPCR experiments were conducted using the protocols described by Bello et al. (2020) and Crandall et al. (2020) referred to hereafter as protocol A and B, respectively. All qPCR reactions were manually assembled into 96-well white plates (Bio-rad MLL9651) containing 10 µl of the Prime-Time Gene Expression Master Mix (IDT, Skokie, IL), 2µl of template DNA, and 8 µl of a solution

containing primers, probes and internal controls as described in Table 3-1. Negative control reactions lacking a DNA template were included in each plate run. The qPCR protocols were run on a CFX 96 Touch qPCR system (Bio-rad); the cycling conditions are summarized in Table 3-1. Two technical replicates of each sample were run and the average Cq and standard deviation were calculated using Bio-rad CFX Manager software (version 3.1).

Specificity and sensitivity of qPCR assays. The sensitivity and specificity of the qPCR protocols were tested using ten-fold dilutions of genomic DNA from two independent DNA extractions of each isolate (CDM23, CDM-YUM and HDM19). Three technical replicates of each sample dilution were tested using both qPCR protocols (Table 3-1) and the average C_q values with standard deviation were calculated using Bio-rad CFX Manager software. Mean C_q values were plotted against the $\log_{10}$ of template DNA concentrations and used to generate standard curves. To assess the specificity of the qPCR protocol B, samples of mixed DNA from the three isolates were evaluated to determine whether the assay could detect *P. cubensis* (clades 1 and 2) and *P. humuli*. Ten-fold dilutions of genomic DNA from each isolate were mixed in varying concentrations (Table 3-2) and subjected to qPCR. Three technical replicates of each mixture were run and the average Cq and standard deviations were calculated using Bio-rad CFX Manager software.

To evaluate the relationship between sporangial concentrations and the Cq values from the multiplexed qPCR assays *in vitro*, dilution series containing 1, 3, 5, 10, 25 and 50 sporangia were prepared as described by Crandall et al. (2020) and regressed against the corresponding Cq values of each assay. There were fifteen replicates each for the sporangial counts of 1, 3, and 5 and eight replicates each for

sporangial counts of 10, 25, and 50. DNA was extracted using a NucleoSpin Plant II isolation kit (Macherey-Nagel, Bethlehem, PA) following manufacturer's instructions.

Collection and qPCR evaluation of field samples. Airborne sporangial concentrations were monitored during the growing season (May to August) in 2018 and 2019 using Burkard and impaction spore traps. Each year, a Burkard spore trap and an impaction spore trap were placed side by side approximately 20 m from commercial cucumber fields in the Michigan counties of Muskegon, Allegan, Bay, and Saginaw (Fig. 3-1). In 2019, a cucumber research plot (0.25 ha) at the Michigan State University (MSU) Plant Pathology Farm located in Ingham County was also monitored using a Burkard spore trap and impaction spore trap. An abandoned hop research yard (0.25 ha) with basal shoots infected by *P. humuli* was located 200 m from the cucumber research plot. A Burkard spore trap, only, was placed in a commercial hop yard in Berrien County in 2019 (Fig. 3-1).

Burkard spore traps were set to an approximate airflow rate of 10 l/min. The reel of each spore trap was covered with a melinex tape coated with an adhesive mixture of petroleum jelly and paraffin (9:1 wt/wt) dissolved in sufficient toluene to provide the desired thickness. The tape was removed weekly and cut longitudinally along the center line in two subsection of 9 x 336 mm each (Rogers et al., 2009). The two resulting sub-section were processed as described by Bello et al. (2020). Briefly, the first section was cut at 24-hr segments (48-mm lengths) and subjected to DNA extraction. The second section was also cut at 24-h segments and screened using light microscopy to estimate the number of sporangia captured per day (Granke et al., 2013).

The impaction traps were constructed using a motor (RF-500TB-10750, Mabuchi) that spun at 2700 rpm when powered by a 12-V marine battery. Each

impaction trap was mounted onto a 1.5-m tower that holds the collection rods 1 m above the ground. The impaction traps operated continuously throughout each growing season (May to August), and the greased-coated rods (1.2-by-3.5-mm stainless steel) were collected four times per week at intervals of 24, 24, 24, 96 h (Table 3-3) (Choudhury et al., 2016a). Samples from Burkard and impaction traps were carefully placed into impact-resistant 2mL tubes (Lysing Matrix H, MP Biomedicals) containing 100 µl of PL1 buffer (Macherey-Nagel, Bethlehem, PA). The samples were homogenized using a TissueLyser II (Qiagen, Valencia, CA) for 4 min at 30 Hz and DNA was extracted using NucleoSpin Plant II isolation kit (Macherey-Nagel, Bethlehem, PA) following manufacturer's instructions. Subsequently, 2 µl of the extraction products were evaluated using qPCR. All 2019 samples were assessed using both A and B protocols, however, all the samples collected during 2018 were evaluated using only protocol A.

Correlating C_q values with sporangial counts of field samples. Linear regression using R (version 3.6.1) was used to assess the relationship between the Cq values of each qPCR assay and the number of sporangia in trap samples. The Cq values of each qPCR assay were regressed against the number of sporangia quantified using light microscopy in the second half of the tape of the Burkard spore traps. The linear equation obtained from the regression analysis (Table 3-4) was used to determine the corresponding number of sporangia expressed as N^{Cq} where N represents the number of sporangia calculated using Cq values.

Additionally, binary logistic regression was used to model the relationship between the number of airborne sporangia and the probability of a positive detection in samples collected by Burkard or impaction spore traps. The $\log_{10}$ number of sporangia

quantified in the first half of the Burkard spore traps were regressed with the results from protocol A obtained from trap samples as a categorical (binary) variable. The Cq values of protocol A were categorized using a threshold Cq value of 35.5 (Cq>35.5 negative and Cq≤35.5 positive). The regression was performed independently using the qPCR results from each spore trap separately (i.e. Burkard or impaction). We used this approach to compare between traps and estimate the probability of a positive detection of *P. cubensis* DNA given an approximate number of sporangia in the air. For example, the probability of a positive detection in impaction samples given an estimated number of 10 sporangia in air samples. Assuming that $\boldsymbol{p}$ is the probability of a positive detection by the qPCR, the logistic regression line is described by Equation 1.

Equation 1: Binary logistic regression used to model the relationship between the number of airborne sporangia and the probability of a positive detection in spore trap samples.

$$\boldsymbol{log_{10}\left(\frac{p}{1-p}\right) = \beta_0 + \beta_1 * log_{10}(X_1)}$$

$\boldsymbol{p}$ is the probability of a positive detection. $\boldsymbol{\beta_0}$ to $\boldsymbol{\beta_1}$ are parameters.

RESULTS

Sensitivity and specificity of qPCR assays. Using ten-fold dilutions of genomic DNA, the probes of both protocols detected *P. humuli* and each clade of *P. cubensis* within total DNA template amounts between 100 to 1000 fg ($R^2 \geq 0.99$; $p < 0.05$) (Fig. 3-2 and 3-3). The assays are intended to be used to quantify sporangia in environmental samples, thus, further testing outside of these template amounts was not done. Both protocols detected 100 fg of each taxon with average Cq values below 37.5 as reported

previously (Bello et al., 2020; Crandall et al., 2020; Summers et al. 2015). Most samples with concentrations below 100 fg were not detected reliably (>95% of the times tested), thus, 100 fg of template DNA was considered as the lower limit of detection (LOD) of the qPCR assays for both species (Figs. 3-2 and 3-3).

In singleplex reactions with DNA recovered from isolated sporangia of each *Pseudoperonospora* taxa, unspecific amplification was observed using protocol A (Fig. 3-2 A). On the contrary, singleplex reactions of protocol B using DNA recovered from isolated sporangia allowed the specific detection of each taxon and background amplification of nontarget taxa was not observed (Fig. 3-3 A, B, C). Multiplex reactions containing all the primers and probes of each qPCR protocol yielded the same results.

Small, yet significant differences in the Cq values of mixed and unmixed DNA samples assessed using protocol A were previously reported (Bello et al., 2020). Similar results were also observed using protocol B (Table 3-2). The presence of DNA from a second non-target taxa slightly affected the sensitivity of the probes Pcub2 and Pcub_RFLP_qP1 designed for the detection of *P. cubensis* clades II and I, respectively (Table 3-1). When 100 fg of *P. cubensis* clade II DNA were mixed in a 1:1 or 1:100 ratio with DNA from a second taxon, no amplification or a significant increase in the Cq value was observed with the Pcub2 probe. Similarly, when 100 fg of *P. cubensis* clade I DNA were mixed in a 1:100 ratio with DNA from a second taxon, no amplification was observed with the probe Pcub_RFLP_qP1 (Table 3-2).

The regression between sporangial concentrations and the Cq values of both assays (A and B) demonstrated reliable pathogen detection with as few as three sporangia for each taxon (Fig. 3-11 and 3-12). Amplification results of DNA from a

single sporangium were inconsistent and outside of the linear relationship between sporangial counts and C_q values.

Correlation between Cq values and sporangial counts of Burkard spore trap samples. DNA of *P. cubensis* clade II and *P. humuli* was detected using both qPCR protocols on field samples containing fewer than 10 sporangia (Fig. 3-4). Regression analysis indicated that the number of sporangia on the second half of the tape of field samples (quantified using light microscopy) explained 37% and 60% of the variation in the C_q values of *P. cubensis* clade II DNA obtained using protocols A and B, respectively (Fig. 3-4 A). Significant differences between the protocols were detected using regression analysis ($p<2.24e-05$, Table 3-4) with a more inclined regression line observed for protocol B (Fig. 3-4 A). Similarly, the number of sporangia on the second half of the tape explained 27% and 30% of the variation in the C_q values of *P. humuli* DNA obtained using protocols A and B, respectively (Fig. 3-4 B). No significant differences between the protocols were detected ($P=0.26$, Table 3-4) using regression analysis. β estimates of equations 2 and 3 that describe the relationship between the Cq values of each qPCR assay and the sporangial numbers of each species are summarized in Table 3-4.

Equation 2: Regression line that describes the relationship between Cq values and sporangial numbers of *Pseudoperonospora cubensis* clade II.

$$\boldsymbol{Cq_{P.cub\,2} = \beta_0 - \beta_1\, log_{10}(Sporangia) + \beta_2\, log_{10}(qPCR) \beta_3\, log_{10}(Sporangia)(qPCR)}$$

The values of the β_0, β_1, β_2, β_3 parameters are summarized in Table 3-4. The qPCR assay is express as a binary variable: qPCR assay A = 1, qPCR assay B = 0.

Equation 3: Regression line that describes the relationship between Cq values and sporangial numbers of *Pseudoperonospora humuli.*

$$Cq_{P.hu} = \beta_0 - \beta_1 \, log_{10}(Sporangia)).$$

The values of the β_0 to β_1 parameters are summarized in Table 3-4.

Logistic regression. After categorizing the qPCR results of both spore traps (positive/negative) a higher number of impaction samples were negative compared to the Burkard samples (Fig. 3-5 C, D). This occurred most frequently when the atmospheric concentration of sporangia was below 100 sporangia/day as estimated using microscopic analysis of the Burkard tape. Using a logistic regression to model the relationship between the number of atmospheric sporangia and the probability of detection, higher estimates were obtained for the Burkard traps (Table 3-5). Therefore, a higher probability of *P. cubensis* detection given any number of sporangia was estimated for Burkard trap samples (Figs. 3-5 A, B). A probability of detection above 90% was obtained for Burkard and impaction trap samples with an approximate number of sporangia equal to 15 and 120 sporangia, respectively.

Assessment of field samples using light microscopy and qPCR. During 2018 and 2019, an average of 15 reels of Burkard spore traps were collected from May to August in all the locations monitored (Table 3-3, Figs. 3-5 to 3-10). The tape from each reel was divided by days for microscopic and qPCR analysis generating a total of 105 to 112 samples of 24 h per location each year (Table 3-3, Figs. 3-5 to 3-10). Similarly, during both years a total of 544 impaction trap samples were collected from May to August among all the locations monitored. An average of 45 and 15 impaction

trap samples per location were collected every 24 and 96 h, respectively (Table 3-3, Figs. 3-5 to 3-10). The qPCR assays detected *Pseudoperonospora* spp. DNA on 41.84% of the 24 h-samples collected using Burkard spore traps (Table 3-3). Similarly, detection of *Pseudoperonospora* spp. DNA occurred in 23.35 and 29.81% of the impaction trap samples collected every 24 and 96h, respectively (Table 3-3).

In 2018, *Pseudoperonospora* spp. sporangia were first observed in May or June across the monitored cucumber fields (Figs. 3-6 and 3-7). During May, June and July, the number of sporangia observed in the tape of Burkard spore traps remained below 10 sporangia/day and *P. cubensis* clade II DNA was detected with Cq values above 31 (Fig. 3-6 and 3-7). This Cq value corresponds to $<3^{Cq}$ sporangia according to the regression line that describes the relationship between Cq values and sporangial numbers (Equation 2 and Table 3-4). Using light microscopy, 10 to 40 sporangia/day were detected in June in Bay Co. (22, 27 June) and Allegan Co. (6, 7, 24 June) and were identified as *P. humuli* using qPCR with Cq values between 31 and 27 (corresponding to 3^{Cq} to 15^{Cq} sporangia) (Figs. 3-6 B and 3-7 A). In all locations, the number of airborne *Pseudoperonospora* spp. sporangia observed in the tape of the Burkard tape increased during the last week of July and reached a maximum in the second or third week of August. During this time, *P. cubensis* clade II DNA was regularly detected in all fields with Cq values that range between 31 and 22 (corresponding to 3^{Cq} and 1200^{Cq} sporangia) but *P. humuli* was not detected (Figs. 3-6 and 3-7). In 2018, CDM symptoms were detected in August for each monitored cucumber field, after 12 to 40 sporangia/day were observed in the Burkard spore trap tape. Correspondingly, before symptoms were observed in the fields, *P. cubensis* clade

II detection using qPCR occurred one to seven days earlier with Cq values below 31 (equivalent to $>3^{Cq}$ sporangia) (Figs. 3-6 and 3-7).

Similar results were also obtained after the evaluation of impaction trap samples using qPCR in 2018. However, when the number of sporangia per day was low (<20 sporangia/day), pathogen detection in impaction trap samples using qPCR was less consistent. For instance, 1 to 20 *P. humuli* sporangia were observed in the first half of the Burkard spore trap tape in June (Bay and Allegan Counties) and detected in the second half using qPCR, but *P. humuli* detection did not occur in the impaction trap samples of the same dates (Figs. 3-6B and 3-7A). Similarly, before CDM symptoms were observed, *P. cubensis* DNA was consistently detected in Burkard samples in all the fields monitored, but it was only detected in impaction trap samples in Muskegon and Allegan Counties. (Figs. 3-6 A and 3-7 A). Using the Burkard spore trap, *P. cubensis* clade II DNA was detected with Cq values below 31 approximately 10 days before CDM symptoms were observed in the field (Figs. 3-6 and 3-7). On the other hand, *P. cubensis* clade II DNA was detected in impaction trap samples approximately 7 days before symptoms were observed in the field only in Muskegon and Allegan Counties. (Figs. 3-6 and 3-7, Table 3-6).

In 2019, the number of sporangia observed in Burkard samples from May to July were generally below 10 sporangia/day, but exceptions occurred in May and/or June in Muskegon, Allegan, Saginaw, Ingham and Berrien Counties where daily counts reached values between 10 to 40 sporangia (Figs. 3-8, 3-9 and 3-10). From May to July, *P. cubensis* clade II DNA was occasionally detected with Cq values above 36 (corresponding to $<3^{Cq}$ sporangia) in all fields monitored. When sporangial numbers were above 10 sporangia/day, the Cq values for *P. humuli* detection reached values

between 31 and 25. These Cq values correspond to >3^{Cq} and 50 ^{Cq} sporangia according to the regression line that describes the relationship between Cq values and sporangial numbers (Equation 2 and Table 3-4). Most Cq values for *P. humuli* detection below 31 were detected only during June, when the highest numbers of sporangia (>40) were observed using light microscopy.

In the commercial cucumber fields monitored, the concentration of *Pseudoperonospora* spp. sporangia estimated using light microcopy increased during August but did not reach the numbers observed in 2018 (Figs. 3-8 and 3-9). At these locations, CDM symptoms were detected during the third or fourth week of August. More regular detection of *P. cubensis* clade II DNA in Burkard trap samples with Cq values between 31 and 20 (corresponding to 3^{Cq} to 400^{Cq} sporangia) occurred after the observation of CDM symptoms. *P. cubensis* detection using qPCR before CDM symptoms were observed in the cucumber fields occurred one two seven days earlier with Cq values between 36 and 30 (corresponding >3^{Cq} to 10^{Cq} sporangia) (Figs. 3-8 and 3-9). On the other hand*, P. humuli* DNA was detected almost every day from May to August in the commercial hop yard (Fig. 3-10 B) and from May to July in the cucumber research plot (Fig. 3-10 A). At these two locations, concentrations between 10 and 40 sporangia were observed from the Burkard trap tapes during May and June and Cq values between 31 and 23 (corresponding to >3^{Cq} to 100^{Cq} sporangia) were registered (Fig. 3-10).

The monitoring of *Pseudoperonospora* spp. using impaction trap samples in the commercial cucumber fields had similar results to those of the Burkard spore traps in 2019 (Fig. 3-8, 3-9 and 3-10). However, when atmospheric concentrations of *P. cubensis* sporangia were below 10 sporangia/day (estimated with the aid of a light

microscope), DNA detection occurred less frequently in samples collected by impaction spore traps compared to the Burkard spore traps. Using qPCR, *P. cubensis* was detected in samples from both traps approximately two weeks before symptoms were observed in the cucumber fields monitored in Muskegon, Allegan and Saginaw counties. Only in Bay county, *P. cubensis* was not detected two weeks before symptoms developed in impaction trap samples (Table 3-6). Generally*, P. cubensis* detection in 2019 occurred with higher Cq values compared to 2018.

DISCUSSION

Early detection and quantification of airborne *P. cubensis* sporangia could improve the timing of fungicide initiation in Michigan as the pathogen is reintroduced to northern U.S. production regions each year (Bello et al., 2020). The Burkard spore traps have been used in the state for this purpose since 2008, however, the inability to distinguish between the morphologically identical sporangia of *P. humuli* and *P. cubensis* has been a significant shortcoming. Using an improved qPCR assay (Crandall et al., 2020), we were able to distinguish between three host-adapted *Pseudoperonospora* taxa in spore trap samples: *P. humuli*, *P. cubensis* clade I, and *P. cubensis* clade II. During two years of monitoring using Burkard and impaction spore traps coupled with qPCR in commercial cucumber fields, *P. cubensis* clade II sporangia were detected 2 to 10 days before CDM symptoms were observed. Both spore traps recorded similar trends in the airborne concentration of *P. humuli* and *P. cubensis* (clade I and II) sporangia, however, in our study, the Burkard spore trap was a more efficient instrument for detecting *P. cubensis* sporangia.

The multiplex qPCR assay developed by Crandall et al. (2020) that targets the open reading frames (*orf* 374, *orf* 367, *orf* 329) in the mitochondrial genome of each taxon provided high specificity for detecting DNA of *P. humuli* and each clade of *P. cubensis* (Crandall et al., 2020). This qPCR assay allowed us to estimate the concentrations of *P. cubensis* and *P. humuli* sporangia in Burkard and impaction spore trap field samples. The new multiplex qPCR assay had the same sensitivity of the qPCR assay developed by Summers et al. (2015), which was also developed to target a mitochondrial DNA region. Both assays detected *P. cubensis* and *P. humuli* DNA at amounts ranging from 100-1000 fg *in vitro* and were equally sensitive to a qPCR assay targeting a nuclear DNA region (Rahman et al., 2020). This high sensitivity was validated with the detection of less than 10 sporangia of each species in field spore trap samples. *In vitro*, samples containing three sporangia of each clade were reliably detected (Crandall et al., 2020) using these qPCR assays. Comparatively, the qPCR assay that targets the single-copy nuclear gene c255.3e7 showed a detection limit of 10 sporangia (Rahman et al., 2020). Additionally, the detection of each taxon without cross reactivity in samples containing mixed DNA of *P. humuli* and either clade of *P. cubensis* validated the high specificity of the assay developed by Crandall et al. (2020). This improved specificity was possible because the primers and probes of this new qPCR assay target more polymorphic regions in the mitochondrial genome compared to the single nucleotide polymorphism used for differentiation in the assay developed by Summer et al. (2015).

Improving the specificity also resulted in an increased linear correlation between the number of *P. cubensis* sporangia quantified with the aid of a light microscope and the Cq values of the qPCR (R^2=0.6). We used the equation that describes this

relationship to calculate the number of sporangia based on Cq values; however, the standard error of the β estimates used in this equation suggests a low precision for the quantification of sporangia using qPCR in spore trap samples. Multiple factors such as high variation during DNA extraction (Summers et al., 2015a), user variation during qPCR, and the multicopy nature of the target mitochondrial genes (González-Domínguez et al., 2020) could explain these results. The number of mitochondria can vary greatly among cells (O'Hara et al., 2019) reducing the precision for the quantification of cells using qPCR assays that target mitochondrial genes, however, the additional number of mitochondria per cell can increase the ability to detect low concentrations of sporangia. The more precise the assay (i.e. regression model) the closer predictions are to the observed number of sporangia. In this study, the use of Cq values to predict the number of sporangia resulted in misestimates compared to the quantification using light microscopy. Single-copy nuclear genes are thought to offer more precision for cell quantification compared to mitochondrial genes. However, the correlation of Cq values obtained from the amplification of the single-copy nuclear gene c255.3e7 with sporangial numbers revealed a standard deviation across more than three amplification cycles for samples with the same number of sporangia (Rahman et al., 2020). Similar results were obtained using the mitochondrial genes *orf* 374, *orf* 367and *orf* 329 (Crandall et al., 2020) suggesting that the precision for cell quantification using qPCR is not significantly increased with the utilization of nuclear genes as amplification targets.

During the two years of monitoring in commercial cucumber fields in Michigan, *P. humuli* detection occurred early in the growing season. This was expected because hop downy mildew is prevalent in the state (Higgins et al., 2020; Lizotte et al., 2020) and the

pathogen overwinters in dormant hop crowns, growing into expanding basal shoots in the spring (Coley-Smith, 1962). Similarly, detection of *P. cubensis* clade II occurred as expected because airborne sporangia are dispersed every year from overwintering sources resulting in CDM outbreaks in cucumber production regions of the upper Midwest (Ojiambo et al., 2011; Naegele et al., 2016). However, *P. cubensis* clade I was not detected in the 980 Burkard and 544 impaction spore trap samples that were collected over the two years of sampling from May to August. The absence of *P. cubensis* clade I sporangia in the air samples collected at the monitored cucumber fields may be due to the reduced number of crops planted in the state that are known to be hosts of this clade (i.e. *C. pepo, C. moschata, C. maxima, and C. lanatus*) (Wallace et al., 2020). Approximately 6000 ha of *C. maxima* (pumpkin), *C. pepo* (squash). *C. moschata* (butternut squash) and *C. lanatus* (watermelon) are planted in Michigan, compared to the more than 15000 ha of *C. sativus* (cucumber) planted in the state every year (USDA, 2020).

In North Carolina, the hectares of cucumber planted annually are also greater compared than those planted with other cucurbits; clade I was consistently detected using spore traps in the fall (September and October), while clade II was detected in the summer and fall (Rahman et al., 2020). In our study, we report on the airborne concentration of *P. cubensis* sporangia through August and most of the cucumber acreage is harvested by this time. In Michigan, the foliage of pumpkins and hard squash during September and October begins to senesce and is compromised by powdery mildew; CDM is rarely reported on these crops in the state. Determining if sporangia from both clades are dispersed to the Great Lakes cucurbit growing regions during September to October remains to be seen by future studies. *P. cubensis* clade I was not

detected in North Carolina and Michigan during the summer probably due to the total area planted to hosts susceptible to this clade. In the absence of airborne *P. cubensis* clade I sporangia, an intensive fungicide program for CDM may be unnecessary in non-cucumber hosts. Timely regional information on the atmospheric concentrations of each clade of *P. cubensis* could inform control measures to minimize the negative impact of CDM across different cucurbits.

This information could be used as a decision-making tool to initiate fungicide sprays to protect susceptible crops, as it is used in other crop production systems (Carisse et al., 2009; Fall et al., 2015; Dhar et al., 2019; Van der Heyden et al., 2020). In lettuce, a threshold Cq value of 24, equivalent to 324 *Bremia lactucae* sporangia/day, is used to determine whether fungicides should be applied. This approach reduced the number of fungicide applications to control downy mildew in small lettuce plots without a significant increase in disease incidence (Dhar et al., 2019). Similarly, in our study, CDM symptoms were observed after airborne sporangial concentrations exceeded 10-15 sporangia/day (estimated using light microscopy) or Cq values between 33 to 30 (qPCR assay B) were detected in Burkard spore trap samples. This suggests that the critical concentration to trigger fungicide sprays against CDM could be close to these numbers. However, further research is required to better understand the interaction between sporangial concentrations, environmental conditions, and symptom development (Fall et al., 2015), which could ultimately lead to the establishment of spore concentration thresholds to trigger fungicide application.

Accurate sampling of low inoculum loads and real-time monitoring is critical to develop a biosurveillance system that accurately assesses the risk of CDM in cucurbits. Burkard and impaction spore traps are the most widely used devices for atmospheric

sampling in plant pathology (Frenz, 1999) and have played a significant role in epidemiological studies in horticultural and agricultural settings (Granke et al., 2013; Choudhury et al., 2016a; Carisse et al., 2017; Wyka et al., 2017). They have also been used to accelerate the detection of airborne plant pathogens (Jackson and Bayliss, 2011) prior to symptom development (Villari et al., 2016; Thiessen et al., 2017; Dung et al., 2018; Dhar et al., 2019). However, Burkard and impaction spore traps had not been used side by side to monitor *Pseudoperonospora* spp. sporangia. After two years of monitoring, our results suggest that the Burkard spore traps are a more efficient device detecting airborne sporangia at low concentrations (<100 sporangia/day). This is consistent with theoretical expectations that impaction spore traps are likely to offer lower particle recoveries than Burkard spore traps (Frenz, 1999).

We found that the probability of *P. cubensis* detection is above 90% for Burkard and impaction samples that contain approximately 15 and 120 sporangia, respectively. These results indicate that Burkard spore traps can collect at least eight times (120/15) more sporangia than impaction spore traps at the conditions tested. The difference in the spore recovery between these two spore traps is expected to increase inversely proportional to the size of the particles being collected. According to Aylor (1993), Burkard spore traps can recover three times more particles than impaction spore traps when the particle size is approximately the same as that of *P. cubensis* sporangia (40 µm). However, differences of up to seven times in particle recovery between these two collection devices have also been reported (Solomon et al., 1980).

Wind direction and wind velocity can also affect the particle collection efficiency of both spore traps (West and Kimber, 2015), but the more important factors in the performance of impaction spore traps are sampling surface width and angular velocity

(Solomon et al., 1980). We used rods with similar width surface (1.2-by-3.5-mm stainless steel) to rods utilized in previous studies (Klosterman et al., 2014; Rahman et al., 2020) but increasing the collection surface of the impaction rod samplers could result in higher particle recovery and should be considered for future monitoring studies. Other factors to consider for increasing the recovery of *P. cubensis* sporangia by impaction spore traps include using multiple traps per location and longer deployment times of spore traps before rod collection. In California, at least two impaction spore traps are utilized to monitor *B. lactucae* spore loads in lettuce fields 50 to 200 times smaller than the commercial fields monitored in this study (Dhar et al., 2019); doubling the sample surface and the amount of air sampled could increase the chances for impaction of airborne sporangia in daily samples. We also observed a higher proportion of positive samples among the impaction spore trap samples collected over a longer period of time (96 h) which indicates that the adhesive medium we used on the rods (High-Vacuum Grease) was not completely saturated. It may not be necessary to change the impaction rods every 24 to 72 hours. Considering the expense of Burkard spore traps and the relatively low cost of impaction spore traps and their ease of use, it is important to improve the efficiency of sporangia detection using impaction spore traps.

The combination of Burkard and impaction spore traps with the qPCR assay developed by Crandall et al., 2020 facilitated the sensitive and specific monitoring of *P. humuli* and two host-adapted clades *P. cubensis* in Michigan. Using spore traps and qPCR, we detected *P. cubensis* clade II sporangia three to seven days before disease onset in commercial cucumber fields. During two years of monitoring, *P. cubensis* clade I was never detected during the summer season (May to August) in the fields

monitored. Our data suggest that Burkard spore traps are more efficient than impaction traps for the detection of airborne *Pseudoperonospora* spp. sporangia at low concentrations (<100 sporangia/day). Impaction spore traps could be modified to increase the probability for the collection of sporangia. In the future, the ability to rapidly detect both clades of *P. cubensis* using qPCR could be incorporated with environmental data and disease development information as part of a CDM risk advisory system to time fungicide applications that protect cucurbit crops in Michigan.

APPENDIX

APPENDIX

Table 3-1. **qPCR assays designed for the differentiation of *Pseudoperonospora humuli and Pseudoperonospora cubensis* clade I and II.**

Assay	Primers/probes	Final concentration[a]	Sequence 5'->3'	Protocol[b]
A[c]	RT33F	60 µm	AACTCCCGTTATGGAAGGTATT	95°C for 3 min followed by 40 cycles of 95°C for 10 s and 65°C for 45 s
	RT182R	60 µm	CCATGTACAACAGTAGCTGGA	
	CUBprobeSNP105	2.5 µm	HEX/A+C+AAA+C+G+AATA+CT/BHQ	
	HUMprobeSNP105	5 µm	FAM/AA+C+AAA+C+A+AATA+CTG/BHQ	
	InCp_J2	5 µm	CYS/A+GCATTATT+GTTTAT+CATATATACA/BHQ	
	Internal control (IC)	7.5 x10^{-10} nM	AACTCCCGTTATGGAAGGTATTATCATTAATCATGATTTGTA TATATGATAAACAATAATGCTATAACATAGAGTC TCTTTCAT GAATAATCCAGCTACTGTTGTACATGG.	
B[d]	PC_RFLP_2F	20 µm	CTGCTTTATCTTTTTCTTTTTG	95ºC for 3 minutes followed by 45 cycles of 95ºC for 15 s and 58ºC for 45 s
	PC_RFLP_3R	10 µm	AGAGAAGATTTAGATTATAATTC	
	PH_RFLP_4R	10 µm	AGAGACGATTTGGATTATAATT	
	PC-4 F	10 µm	CAAGACCACCATTTTTATGTC	
	PC-4 R	10 µm	TGGAAATTAAAAATTTTCTATTAC	
	Pcub_RFLP_qP1	5 µm	FAM/AACAAACTCAAGTAGAACTTCAACAAA/BHQ	
	Pcub2	10 µm	HEX/AGGATTGATTTTCATTAATTCCTTTTTGTAATAGAA/BHQ	
	Phum_RFLP_qP4	5 µm	RED/CCAACAGTTATACTTGTAATAAAC ATCAAG/BHQ	

Table 3-1. ***(cont'd)***

a. Final concentrations used in a 20 ul qPCR reaction.
b. The amplification protocols run on a CFX 96 Touch qPCR system (Bio-rad).
c. This set of primers and probes were adapted from (Summers et al., 2015a). Locked nucleic acids in the probes are followed by a plus (+) sign.
d. This set of primers and probes were adapted from (Crandall et al., 2020).

Table 3-2. **Threshold cycle (Cq) values of the qPCR protocol B using varying concentrations of genomic DNA from *Pseudoperonospora cubensis clade 1 and 2 and P. humuli***

Mix ratio	Species/Clade DNA			Probe		
	P. cubensis clade I	***P. cubensis clade II***	***P. humuli***	**Pcub_ RFLP_qP1 Cq±SD**	**Pcub2 Cq±SD**	**Phum_ RFLP_qP4 Cq±SD**
Un-mixed	10.000 fg	--	--	27.53±0.35[a]	NA	NA
	1.000 fg	--	--	31.69±0.21[b]	NA	NA
	100 fg	--	--	34.76±0.94[c]	NA	NA
	--	10.000 fg	--	NA	28.17±0.47[a]	NA
	--	1.000 fg	--	NA	32.01±1.1[b]	NA
	--	100 fg	--	NA	34.11±0.25[c]	NA
	--	--	10.000 fg	NA	NA	27.21±0.69[a]
	--	--	1.000 fg	NA	NA	31.11±1.1[b]
	--	--	100 fg	NA	NA	35.64±1.2[c]
1/1	10.000 fg	10.000 fg	--	27.75±0.02[a]	28.15±0.05[a]	NA
	1.000 fg	1.000 fg	--	31.91±0.38[b]	32.82±0.47[b]	NA
	100 fg	100 fg	--	34.67±0.41[c]	38.65±0.15*	NA
	--	10.000 fg	10.000 fg	NA	28.58±0.15[a]	26.57±0.31[a]
	--	1.000 fg	1.000 fg	NA	33.27±0.12*	31.25±0.05[b]
	--	100 fg	100 fg	NA	**NA****	34.71±0.7[c]
	10.000 fg	--	10.000 fg	27.39±0.07[a]	NA	27.85±0.22[a]
	1.000 fg	--	1.000 fg	31±0.28*	NA	31.33±0.64[b]
	100 fg	--	100 fg	34.73±0.5[c]	NA	35.73±0.34[c]

Table 3-2*. (cont'd)*

Mix ratio	Species/Clade DNA			Probe		
	P. cubensis clade I	***P. cubensis clade II***	***P. humuli***	**Pcub_ RFLP_qP1 Cq±SD**	**Pcub2 Cq±SD**	**Phum_ RFLP_qP4 Cq±SD**
1/10	10.000 fg	1.000 fg	--	27.61±0.01[a]	31.9±0.56[b]	NA
	1.000 fg	10.000 fg	--	**NA****	28.21±0.18[a]	NA
	--	10.000 fg	1.000 fg	NA	28.24±0.52[a]	29.51±0.13*
	--	1.000 fg	10.000 fg	NA	33.24±1.77[b]	26.32±0.32[a]
	10.000 fg	--	1.000 fg	27.78±0.33[a]	NA	31.06±1.11[b]
	1.000 fg	--	10.000 fg	34.25±0.48*	NA	27.87±0.25[a]
1/100	10.000 fg	100 fg	--	27.66±0.06[a]	**NA****	NA
	100 fg	10.000 fg	--	**NA****	28.11±0.05[a]	NA
	10.000 fg	--	100 fg	27.61±0.17[a]	NA	35.76±0.26[c]
	100 fg	--	10.000 fg	**NA****	NA	27.92±0.55[a]
	--	10.000 fg	100 fg	NA	28.08±0.78[a]	33.04±0.9*
	--	100 fg	10.000 fg	NA	**NA****	26.65±0.52*

Cq values with the same letter are not significantly different. Cq values with the symbol * are significantly different from values obtained for un-mixed samples with the same concentration of DNA (t-Test; P=0.05). --: not DNA added. NC: not used for comparison in the t-Test. NA: not defined.

Table 3-3. **Percentage of qPCR positive samples collected by Burkard and impaction spore traps**

Location	Year	Burkard			Impaction			
		24 h[a]			24 h[b]		96 h[c]	
		Reel	N[d]	Positive[e]	N[d]	Positive	N[d]	Positive[e]
Muskegon	2018	15	105	40.95%	45	33.33%	16	25.00%
	2019	16	112	33.04%	45	8.89%	15	40.00%
Bay	2018	15	105	39.05%	45	13.33%	16	18.75%
	2018	16	112	43.75%	45	20.00%	15	40.00%
Allegan	2018	15	105	48.57%	45	26.67%	15	13.33%
	2019	16	112	33.93%	45	20.00%	15	33.33%
Saginaw	2018	15	105	24.76%	48	12.50%	16	31.25%
	2019	16	112	41.96%	45	28.89%	15	20.00%
Ingham	2018	--	--	--	--	--	--	--
	2019	16	112	70.54%	43	46.51%	15	46.67%
Average		15.6	108	41.84%	45	23.35%	15	29.81%

a. Reels were collected every 7 days and the tape was divided every 24 hours.
b. Rod samples collected every 24 hours.
c. Rod samples collected every 96 hours.
d. Total number of samples collected.
e. Percentage of samples collected that tested positive for *P. cubensis* or *P. humuli.*

Table 3-4. **Linear regression analysis of Cq values as a function of the number *Pseudoperonospora spp.* sporangia**

Taxon	Variables[a]	β	Estimate	S.E	t value	Pr(>|t|)	Pr(>F)
P. humuli	Intercept	β_0	32.33	0.42	76.13	<2e-16	--
	$\log_{10}(X^b)$	β_1	-4.77	0.47	-10.05	<2e-16	<2e-16
	$qPCR_{(A/B)}$	β_2	-0.77	0.55	-1.40	0.16	0.39
	$\log_{10}(X^b)$*$qPCR_{(A/B)}$ [c]	β_3	0.71	0.63	1.12	0.26	0.26
P. cubensis **clade II**	Intercept	β_0	33.69	0.59	57.03	<2e-16	--
	$\log_{10}(X^b)$	β_1	-5.34	0.49	-10.89	<2e-16	<2.20e-16
	$qPCR_{(A/B)}$	β_2	-2.30	0.65	-3.50	5.1e-04	0.91
	$\log_{10}(X^b)$*$qPCR_{(A/B)}$ [c]	β_3	2.27	0.53	4.28	2.2e-05	<2.2e-05

a. Linear regression equation: $Cq_{P.cub} = \beta_0 - \beta_1 \, log_{10}(Sporangia) + \beta_2 \, log_{10}(qPCR) + \beta_3 \, log_{10}(Sporangia)(qPCR)$, $Cq_{P.hu} = \beta_0 - \beta_1 \, log_{10}(Sporangia)$).

b. X = number of sporangia.

c. qPCR assay express as a binary variable: qPCR assay A = 1, qPCR assay B = 0.

Table 3-5. β estimates of logistical models developed to predict the probability of *Pseudoperonospora cubensis* detection in Burkard and impaction spore trap samples

Spore trap	β_0	SD	P_{value}	β_1	SD	P_{value}	AIC
Burkard	-1.57	0.10	<2e-16	2.16	0.16	<2e-16	1333.8
Impaction	-2.33	0.21	<2e-17	1.60	0.21	6.e-14	405.4

Logistic regression models were developed using the spore trapping data collected in Allegan, Muskegon, Saginaw, Berrien and Bay counties in 2018 and 2019. Cq values of the qPCR protocol A were categorized as a binary variable using a threshold value of 35.5 (0>35.5 and 1≤35.5). To predict the probability o*f P. cubensis* detection in Burkard and impaction spore traps as a function of the number of sporangia β estimates should be replaced in equation 1.

Table 3-6. **Detection of *Pseudoperonospora cubensis* using Burkard spore traps coupled with qPCR and detection of symptoms**

Year	Location	qPCR	Spore trap	CDM Symptoms	qPCR detection of *P. cubensis* pre-symptoms[a]	qPCR detection[b]
2018	Muskegon	A	Burkard	Aug 7	Jul 23, 24, 26, 28, 29, 30, 31 and Aug 1, 2, 3, 4, 5, 6	16 days
			Impaction		Jul 27, 28, 29, 30, 31and Aug 1, 2, 3, 4, 5, 6	12 days
	Bay	A	Burkard	Aug 7	Jul 27, 30 and Aug 5, 6	11 days
			Impaction		---	---
	Allegan	A	Burkard	Aug 21	Aug 4, 6, 7, 8, 9, 10, 11, 12, 13, 14	17 days
			Impaction		Aug 2, 3, 4, 5, 6, 7, 14	19 days
	Saginaw	A	Burkard	Aug 2	Jul 27, 31	6 days
			Impaction		---	---
2019	Muskegon	B	Burkard	Aug 16	Aug 5, 6, 7, 9, 11, 12, 13, 14, 15	11 days
			Impaction		Aug 8, 9, 10, 11, 12, 13, 14, 15	9 days
	Bay	B	Burkard	Aug 20	Aug 12	8 days
			Impaction		---	---
	Allegan	B	Burkard	Aug 16	Aug 5, 8, 11, 12, 13, 14, 15	11 days
			Impaction		Aug 8, 9, 10, 11, 15	9 days
	Saginaw	B	Burkard	Aug 22	Aug 11, 19, 21	11 days
			Impaction		Aug 15, 16, 17, 18, 19	9 days
	Ingham	B	Burkard	Aug 21	Aug 1, 19, 20	21 days
			Impaction		---	---

a. qPCR detection within a window of three weeks before symptoms were observed in the field
b. Number of days between the first detection of *P. cubensis* DNA using qPCR and the detection of CDM symptoms in the field

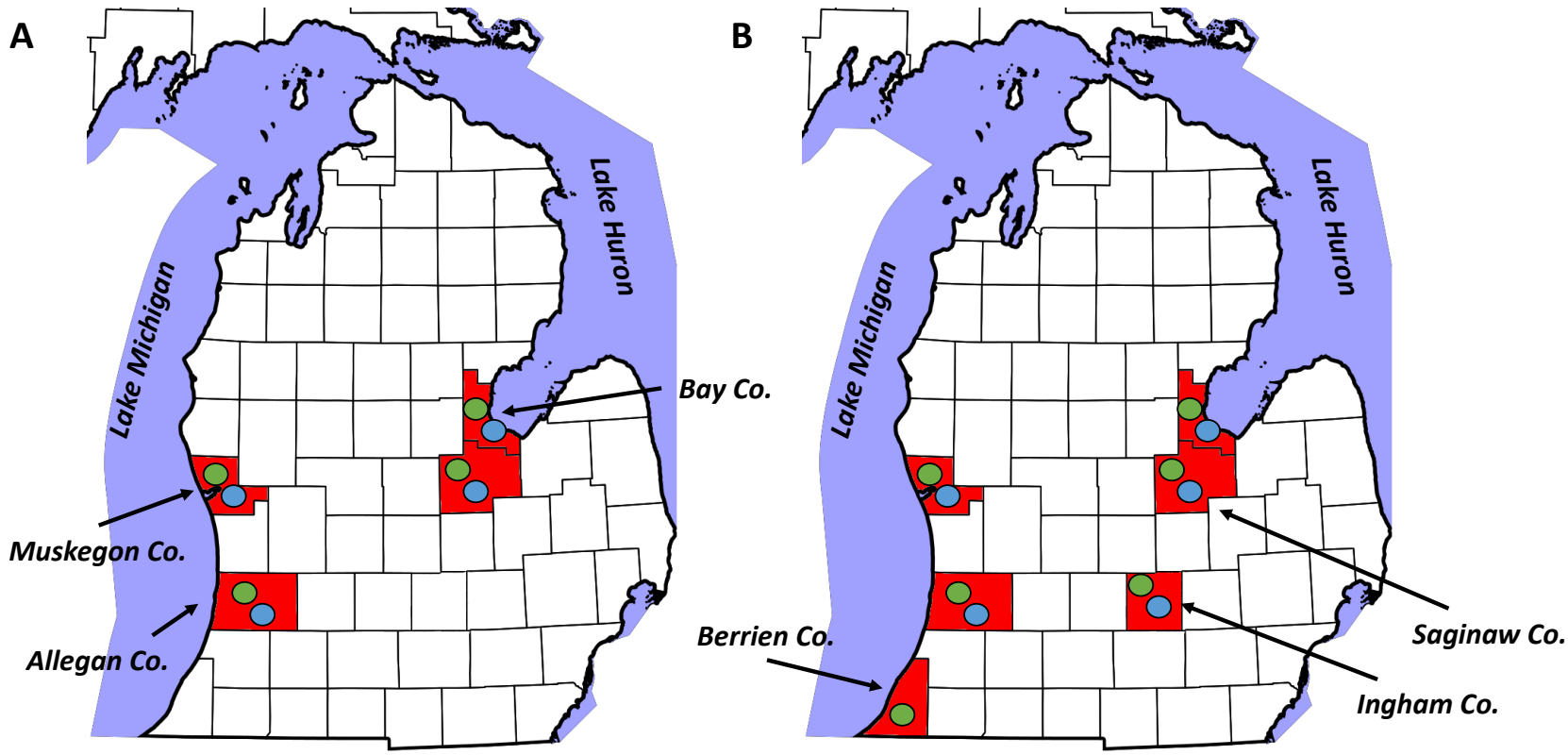

Figure 3-1. **Location of spore traps by county in 2018 (A) and 2019 (B). Green and blue dots indicate Burkard and impaction spore traps, respectively.**

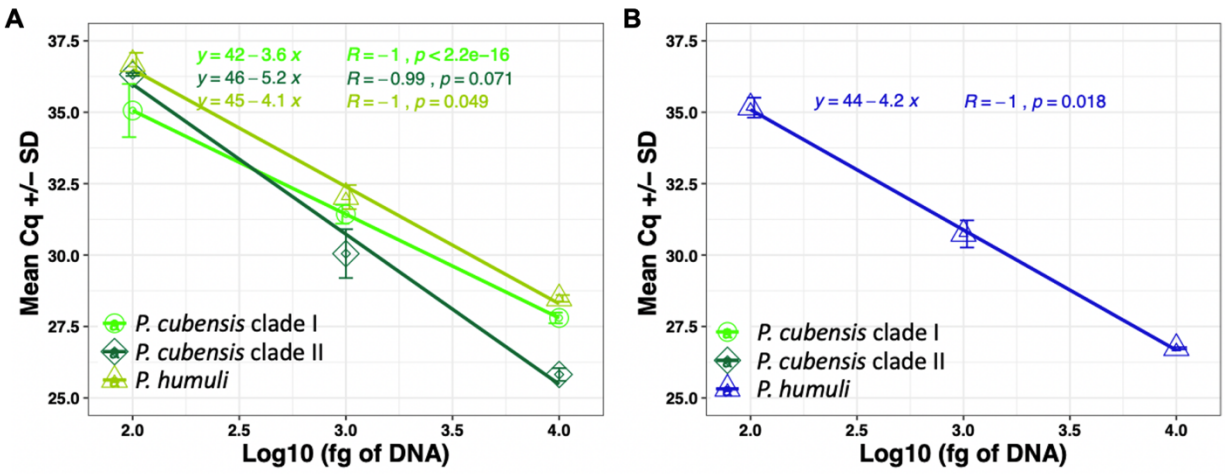

***Figure 3-2*. Standard curves for the quantification of *Pseudoperonospora cubensis* clade I, *P. cubensis* clade II and *P. humuli* DNA using the qPCR protocol A.**

Standard curves of the protocol A using **(A)** the probe CUBprobeSNP105 for *P. cubensis* detection and **(B)** the probe HUMprobeSNP105 for *P. humuli* detection. The curves were constructed assessing the DNA from all taxa independently. Detection of *P. cubensis* clade I and II was observed using the probe HUMprobeSNP105. The log_{10} of DNA fg is plotted against the quantification cycle values (Cq). All data points are from three technical replicates derived from two DNA extractions. The centerline represents the line of fit and error bars represent standard deviation.

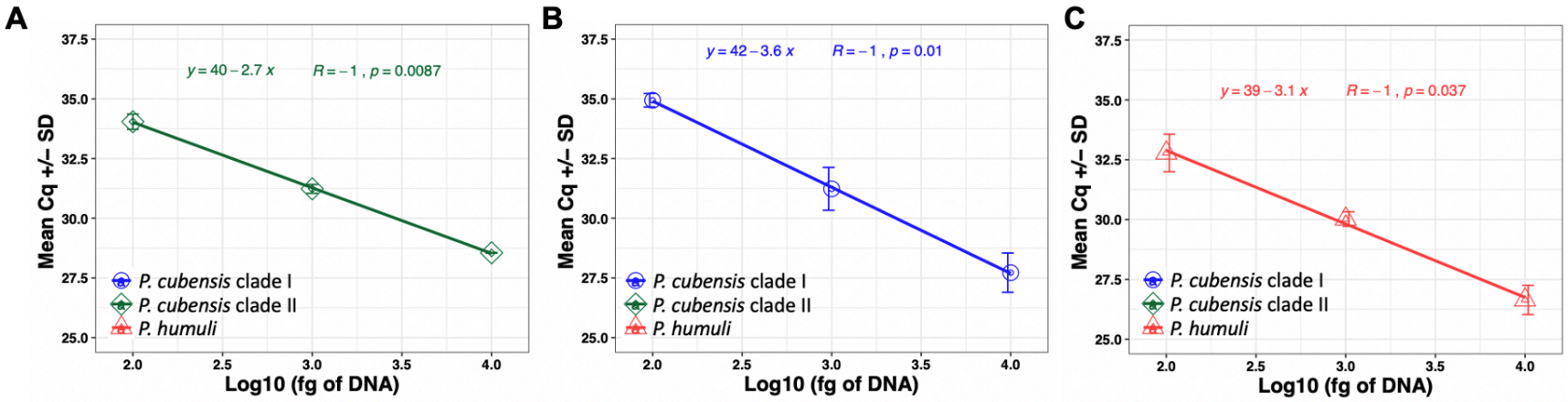

Figure 3-3. **Standard curves for the quantification of *Pseudoperonospora cubensis* clade I, *P. cubensis* clade II and *P. humuli* DNA using the qPCR protocol B**

Standard curves of the protocol B using the probes Pcub2 **(A),** Pcub_RFLP_qP1 **(B)** and Phum_RFLP_qP4 **(C)** for detection of *P. cubensis* clade II, *P. cubensis* clade I and *P. humuli*, respectively**.** The curves were constructed assessing the DNA from all taxa independently. Amplification of non-target taxa was not observed. The $\log_{10}$ of DNA fg is plotted against the quantification cycle values (Cq). All data points are from three technical replicates derived from two DNA extractions. The centerline represents the line of fit and error bars represent standard deviation.

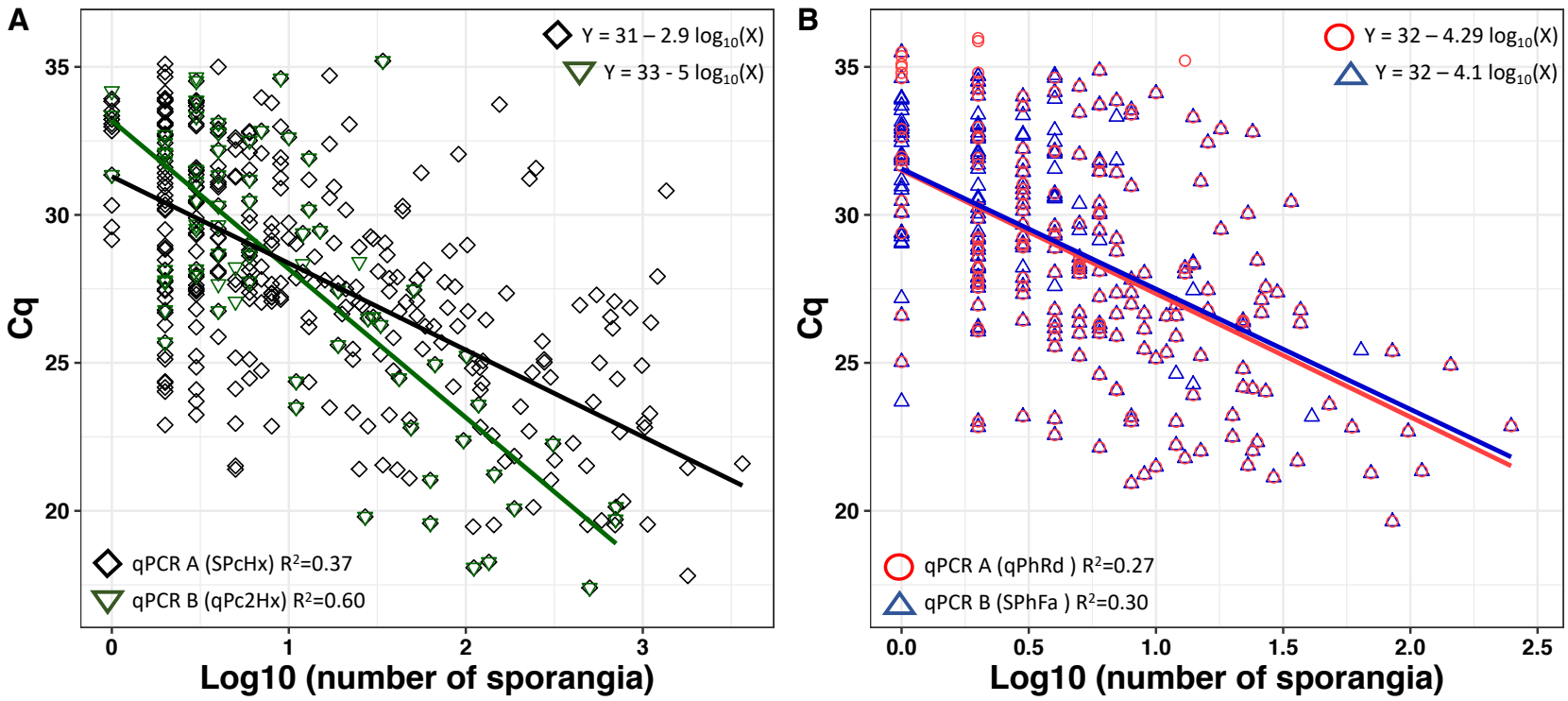

***Figure 3-4*. Linear regression of Cq values as a function of sporangial numbers.**

(A) Linear regression of *Pseudoperonospora* spp. sporangia counted using light microscopy against corresponding mean Cq values of the protocol A (rhomboids) and B (triangles). **(B)** Linear regression of *Pseudoperonospora* spp. sporangia counted using light microscopy against corresponding mean Cq values of the protocol A (circles) and B (triangles). The $\log_{10}$ number of sporangia is plotted against the quantification cycle values (Cq).

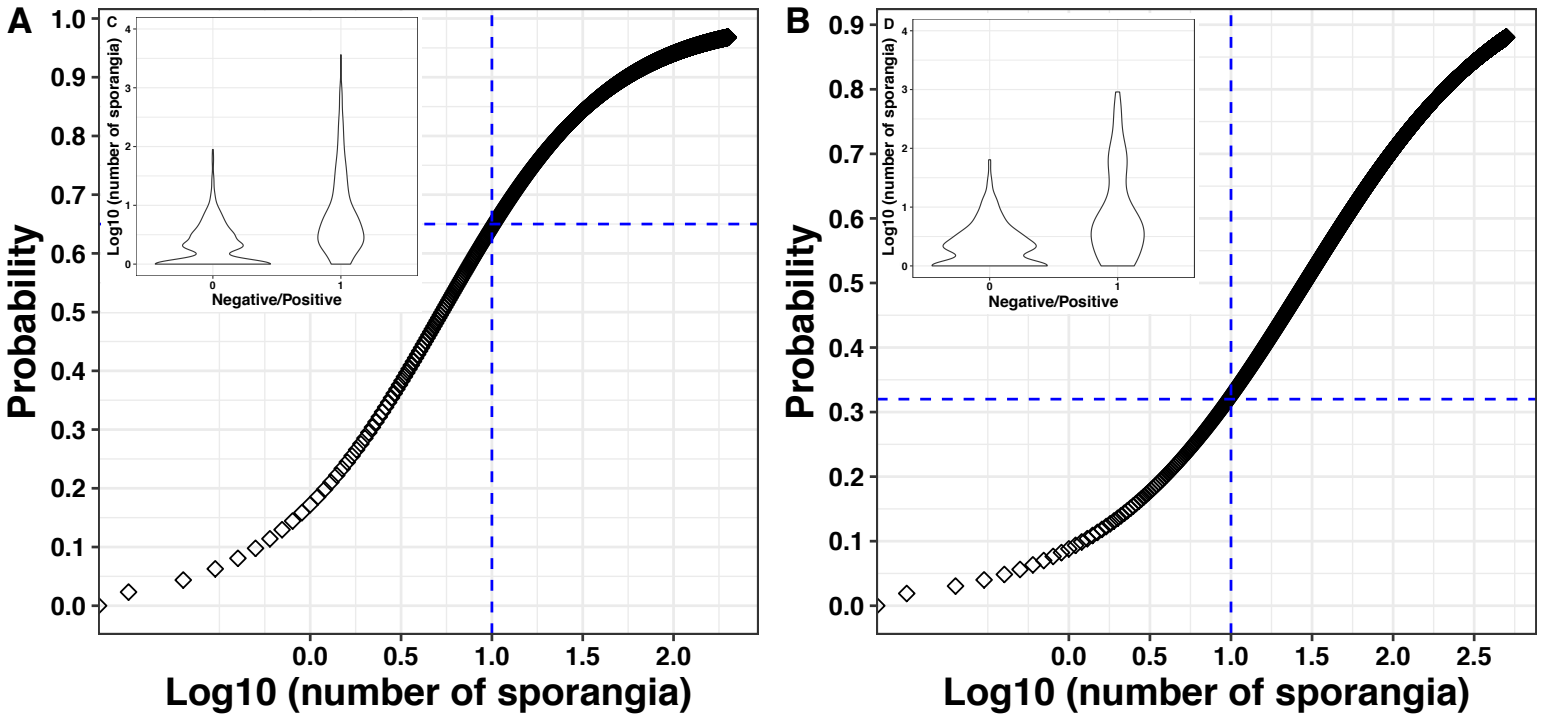

Figure 3-5. Logistic regression of qPCR results from Burkard (A) and impaction (B) spore traps as a function of sporangial numbers**.**

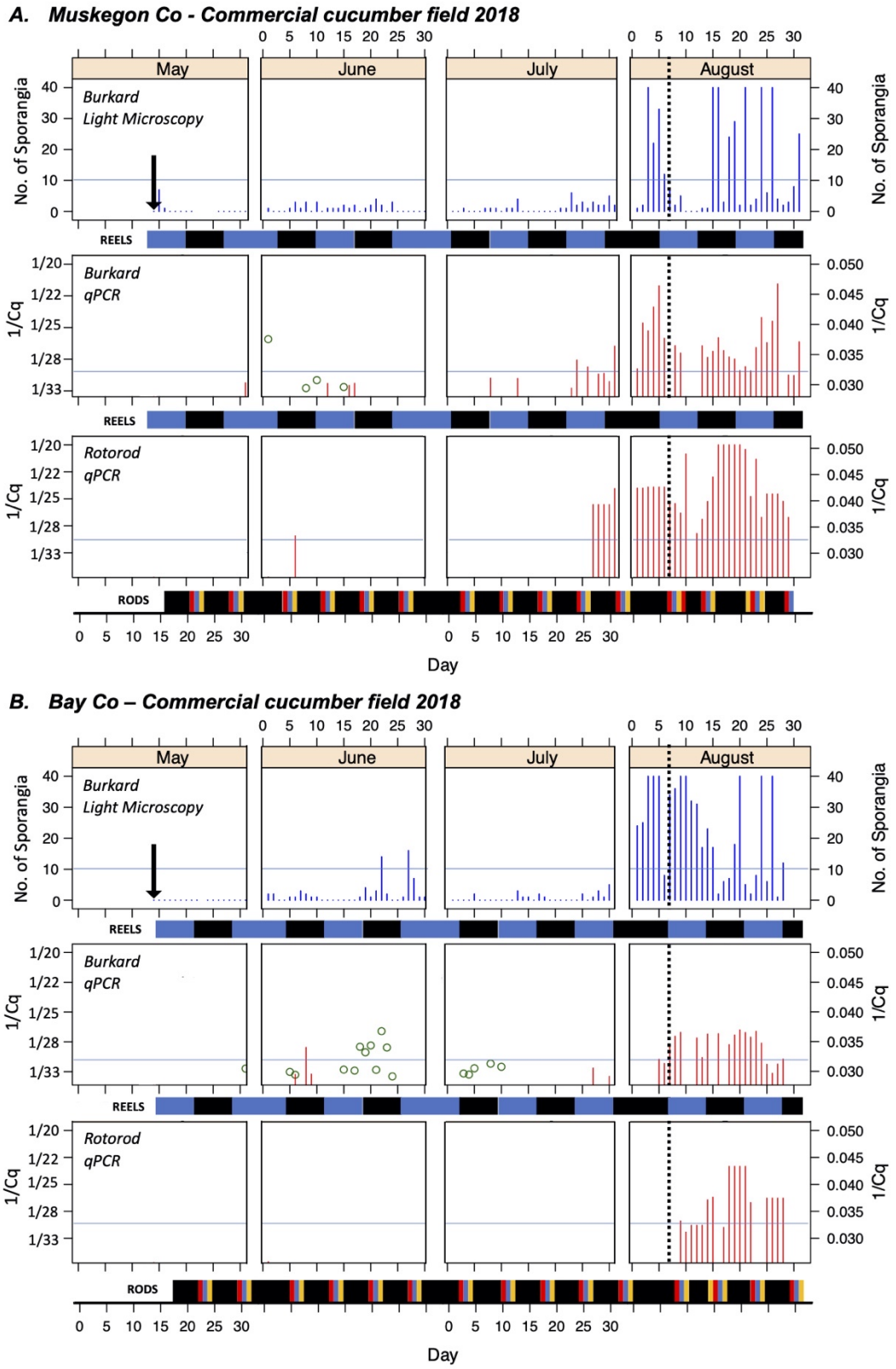

Figure 3-6. Monitoring of *Pseudoperonospora cubensis* and *P. humuli* sporangia using spore traps in Muskegon (A) and Bay (B) counties in 2018 (Location B).

Figure 3-6. ***(cont'd)***

The data from each county was divided into three rows of panels. **The first row panels** represent the daily sporangial numbers estimated through the analysis of Burkard spore trap samples using light microscopy (blue bars). The y-axis was trimmed to 40 sporangia to facilitate the visualization of low counts. **The middle panels** represent the qPCR results of protocol A for the detection of *P. cubensis* (red bars) and *P. humuli* (green circles) in the tape of Burkard spore traps. **The bottom panels** represent the qPCR results of protocol A for the detection of *P. cubensis* (red bars) and *P. humuli* (green circles) in the rods of impaction spore traps. A black arrow denotes the monitoring starting date. The dashed line denotes the date of cucurbit downy mildew symptom detection in the field. Scouting efforts to detect CDM symptoms in growing cucumber regions are increased once sporangial loads exceed 10 sporangia/day. Bars below the x-axis denote the time the reels and rods were changed from each trap.

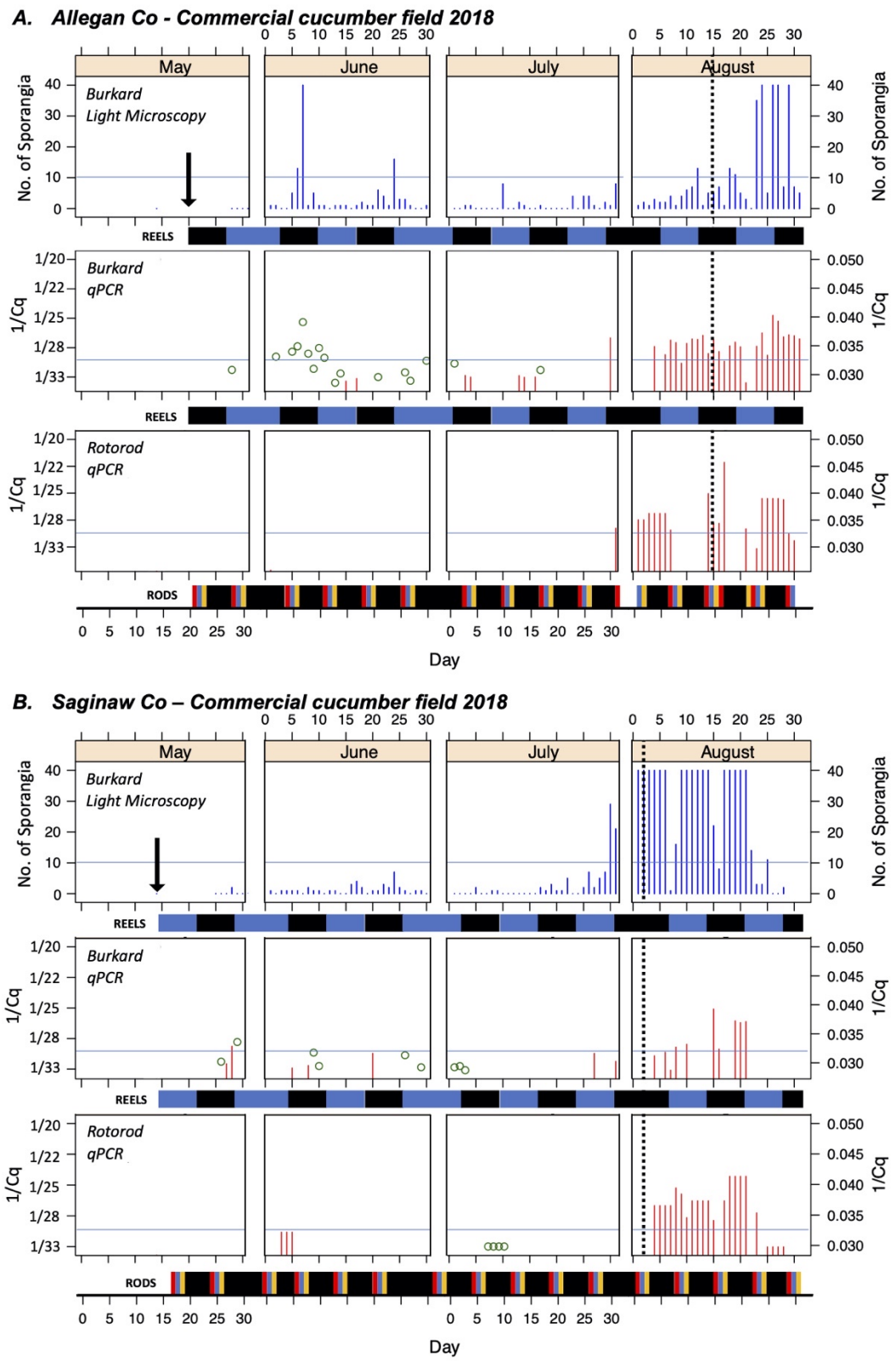

Figure 3-7. Monitoring of *Pseudoperonospora cubensis* and *P. humuli* sporangia using spore traps in Allegan (A) and Saginaw (B) counties in 2018**.**

Figure 3-7*. (cont'd)*

The data from each county was divided into three rows of panels. **The first row panels** represent the daily sporangial numbers estimated through the analysis of Burkard spore trap samples using light microscopy (blue bars). The y-axis was trimmed to 40 sporangia to facilitate the visualization of low counts. **The middle panels** represent the qPCR results of protocol A for the detection of *P. cubensis* (red bars) and *P. humuli* (green circles) in the tape of Burkard spore traps. **The bottom panels** represent the qPCR results of protocol A for the detection of *P. cubensis* (red bars) and *P. humuli* (green circles) in the rods of impaction spore traps. A black arrow denotes the monitoring starting date. The dashed line denotes the date of cucurbit downy mildew symptoms detection in the field. Scouting efforts to detect CDM symptoms in growing cucumber regions are increased once sporangial loads exceed 10 sporangia/day. Bars below the x-axis denote the time the reels and rods were changed from each trap.

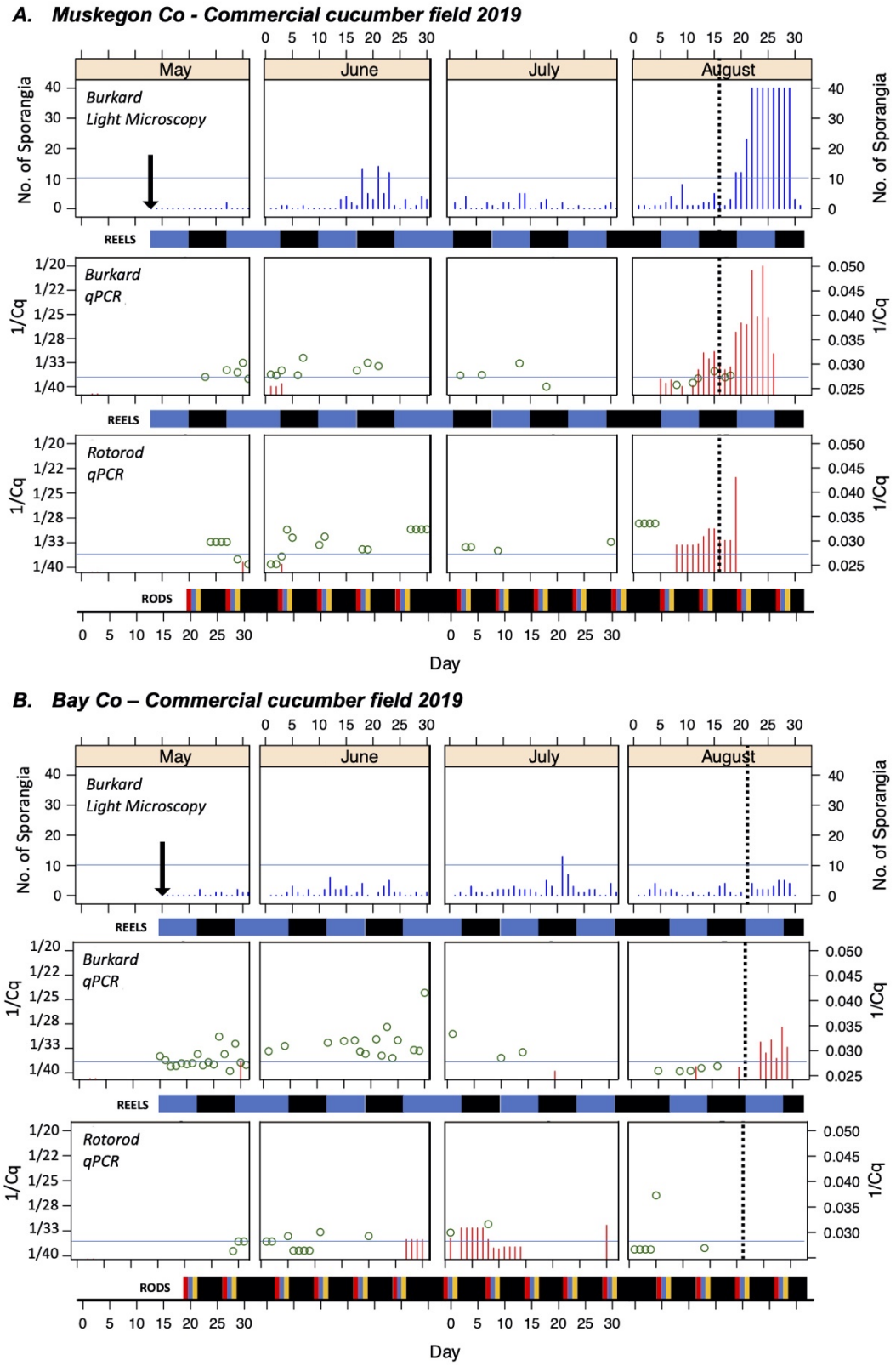

Figure 3-8. Monitoring of *Pseudoperonospora cubensis* and *P. humuli* sporangia using spore traps in Muskegon (A) and Bay (B) counties in 2019.

Figure 3-8*. (cont'd)*

The data from each county was divided into three rows of panels. **The first row panels** represent the daily sporangial numbers estimated through the analysis of Burkard spore trap samples using light microscopy (blue bars). The y-axis was trimmed to 40 sporangia to facilitate the visualization of low counts. **The middle panels** represent the qPCR results of protocol B for the detection of *P. cubensis* (red bars) and *P. humuli* (green circles) in the tape of Burkard spore traps. **The bottom panels** represent the qPCR results of protocol B for the detection of *P. cubensis* (red bars) and *P. humuli* (green circles) in the rods of impaction spore traps. A black arrow denotes the monitoring starting date. The dashed line denotes the date of cucurbit downy mildew symptoms detection in the field. Scouting efforts to detect CDM symptoms in growing cucumber regions are increased once sporangial loads exceed 10 sporangia/day. Bars below the x-axis denote the time the reels and rods were changed from each trap.

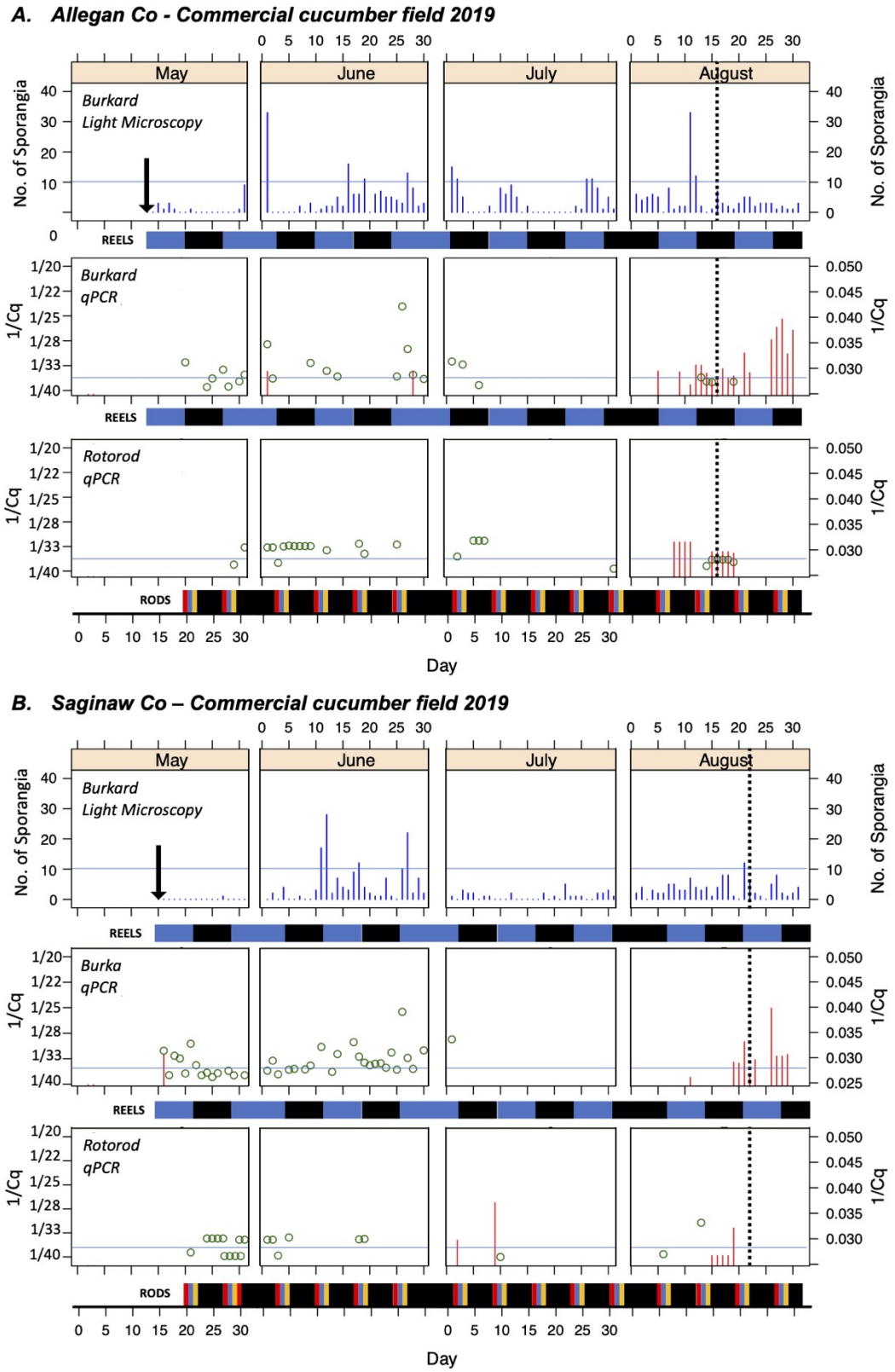

Figure 3-9. Monitoring of *Pseudoperonospora cubensis* and *P. humuli* sporangia using spore traps in Allegan (A) and Saginaw (B) counties in 2019.

Figure 3-9*. (cont'd)*

The data from each county was divided into three rows of panels. **The first row panels** represent the daily sporangial numbers estimated through the analysis of Burkard spore trap samples using light microscopy (blue bars). The y-axis was trimmed to 40 sporangia to facilitate the visualization of low counts. **The middle panels** represent the qPCR results of protocol B for the detection of *P. cubensis* (red bars) and *P. humuli* (green circles) in the tape of Burkard spore traps. **The bottom panels** represent the qPCR results of protocol B for the detection of *P. cubensis* (red bars) and *P. humuli* (green circles) in the rods of impaction spore traps. A black arrow denotes the monitoring starting date. The dashed line denotes the date of cucurbit downy mildew symptoms detection in the field. Scouting efforts to detect CDM symptoms in growing cucumber regions are increased once sporangial loads exceed 10 sporangia/day. Bars below the x-axis denote the time the reels and rods were changed from each trap.

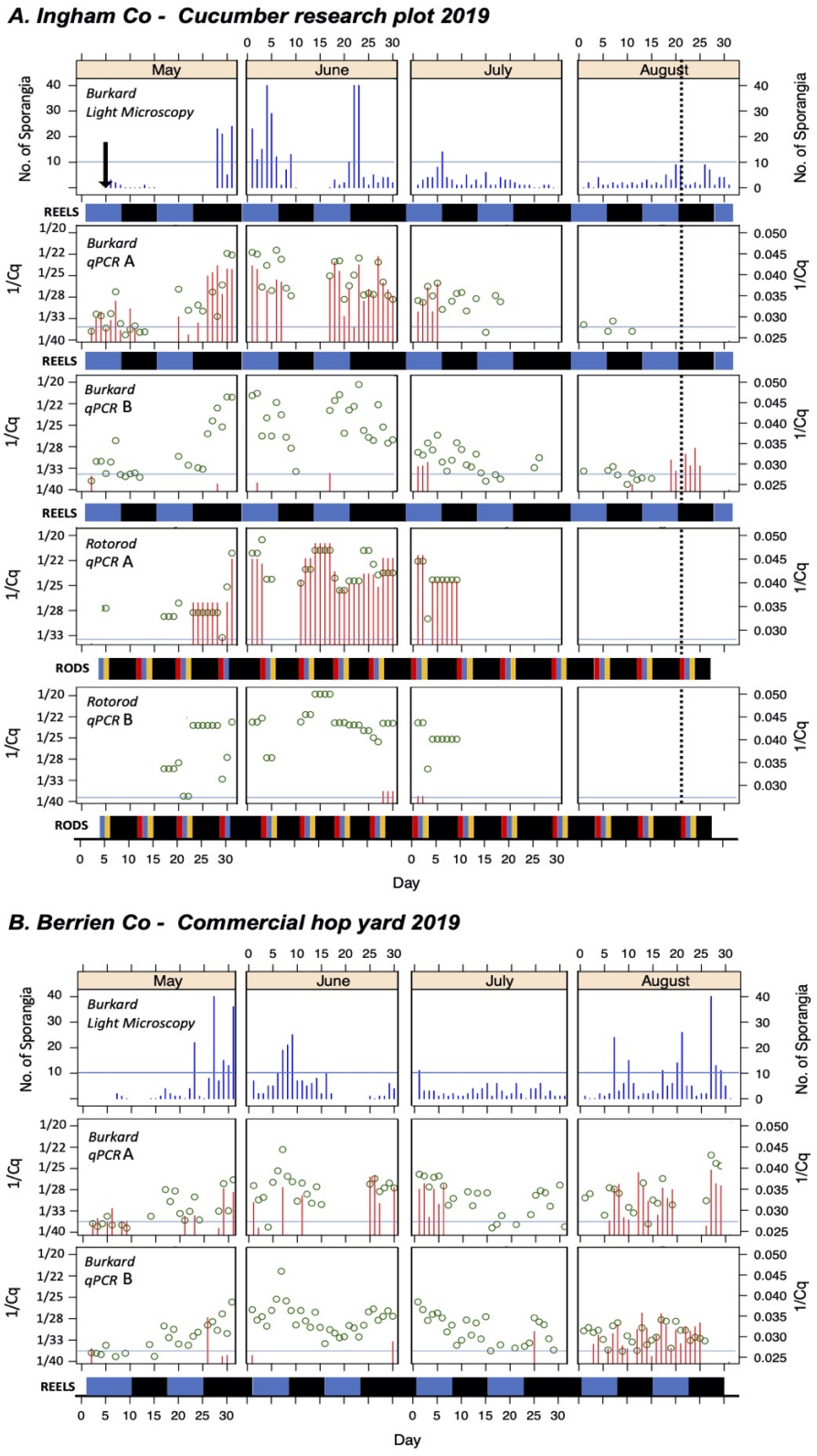

Figure 3-10. Monitoring of *P cubensis* and *P. humuli* sporangia using spore traps in Ingham (A) and Berrien (B) counties in 2019.

Figure 3-10*. (cont'd)*

The data from Ingham county was divided into five rows of panels. **The first row panels** represent the daily sporangial numbers estimated through the analysis of Burkard spore trap samples using light microscopy (blue bars). The y-axis was trimmed to 40 sporangia to facilitate the visualization of low counts. **The middle second and third row panels** represent the qPCR results of protocol A (row 2) and B (row 3) for the detection of *P. cubensis* (red bars) and *P. humuli* (green circles) in the tape of Burkard spore traps. **The fourth and five row panels** represent the qPCR results of protocol A (row 4) and B (row 5) for the detection of *P. cubensis* (red bars) and *P. humuli* (green circles) in the rods of impaction spore traps. The data from Berrien county was divided into three row panels. **The first row panels** represent the daily sporangial numbers estimated through the analysis of Burkard spore trap samples using light microscopy (blue bars). The y-axis was trimmed to 40 sporangia to facilitate the visualization of low counts. **The middle panels** represent the qPCR results of protocol A for the detection of *P. cubensis* (red bars) and *P. humuli* (green circles) in the tape of Burkard spore traps. **The bottom panels** represent the qPCR results of protocol B for the detection of *P. cubensis* (red bars) and *P. humuli* (green circles) in the tape of Burkard spore traps. A black arrow denotes the monitoring starting date. The dashed line denotes the date of cucurbit downy mildew symptoms detection in the field. Scouting efforts to detect CDM symptoms in growing cucumber regions are increased once sporangial loads exceed 10 sporangia/day. Bars below the x-axis denote the time the reels and rods were changed from each trap.

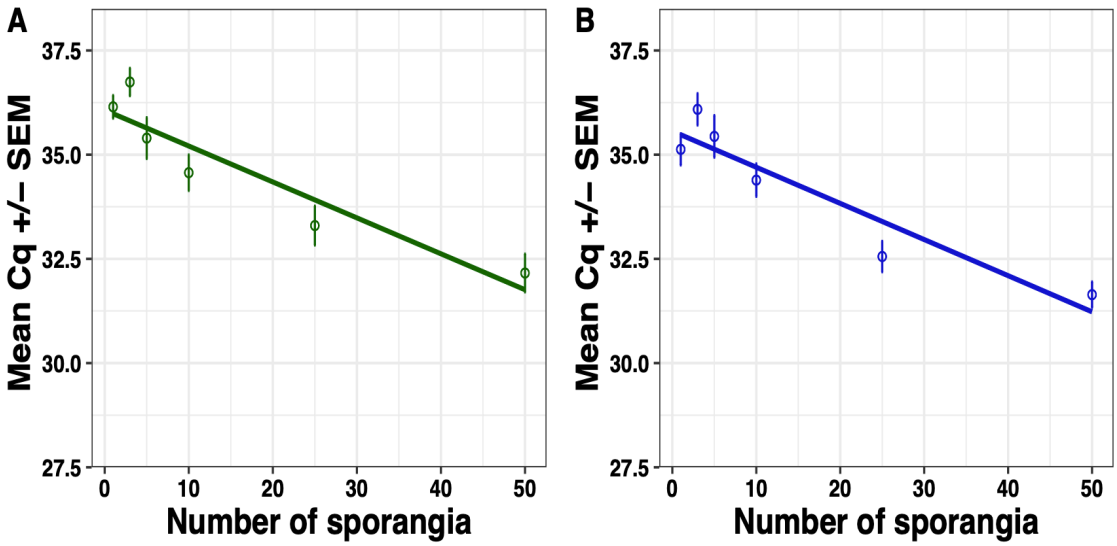

***Figure 3-11*. Standard curves for the quantification of *Pseudoperonospora cubensis* and *P. humuli* sporangia using the qPCR protocol A.**

Five-point standard curves for protocol A using **(A)** the probe CUBprobeSNP105 for *P. cubensis* detection and **(B)** the probe HUMprobeSNP105 for *P. humuli* detection. All data points represent an average of 8 to 15 replicate spore-count samples of each species. Error bars on points represent the standard error of the mean. There was inconsistent amplification for the 1-count sporangium samples and they were excluded from the final linear regression.

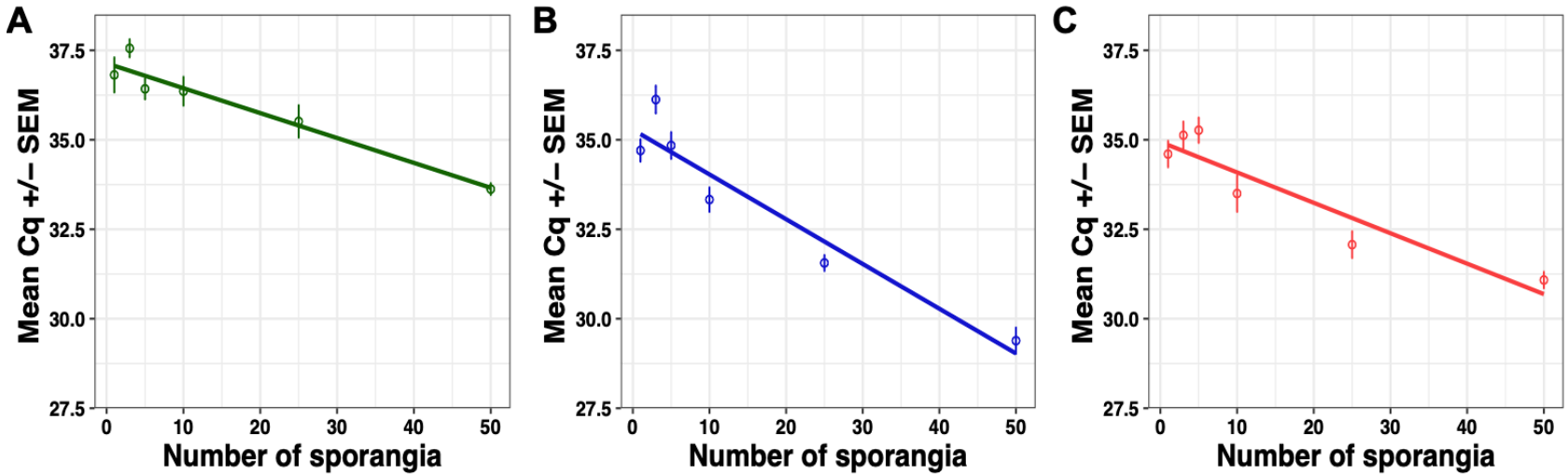

Figure 3-12. **Standard curves for the quantification of *Pseudoperonospora cubensis* clade I, *P. cubensis* clade II and *P. humuli* sporangia using the qPCR protocol B.**

Five-point standard curves for protocol B using the probes Pcub2 **(A),** Pcub_RFLP_qP1 **(B)** and Phum_RFLP_qP4 **(C)** for detection of *P. cubensis* clade II, *P. cubensis* clade I and *P. humuli*, respectively**.** All data points represent an average of 8 to 15 replicate spore-count samples of each taxa. Error bars on points represent the standard error of the mean. There was inconsistent amplification for the 1-count sporangium samples and they were excluded from the final linear regression.

LITERATURE CITED

LITERATURE CITED

Adams, M., D'Arcangelo, K, Collins, H, Quesada-Ocampo, L (2019) Evaluation of cultivars for control of downy mildew on squash, Kinston 2018. Plant Dis Manag Reports 13: V124

Aylor, D.E. (2017) Chapter 20: Aerial Sampling. Aerial dispersal of pollen and spores. The American Phytopathological Society, pp 339–360

Aylor, D.E. (1993) Relative collection efficiency of Rotorod and Burkard spore samplers for airborne *Venturia inaequalis* ascospores. Phythopathology 83: 1116–1119

Bello, J.C., Sakalidis, M.L., Perla, D.E., Hausbeck, M.K. (2020) Detection of airborne sporangia of *Pseudoperonospora cubensis* in Michigan using Burkard spore traps coupled to qPCR. Accepted in Plant Dis.

Blum, M., Waldner, M., Olaya, G., Cohen, Y., Gisi, U., Sierotzki, H. (2011) Resistance mechanism to carboxylic acid amide fungicides in the cucurbit downy mildew pathogen *Pseudoperonospora cubensis*. Pest Manag Sci 67: 1211–1214

Carisse, O., McNealis, V., Kriss, A. (2017) Association between weather variables, airborne inoculum concentration, and raspberry fruit rot caused by *Botrytis cinerea*. Phytopathology 108: 70–82

Carisse, O., Tremblay, D.M., Lévesque, C.A., Gindro, K., Ward, P., Houde, A. (2009) Development of a Taqman real-time PCR assay for quantification of airborne conidia of *Botrytis squamosa* and management of Botrytis leaf blight of onion. Phytopathology 99: 1273–1280

Choudhury, R.A., Koike, S.T., Fox, A.D., Anchieta, A., Subbarao, K.V., Klosterman, S.J., McRoberts, N. (2016a) Season-long dynamics of spinach downy mildew determined by spore trapping and disease incidence. Phytopathology 106: 1311–1318

Choudhury, R.A., Koike, S.T., Fox, A.D., Anchieta, A., Subbarao, K.V., Klosterman, S.J., McRoberts, N. (2016b) Spatiotemporal patterns in the airborne dispersal of spinach downy mildew. Phytopathology 107: 50–58

Coley-Smith, J.R. (1962) Overwintering of hop downy mildew *Pseudoperonospora humuli* (Miy. and Tak.) Wilson. Ann Appl Biol 50: 235–243

Crandall, S. G., Ramon, M. L., Burkhardt, A. K., Bello J. C., Adair, N., Gent, D. H., Hausbeck, M. K., Quesada-Ocampo, L. M. and Martin, F. N. A multiplex TaqMan qPCR assay for detection and quantification of clade 1 and clade 2 isolates of *Pseudoperonospora cubensis* and *P. humuli.* Under review in Plant Dis.

Dhar, N., Mamo, B.E., Subbarao, K., Koike, S., Fox, A., Anchieta, A., Klosterman, S.J .(2019) Measurements of aerial spore load by qPCR facilitates lettuce downy mildew risk advisement. Plant Dis 104: 82–93

Dung, J.K.S., Scott, J.C., Cheng, Q., Alderman, S.C., Kaur, N., Walenta, D.L., Frost, K.E., Hamm, P.B. (2018) Detection and quantification of airborne *Claviceps purpurea* sensu lato ascospores from Hirst-type spore traps using real-time quantitative PCR. Plant Dis 102: 2487–2493

Fall. M.L., Van der Heyden, H., Brodeur, L., Leclerc, Y., Moreau, G., Carisse, O. (2015) Spatiotemporal variation in airborne sporangia of *Phytophthora infestans*: characterization and initiatives towards improving potato late blight risk estimation. Plant Pathol 64: 178–190

Frenz, D.A. (1999) Comparing pollen and spore counts collected with the Rotorod Sampler and Burkard spore trap. Ann Allergy, Asthma Immunol 83: 341–349

González-Domínguez, E., Berlanas, C., Gramaje, D., Armengol, J., Rossi, V., Berbegal, M. (2020) Temporal dispersal patterns of *Phaeomoniella chlamydospora*, causal agent of petri disease and esca, in vineyards. Phytopathology 110: 1216–1225

Granke, L.L., Hausbeck, M.K. (2011) Dynamics of *Pseudoperonospora cubensis* sporangia in commercial cucurbit fields in Michigan. Plant Dis 95: 1392–1400

Granke, L.L., Morrice, J.J., Hausbeck, M.K. (2013) Relationships between airborne *Pseudoperonospora cubensis* sporangia, environmental conditions, and cucumber downy mildew severity. Plant Dis 98: 674–681

Hausbeck, M., Brisco-McCann, E., Goldenhar, K., Cook, A. (2017) Evaluation of fungicide programs for control of downy mildew of cucumber, 2016. Plant Dis Manag Reports 11: V063

Hausbeck, M.K., Perla, D.E., Cook, A.J. (2019) Evaluation of single fungicide products for control of downy mildew of cucumber, 2018. Plant Dis Manag Reports 139: V13

Hollomon, B. (2007) Fungicide resistance in crop pathogens: How can it be managed?, 2nd ed. FRAC, Brussels

Holmes, G.J., Ojiambo, P.S., Hausbeck, M.K., Quesada-Ocampo, L., Keinath, A.P. (2014) Resurgence of cucurbit downy mildew in the united states: a watershed event for research and extension. Plant Dis 99: 428–441

Jackson, S.L., Bayliss, K.L. (2011) Spore traps need improvement to fulfil plant biosecurity requirements. Plant Pathol 60: 801–810

Keinath, A.P. (2015) Utility of a cucumber plant bioassay to assess fungicide efficacy against *Pseudoperonospora cubensis*. Plant Dis 100: 490–499

Klosterman, S.J., Anchieta, A., McRoberts, N., Koike, S.T., Subbarao, K.V., Voglmayr, H., Choi, Y-J., Thines, M., Martin, F.N. (2014) Coupling spore traps and quantitative PCR assays for detection of the downy mildew pathogens of spinach (*Peronospora effusa*) and beet (*P. schachtii*). Phytopathology 104: 1349–1359

Kunjeti, S.G., Anchieta, A., Martin, F.N., Choi, Y-J., Thines, M., Michelmore, R.W., Koike, S.T., Tsuchida, C., Mahaffee, W., Subbarao, K. V., et al (2016) Detection and quantification of *Bremia lactucae* by spore trapping and quantitative PCR. Phytopathology 106: 1426–1437

Lizotte, E., and Miles, T.D. (2020) Hop disease management in Michigan for 2020. MSU Ext., https://www.canr.msu.edu/news/managing-hop-downy-mildew-in-michigan

Naegele, R.P., Quesada-Ocampo, L.M., Kurjan, J.D., Saude, C., Hausbeck, M.K. (2016) Regional and temporal population structure of *Pseudoperonospora cubensis* in Michigan and Ontario. Phytopathology 106: 372–379

O'Hara, R., Tedone, E., Ludlow, A., Huang, E., Arosio, B., Mari, D., Shay, J.W. (2019) Quantitative mitochondrial DNA copy number determination using droplet digital PCR with single-cell resolution. Genome Res 29: 1878–1888

Ojiambo, P.S., Gent, D.H., Quesada-Ocampo, L.M., Hausbeck, M.K., Holmes, G.J. (2015) Epidemiology and population biology of *Pseudoperonospora cubensis*: a model system for management of downy mildews. Annu Rev Phytopathol 53: 223–246

Ojiambo, P.S., Holmes, G.J. (2010) Spatiotemporal spread of cucurbit downy mildew in the Eastern United States. Phytopathology 101: 451–461

Ojiambo, P.S., Holmes, G.J., Britton, W., Babadoost, M., Bost, S.C., Boyles, R., Brooks, M., Damicone, J., Draper, M.A., Egel, D.S., et al (2011) Cucurbit downy mildew IPMpipe: a next generation web-based interactive tool for disease management and extension outreach. Plant Heal Prog 12: 26

Perla, D., Hausbeck, M.K., Cook, A. (2019) Evaluation of fungicide programs for control of downy mildew of cucumber, 2018. Plant Dis Manag Reports 147: V13

Rahman, A., Standish, J., D'Arcangelo, K.N., Quesada-Ocampo, L.M. (2020) Clade-specific biosurveillance of *Pseudoperonospora cubensis* using spore traps for precision disease management of cucurbit downy mildew. Phytopathology.

Reuveni, M., Eyal, H., Cohen, Y. (1980) Development of resistance to metalaxyl in *Pseudoperonospora cubensis*. Plant Dis 64: 1108–1109

Rogers, S.L., Atkins, S.D., West, J.S. (2009) Detection and quantification of airborne inoculum of *Sclerotinia sclerotiorum* using quantitative PCR. Plant Pathol 58: 324–331

Savory, E.A., Granke, L.L., Quesada-Ocampo, L.M., Varbanova, M., Hausbeck, M.K., Day, B. (2011) The cucurbit downy mildew pathogen *Pseudoperonospora cubensis*. Mol Plant Pathol 12: 217–26

Solomon, W.R., Burge, H.A., Boise, J.R., Becker, M. (1980) Comparative particle recoveries by the retracting rotorod, rotoslide and Burkard spore trap sampling in a compact array. Int J Biometeorol 24: 107–116

Summers, C., Adair, N., Gent, D., Mcgrath, M., Christine, S. (2015a) *Pseudoperonospora cubensis* and *P. humuli* detection using species-specific probes and high definition melt curve analysis. Can J Plant Pathol 37: 150605144651006

Summers, C.F., Gulliford, C.M., Carlson, C.H., Lillis, J.A., Carlson, M.O., Cadle-Davidson, L., Gent, D.H., Smart, C.D. (2015b) Identification of genetic variation between obligate plant pathogens *Pseudoperonospora cubensis* and *P. humuli* using RNA sequencing and genotyping-by-sequencing. PLoS One 10: e0143665

Thiessen, L.D., Neill, T.M., Mahaffee, W.F. (2017) Timing fungicide application intervals based on airborne *erysiphe necator* concentrations. Plant Dis 101: 1246–1252

Thomas, A., Carbone, I., Choe, K., Quesada-Ocampo, L.M., Ojiambo, P.S. (2017) Resurgence of cucurbit downy mildew in the United States: Insights from comparative genomic analysis of *Pseudoperonospora cubensis*. Ecol Evol 7: 6231–6246

USDA (2020) United States Department of Agriculture. 2019. Vegetables Annual Summary.

Van der Heyden, H., Bilodeau, G., Carisse, O., Charron, J-B. (2020) Monitoring of *Peronospora destructor* primary and secondary inoculum by Real-Time qPCR. Plant Dis. doi: 10.1094/PDIS-03-20-0687-RE

Villari, C., Mahaffee, W.F., Mitchell, T.K., Pedley, K.F., Pieck, M.L., Hand, F.P. (2016) Early detection of airborne inoculum of *Magnaporthe oryzae* in turfgrass fields using a quantitative LAMP assay. Plant Dis 101: 170–177

Wallace, E.C., D'Arcangelo, K.N., Quesada-Ocampo, L.M. (2020) Population analyses reveal two host-adapted clades of *Pseudoperonospora cubensis*, the causal agent of cucurbit downy mildew, on commercial and wild cucurbits. Phytopathology. doi: 10.1094/PHYTO-01-20-0009-R

West, J., Kimber, R. (2015) Innovations in air sampling to detect plant pathogens. Ann Appl Biol 166: 4–17

Wyka, S.A., McIntire, C.D., Smith, C., Munck, I.A., Rock, B.N., Asbjornsen, H., Broders, K.D. (2017). Effect of climatic variables on abundance and dispersal of *Lecanosticta acicola* spores and their impact on defoliation on eastern white pine. Phytopathology 108: 374–383

Zhu, S.S., Liu, X.L., Wang, Y., Wu, X.H., Liu, P.F., Li, J.Q., Yuan, S.K., Si, N.G. (2007) Resistance of *Pseudoperonospora cubensis* to flumorph on cucumber in plastic houses. Plant Pathol 56: 967–975

CHAPTER IV: GENOTYPING OF THE OBLIGATE PLANT PATHOGENS *PSEUDOPERONOSPORA CUBENSIS* AND *P. HUMULI* USING TARGET ENRICHMENT SEQUENCING

ABSTRACT

Technological advances in genome sequencing have improved our ability to catalog genomic variation and have led to an expansion of the scope and scale of genetic studies over the past decade. Yet, for agronomically important plant pathogens such as the downy mildews (*Peronosporaceae*) the scale of genetic studies remains limited. This is, in part, due to the difficulties associated with maintaining obligate pathogens, and the logistical constraints involved in the genotyping of these species (e.g. obtaining DNA of sufficient quantity and quality). To gain an evolutionary and ecological perspective of downy mildews, adaptable methods for the genotyping of their populations are required. Here, we describe a targeted enrichment (TE) protocol to genotype isolates from two *Pseudoperonospora* species (*P. cubensis* and *P. humuli*) using less than 50 ng of mixed pathogen and plant DNA for library preparation. We were able to enrich 736 target genes across 101 samples and identified 2,978 high-quality SNP variants. Using these SNPs, we detected significant genetic differentiation (AMOVA, p=0.01) between *P. cubensis* subpopulations from *Cucurbita moschata* (clade I) and *Cucumis sativus* (clade II) in Michigan (U.S.). No evidence of location-based differentiation was detected within the *P. cubensis* (clade II) subpopulation of Michigan. However, a significant effect of location on the genetic variation of the *P. humuli* subpopulation was detected in the state (AMOVA, p=0.01). Mantel tests found evidence that the genetic distance among *P. humuli* samples was associated with the physical distance of the hop yards from which the samples were collected (p=0.005). The differences in the distribution of genetic variation of the *P. humuli* and *P. cubensis* subpopulations of Michigan suggest differences in the dispersal of these two species.

The TE protocol described here provides an additional tool for genotyping obligate biotrophic plant pathogens and the execution of new genetic studies.

INTRODUCTION

Downy mildew (DM) pathogens (*Peronosporaceae*) cause foliar disease in several agronomically important plant species (Gent et al., 2009; Kanetis et al, 2013; Kunjeti et al., 2016; Lane et al., 2005; Rivera et al., 2016; Wallace & Quesada-Ocampo, 2017; Wong & Wilcox, 2001). The group is comprised of at least twenty different genera representing a large portion of the described pathogenic species of oomycetes (Thines, 2014; Choi and Thines, 2015). All DM species are considered obligate biotrophs, growing only in association with living host tissue (Bourret et al., 2018). Over the past decade, several studies have provided key insight into DM biology, including virulence mechanisms (Savory et al., 2012; Baxter et al., 2010; Burkhardt & Day, 2016; Purayannur et al., 2020), host specificity (Choi and Thines, 2015; Summers et al., 2015b; Rivera et al., 2016; Wallace et al., 2020), and fungicide resistance (Gisi and Sierotzki, 2008; Blum et al., 2011). Despite this progress, several unresolved research questions in ecology and evolution remain, many of which could be addressed with emerging genomic and genetic approaches.

Recent technological advances in high-throughput sequencing have facilitated the genotyping of dozens of samples and the analysis of whole plant-pathogen genomes (Savory et al., 2012b; Sharma et al., 2015; Rivera et al., 2016; Withers et al., 2016; Cui et al., 2019; Fletcher et al., 2019; Rahman et al., 2019). The recent availability of genome-wide sequence information from multiple individuals of the same species has facilitated population genomic studies of several plant pathogens

(Grünwald et al., 2017; Tabima et al., 2018; Carleson et al., 2019; Gent et al., 2019). Whole or reduced representation genome sequencing technologies have become increasingly popular to monitor genetic changes in plant-pathogen populations. However, these technologies have not been broadly used to study DM populations due to difficulties in obtaining sufficient amounts of DNA from single obligate biotrophic individuals (Milgroom, 2015).

Traditionally, other genotyping technologies that require significantly lower inputs of DNA such as Sanger sequencing and microsatellites (SSRs) are used with DNA extracted from fresh and stored symptomatic tissue to study DM populations (Quesada-Ocampo et al., 2012; Kitner et al., 2015; Naegele et al., 2016; Rivera et al., 2016; Wallace and Quesada-Ocampo, 2017; Wallace et al., 2020). However, these approaches are limited by the relatively low number of variants that can be obtained when compared to genome-wide sequencing options. DNA from symptomatic tissue can be used for sequencing with high-throughput sequencing technologies but the low concentration of pathogen DNA and large amounts of exogenous material (e.g. plant and bacterial DNA) can add further expense and complexity to the sequencing and bioinformatic analysis (Stassen et al., 2012).

The quality of high-throughput sequencing data depends on the quality and purity of the DNA sample, which means that the target pathogen is ideally present in higher amounts when compared to the host plant before DNA extraction (Jouet et al., 2019). A spore propagation approach using detached susceptible leaves can be used to propagate bulk amounts of DM sporangia from which additional pathogen DNA can be recovered (Summers et al., 2015b; Thomas et al., 2017a; Gent et al., 2019); however,

multiple growing cycles (7-10 days/cycle) are needed making this approach time consuming and labor-intensive (Ali et al., 2011; Gent et al., 2019). Spore propagation is most successful when using freshly collected symptomatic leaves, but propagating sporangia from samples stored over long periods of time or under poor conditions (e.g. samples stored >-80 C) can be complicated. Additionally, sporangial propagation requires continuous maintenance of fresh sporangia on a highly susceptible host, which may bias the genetic composition of the populations under study due to the selection of genotypes by the host and the propagation conditions (Jones et al., 2014; Thomas et al., 2017a). While sporangial propagation can provide large amounts of high-quality DNA needed for sequencing, this approach is impractical for population studies requiring a large number of samples collected over time (i.e. years).

Sequence capture methods may provide a solution for genotyping DM pathogens that excludes non-target DNA while also facilitating high coverage sequencing of several target loci (Kozarewa et al., 2015; Lim & Braun, 2016). These techniques use affinity probes (RNA/DNA) to isolate particular sequences of interest ("target regions") out of a larger pool of DNA fragments (DNA library). Sequence capture methods such as target enrichment (TE) have been used across a variety of genomic studies with model (Gnirke et al., 2009; Clark et al., 2011) and non-model organisms (Faircloth et al., 2015; McCormack et al., 2016; Starrett et al., 2017) and have also facilitated the study of museum specimens with low amounts of poor quality DNA (Cruz-Dávalos et al., 2017). Additionally, sequence capture methods have also been used to study the genetic variation of other plant pathogens such as *Phytophthora infestans*, *Phytophthora □apsica* (Thilliez et al., 2019), and the obligate biotroph *Albugo candida*

(Jouet et al., 2019). These techniques could facilitate the study of DM pathogen populations using symptomatic tissue samples, alleviating the need for sporangial propagation and expanding the type and condition of the samples used.

In this study, we evaluated the genotypic variation of two DM species of the genus *Pseudoperonospora* using TE sequencing. *Pseudoperonospora cubensis* and *Pseudoperonospora humuli* infect cucurbits and hops, respectively, worldwide and are considered the most economically important species of the genus *Pseudoperonospora* (Choi et al., 2005; Mitchell et al., 2011). *P. cubensis* (clades I and II) causes foliar blight (DM) of cucumber (*Cucumis sativus*), melon (*Cucumis melo*), pumpkin (*Cucurbita maxima*), watermelon (*Citrullus lanatus*), and squash (*Cucurbita moschata*) (Summers et al., 2015b; Thomas et al., 2017a; Wallace et al., 2020). *P. humuli* negatively impacts hop (*Humulus lupulus*) cone yield (Gent et al., 2010). We describe an optimized TE procedure for sequencing DM and a bioinformatic pipeline for population genetic analyses using TE data. Evaluation of the structure, diversity, and reproduction of *P. cubensis* and *P. humuli* populations in Michigan was of particular interest.

MATERIALS AND METHODS

Sample collection and DNA extraction. Over a 12 year period (2007-2009, 2012-2013, 2015, and 2018-2019). *P. cubensis* sporangia were obtained from symptomatic cucurbit tissue collected in Michigan, other U.S. states (Indiana, Iowa, Ohio, Florida, and Wisconsin) and one Canadian province: Ontario (Fig. 4-1 A; Supplementary Table 4-1). Sporangia were harvested by gently rinsing infected leaves exhibiting multiple lesions and pathogen signs using a Preval spray power unit (Preval, Chicago) filled with distilled water as described by Mitchell et al. (2011). Dislodged

sporangia were transferred into a centrifuge tube (2 mL), pelleted (14000 rpm for 5 min, 5424 Centrifuge, Eppendorf) and subjected to DNA extraction. A second group of samples was processed by excising single lesions using a sterile scalpel. Sporangia from each lesion were harvested by vigorously shaking the microcentrifuge tube (2 mL) containing the tissue and 1 mL of distilled H_2O for 30 s. Dislodged sporangia were pelleted (14000 rpm for 5 min, 5424 Centrifuge, Eppendorf) and subjected to DNA extraction.

P. humuli samples were processed using methods similar to those described by Chee et al. (2006). Sporangial suspensions were obtained from diseased basal shoots collected from six commercial hop yards and a hop research plot located in Michigan. The three hop yards in the north region were located within a radius of approximately 25 km (hop yards A, B and C) (Fig. 4-1 B). The two hop yards in the west region of the state were separated by approximately 100 km and operated by the same producer (hop yards D and E) (Fig. 4-1 B). The sixth commercial hop yard was located in the east region (hop yard F) and was located approximately 80 km from the research plot (hop yard G) located in the central region (Fig. 4-1B). Diseased basal shoots were brought to the laboratory, stems placed into beakers of water, and shoots individually covered with a plastic bag overnight to induce sporulation. The following day, sporangia were washed from the abaxial leaf surface using a Preval spray power unit filled with distilled water. Sporangial suspensions from single shoots were transferred into centrifuge tubes (2 ml) and pelleted by centrifugation (14000 rpm for 5 min). All DNA extractions were performed on the pelleted sporangial suspensions using the NucleoSpin Plant II

isolation kit (Macherey-Nagel, Bethlehem, PA, U.S.) following manufacturer's instructions.

DNA library construction.

TE libraries: Whole DNA was extracted from 275 samples as described above and quantified using a Qubit 2.0 fluorimeter (Thermo Fisher Scientific). Before fragmentation of DNA using a M220 Focused-ultrasonicator (Covaris, Woburn, MA, U.S.) the presence of *P. cubensis* and/or *P. humuli* in the samples was confirmed by sanger sequencing of the ITS region as described by Quesada-Ocampo et al. (2012). A subset of five samples were divided in two individual tubes and submitted independently for library preparation and enrichment. These samples were used to estimate the number of errors introduced into a sample during the TE workflow. Sequencing libraries were prepared using the KAPA HyperPrep library sequencing preparation kit (Kapa/Roche, Pleasanton, CA, U.S.) following the manufacturer's recommendations and an additional KAPA Pure Bead (Kapa/Roche, Pleasanton, CA, U.S.) cleanup to ensure the libraries were free from any adapters. Insert size and library quality was verified using the Agilent 2100 Bioanalyzer (Agilent Technologies, Santa Clara, CA, U.S.). To optimize the use of the Mybaits custom kit's reactions (80bp baits, Arbor Biosciences, formerly Mycroarray Inc., Ann Arbor, MI, U.S.), good quality libraries were pooled into groups of four libraries for enrichment. Probes (baits) were designed according to manufacturer protocols (probe compatibility, repeat masking, and melting temperature filters) to cover 118 population informative DNA regions and 712 DNA regions annotated as protein genes at a 2X coverage. Protein gene sequences were obtained using bedtools (Quinlan and Hall, 2010) with the coordinates information derived from the genome annotation of *P.*

cubensis available online in the server of the Oregon State University Libraries (dx.doi.org/10.7267/N9TD9V7M; Burkhardt et al., 2014). All the genes annotated as extracellular toxins, hydrolytic enzymes, enzyme inhibitors, cell-entering RxLR effectors, cell-entering crinkler effectors, secreted proteins and transcription factors were targeted for sequencing. These regions were selected to identify annotated genes containing SNPs that may play a role in controlling host-specificity, and selectively neutral regions for population level analyses (Quesada-Ocampo et al., 2012; Kitner et al., 2015; Wallace and Quesada-Ocampo, 2017).

Hybridization of DNA libraries and probes were performed at 65 °C for 24 or 48 h (Supplementary Table 4-1). After hybridization, library pools were bound to Dynabeads MyOne Streptavidin C1 magnetic beads (Life Technologies) for enrichment. Amplification of the enriched libraries was performed using the 2X KAPA HiFi HotStart ReadyMix (Kapa/Roche, Pleasanton, CA, U.S.) and 5 µM of each TruSeq forward and reverse primers. Amplification conditions were 98 °C for 2 min, followed by 6-14 cycles of 98 °C for 20 s, 60 °C for 30 s and 72 °C for 60 s and then a final extension of 72 °C for 5 min. Following PCR, libraries were quantified using a Qubit 2.0 fluorimeter (Invitrogen). Enriched libraries were quality controlled and quantified using a combination of Qubit dsDNA HS and Caliper LabChipGX HS DNA assays. Based on these quantifications the libraries were combined in equimolar amounts into two groups for sequencing. The first set of samples (TES1) included 62 enriched libraries with a hybridization time of 24 h. The second set (TES2) of samples included 72 enriched libraries with a hybridization time of 48 h (Supplementary Table 4-1). Both sets were quantified using the Qubit 2.0 and the Kapa Biosystems Illumina Library Quantification

qPCR kit. Each set was loaded onto one line of an Illumina HiSeq 4000 flow cell and sequenced in a 2x150bp paired-end format.

Low-coverage whole-genome sequencing (Lc-WGS) libraries: In order to assess the performance of TE in comparison to Lc-WGS and to estimate the amount of exogenous material in the DNA samples, ten samples of genomic DNA directly extracted from sporangial suspensions derived from individual lesions were submitted to the Michigan State University Research Technology Support Facility (MSU RTSF) for DNA library preparation and sequencing. Due to the low DNA concentration of some of the samples, the Rubicon ThruPLEX DNA-Seq library preparation kit (Takara Bio, Mountain View, CA, U.S.) was used to prepare the sequencing libraries. Library preparation was performed following manufacturer's recommendations with an additional AMPureXP bead cleanup (Beckman Coulter, Indianapolis, IN, U.S.). Completed libraries were quality controlled and quantified using a combination of Qubit dsDNA HS (Thermo Fisher Scientific/Life Technologies, Carlsbad, CA, U.S.) and Caliper LabChipGX HS DNA assays (PerkinElmer, Waltham, MA, U.S.). Based on these quantifications the libraries were grouped in equimolar amounts into two pools that were quantified using the Kapa Biosystems Illumina Library Quantification qPCR kit (Kapa/Roche, Pleasanton, CA, U.S.). Each pool was loaded into one lane of an Illumina MiSeq standard flow cell (v2) (Illumina, San Diego, CA, U.S.) and sequencing was performed in a 2x250bp paired end format using a v2 500 cycle MiSeq reagent cartridge (Illumina, San Diego, CA, U.S.).

Genotyping and variant calling. In order to assess the performance of TE for the genotyping of *P. cubensis* and *P. humuli*, we analyzed the data in combination with

previously published whole-genome sequencing (WGS) data generated for a comparative genomic analyses of *P. cubensis*. This data set included a total of 10 samples collected from different cucurbits in the U.S. states of Alabama, South Carolina (N=2), Florida, North Carolina (N=2), Georgia, California, New York and Oregon. The datasets can be found in the bioprojects PRJNA360426 (Thomas et al., 2017) and PRJNA675756 (this project) available online through the National Center for Biotechnology Information (NCBI). Sequencing raw reads of all libraries were trimmed and quality filtered using Trimmomatic 0.32 (Bolger et al., 2014). The publicly available *P. cubensis* (Savory et al., 2012b) and *C. sativus* genome sequences were used as references for alignment of the reads. To estimate plant contamination, high-quality reads were initially aligned to the *C. sativus* genome using the Burrows-Wheeler aligner (BWA-0.7.17) (Li and Durbin, 2009). All reads were then aligned to a reference genome of *P. cubensis* containing only the contigs where the target genes are located. Clean reads of the Bioproject PRJNA360426 were also aligned to this subset of the genome. Samtools-0.1.19 (Li et al., 2009) was used to sort the alignments and PCR duplicates were removed with Picard (https://broadinstitute.github.io/picard/). Coverage depth was calculated using BEDTools-2.27.1.

The Next Generation Sequencing Plugin (NGSEP) for analysis of high-throughput sequencing data was used for calling SNPs and producing the variant call format file (VCF) (Perea et al., 2016). The VCF file generated was filtered using the NGSEP plugin in order to retain the most informative SNPs of sufficient quality. Only biallelic SNPs, present in 70% of samples, with a minimum quality of 40 were retained. The resulting VCF file was imported into R using the package *vcfR* (version 1.5.0)

(Knaus and Grünwald, 2017). Missing genotype data were deleted before further analysis (Tabima et al., 2018). Samples with more than 40% of missing variants were removed from the analysis to retain the maximum number of SNPs. Variants with more than 75% of missing information across samples were also removed. To increase the stringency for the genotyping, we excluded all the samples with an average coverage below 50X. A nonparametric Kruskal-Wallis rank-sum test was used to assess the differences among the mean coverage depth across libraries.

Population Assignment. *P. cubensis* samples were assigned to several different subpopulations depending on the analyses. To study the distribution of the genetic variation by host, *P. cubensis* samples were assigned to subpopulations according to its host species. To study the distribution of the genetic variation by geographic location, only the *P. cubensis* samples collected from *Cucumis* spp. were used. The samples collected in the U.S. states of Michigan, Wisconsin, Indiana, Ohio, and the Canadian province of Ontario, CA, were assigned to the Midwest subpopulation (Fig, 4-1 C). Midwest samples excluding those from Michigan were assigned to the Midwest-w/o-MI subpopulation (Fig. 4-1 C). Samples from Michigan were further divided into three subpopulations according to the region of collection (east, west and central) (Fig. 4-1 C). Samples collected from Iowa, Alabama, Oregon, California, South Carolina, Florida, New York, North Carolina, and Georgia, were assigned to their respective state of origin.

P. humuli samples were assigned to either the north or west subpopulation based on their location of collection in Michigan (Fig. 4-1 B, C; Table 4-2; Supplementary Table 4-1). Three hop yards (A, B and C) were located within a radius of

approximately 25 km and comprised the north subpopulation (Fig. 4-1 C). Hop yards D and E in southwest Michigan are operated by one producer and make up the west subpopulation (Fig. 4-1 C). Representative samples from central, east Michigan and Oregon were also included in our analysis.

Genetic differentiation and population structure. The filtered SNPs were used to construct a genetic tree based on Nei's genetic distance (Nei, 1972) and visualize the genetic relationship among all samples, 1000 bootstrap replicates were performed to obtain branch support (Kamvar et al., 2015). Clone-correction was performed by collapsing samples to the average genetic distance detected between technical replicates of sequencing. For this, the "mlg.filter" function of the R package *Poppr* (version 2.4.1) was used with a bitwise distance equal to 0.02 and the farthest neighbor algorithm. Ordination plots based on principal component analysis (PCA) were also constructed to visualize the differentiation of samples within and among subpopulations from different host or regions across the Midwest (Fig. 4-1 C). Three distinct PCAs were constructed to visualize the relationship among i) all *P. cubensis* and *P. humuli* samples by host ii) all *P. cubensis* samples collected from *C. sativus* and iii) all *P. humuli* samples collected in Michigan and Oregon. The PCAs were performed using the "glPca" function of R package Adegenet (Jombart and Ahmed, 2011) and the ordination plots were constructed using the R package Ggplot2. Samples were colored according to host or subpopulations and ellipses of 90% confidence intervals were drawn on the ordination plots.

Genetic differentiation between and within subpopulations was quantified using hierarchical F-statistics (*hierfstat* version 0.04.-22, Goudet, 2005) and analysis of

molecular variance (AMOVA) (*poppr* version 2.4.1, Kamvar et al., 2014) in R version 3.6.1. To test the hypothesis that the *Pseudoperonospora spp.* populations are differentiated by host, we performed an AMOVA and calculated F_{ST} statistics using all the samples collected by *P. cubensis* and *P. humuli* grouped by host. Similarly, to test the hypothesis that the *P. cubensis* subpopulation from *C. sativus* in Michigan is differentiated by geographic location, we performed an AMOVA and calculated F_{ST} statistics using the samples from the Michigan's subpopulations (east, west and central) and the Midwest-w/o-Mi subpopulation. Population differentiation among the *P. humuli* subpopulations of Michigan (north and west) was analyzed in the same way. A Mantel test (Mantel, 1967) was performed to evaluate the relationship between the genetic distance of the samples and the physical distance of the location where the samples originated. This analysis was performed for each species independently (*P. cubensis* and *P. humuli*) using only the samples collected in Michigan. The Mantel test was performed as described by Gent et al. (2019) using the "mantel.rtest" function of the ade4 package (Dray and Dufour, 2007). The genetic and Euclidean-geographic distance matrices were created with the function "bitwise.dist" (Kamvar et al., 2014) and "dist", respectively. Physical distances were calculated using the coordinates of each sample location.

Genotypic diversity. Genotypic diversity was determined using the filtered SNP data (not clone corrected) using the R package *Poppr* (Kamvar et al., 2014). The diversity estimates calculated included genotypic richness (MLG), expected number of genotypes based on rarefaction (eMLG), evenness (E5) and the indices of Shannon-Wiener (Shannon, 1948), Stoddart and Taylor's (Stoddart and Taylor, 1988), and

Simpson's (Simpson, 1949). The within-population gene diversity (Hexp) (Nei, 1978) that describes the proportion of heterozygous genotypes was calculated using the function "basic.stats" of the R package *hierfstat*. The diversity estimates were calculated using i) all *P. cubensis* and *P. humuli* samples grouped by host ii) all *P. cubensis* samples collected from *C. sativus* in each Michigan subpopulation and the Midwest-w/o-Michigan subpopulation iii) the *P. humuli* samples from the north and west subpopulations of Michigan. Only categories or subpopulations with at least five individuals were included for this analysis.

Reproductive Mode. To infer the predominant reproductive mode of *P. cubensis* and *P. humuli* in Michigan (e.g., sexual, clonal, or mixed) we calculated the index of association I_A (Brown et al., 1980; Milgroom, 1996) according to Tabima et al. (2018) using only the *P. cubensis* and *P. humuli* samples collected in the state from *C. sativus* and *H. lupulus*, respectively. For this, we calculated the index of association (I_A) using a subset of 1000 random high-quality SNP and compared to the observed value of simulated populations with 0, 25, 50, 75, and 100% linkage. The mean I_A values of each species were compared independently against the mean I_A values of the simulated populations. Simulations were conducted with a dataset consisting of 2,978 loci analogous to the observed *P. cubensis and P. humuli* data. A nonparametric Kruskal-Wallis rank-sum test was used to assess the differences among means for all I_A distributions. Multiple comparisons between I_A distribution were performed using the nonparametric Kruskal- Wallis test and Tukey's honest significant difference (HSD) test.

RESULTS

Library sequencing and read mapping. The sequencing and alignment results of all libraries used in this study are summarized in Table 4-1. A total of 270 samples containing 2 – 500 ng of DNA were used for library preparation and enrichment. However, we could not generate enough enrichment products from 136 libraries, including 51 libraries prepared from samples with less than 50 ng of DNA. The remaining libraries (N=134) were enriched successfully and were prepared from samples containing 2 – 500 ng of DNA; these libraries included 92 libraries of *P. cubensis* and 42 libraries of *P. humuli* that were sequenced using two lanes of HiSeq4000.

TE libraries: 510 million paired end reads (2 X 150bp) were obtained from the sequencing of these libraries (134) generating approximately 3.9 ± 2.6 SD (standard deviation) million reads per library. A range of 35 to 54% of the reads aligned to the reference genome of *P. cubensis.* The total number of reads obtained per library was influenced by the hybridization time of the libraries with the capture probes for enrichment. The libraries that hybridized for 48 h generated almost two times more aligned reads (2.64 ± 2.6 SD million) than the libraries that hybridized for 24 h (1.34 ± 1.0 SD million) (Table 4-1). Less than 20,000 sequencing reads were generated for only eight libraries that were eliminated (six samples were hybridized for 24 h and two were hybridized for 48 h), leaving 126 enriched libraries for downstream analysis. Five percent of the reads per library that did not align to the reference genome of *P. cubensis* aligned to the *C. sativus* reference genome.

Lc-WGS libraries: Seven libraries of *P. cubensis* and two libraries of *P. humuli* were sequenced without enrichment using MiSeq (Lc-WGS) generating a total of 41 million sequencing reads (2 X 150 bp). Approximately 0.55 ± 0.37 SD million reads were obtained per library, but only 25% of them aligned to the reference genome of *P. cubensis*. Twenty-five percent of the remaining reads aligned to the *C. sativus* reference genome.

WGS libraries: A total of 350 million paired end reads (2 x 150 bp) were obtained from the bioproject PRJNA360426, that included WGS data of 9 libraries of *P. cubensis* and one library of *P. humuli.* An average of 15.6 ± 6 SD million reads per sample we obtained after sequencing. Eighty-nine percent of the total reads aligned to the *P. cubensis* reference genome and approximately 2% of the reads per sample aligned to the reference genome of *C. sativus*.

Genotyping and variant calling. SNPs were retrieved from the sequencing reads generated from 126 enriched DNA libraries and the reads obtained from the 10 libraries sequenced using whole genome sequencing (Bioproject PRJNA360426). Ninety percent of the enriched libraries were prepared from input DNA amounts between 2 to 100 ng (Fig. 4-2 B). After mapping the reads to the reference genome of *P. cubensis*, 5,957 biallelic SNPs were identified across 70% of the 136 samples. To retain the maximum number of SNPs, we excluded 31 of the samples prepared using TE as they contained more than 40% missing data (24 of these were hybridized for 24 h, with the remaining libraries hybridized for 48 h) (Table 4-1). SNPs with more than 75% of the missing data across the entire data set were also excluded. This resulted in a total of 2,978 high-quality (HQ) SNPs with <10% missing data for downstream

analysis. All HQ SNPs were located within 127 out of the 812 genes targeted, 66% of the SNPs were found within secreted and effectors proteins. The remaining 44% of the SNPs were contained within esterases (16.3%), glucanasas (3%), lyases (3%), SSRs (4%), and other (7%) genes.

The coverage depth (CD) across the 2,978 HQ SNPs was variable among samples and significant differences in the CD were observed between the libraries genotyped using TE and the libraries genotyped using WGS (Kruskal-Wallis p = 2.2e-16; Fig. 4-2 A). The enriched libraries with a hybridization time of 48 h (TES3) exhibited a significantly higher CD than the enriched libraries generated with 24 h of hybridization time (TES2) or the libraries genotyped using WGS (Kruskal-Wallis p = 2.2e-16; Fig. 4-2 A). The CD across all HQ SNPs had an average of 262 ± 546 SD and 358 ± 546 SD for the libraries with hybridization times of 24 and 48 h, respectively (Table 4-1; Fig. 4-2 A). Among the samples sequenced using WGS, the CD across HQ SNPs had an average of 180 ± 116 SD (Table 4-1). No correlation was observed between the amount of input DNA used for library preparation and the CD across HQ SNPs ($p > 0.05$, Fig. 4-2 B).

Characterization of technical error. Technical replicates were used to characterize the number of errors introduced into a sample during TE. Of the five samples with two technical replicates submitted for enrichment, only three samples (18-35, L32 and L682) and their corresponding replicates were retained after the quality filtering of the SNPs. Differences in the average coverage between technical replicates of the same sample were observed (Fig. 4-3 A), however, only a small proportion of loci were different between replicates (Fig. 4-3 B). On average, 30 SNPs (out of 2,978 total

SNPs) differed between technical replicates, suggesting an error rate of roughly 1% within the high-quality variants.

Genetic differentiation and population structure . In the genetic distance tree of HQ SNPs (2,978) all 101 samples genotyped fell into one of two clades (100% bootstrap support); either *P. cubensis* (67 samples) or *P. humuli* (34 samples) (Fig. 4-4). Within the *P. cubensis* clade, samples were either clade I or II of *P. cubensis* (Thomas et al., 2017). The majority of samples from *Cucumis* spp. aligned with clade II of *P. cubensis*, while the remaining samples collected from *C. moschata* and *C. lanatus* aligned with clade I (Fig. 4-4).

Samples in the ordination plot formed 3 clusters corresponding to *P. humuli*, *P. cubensis* clade I, and *P. cubensis* clade II; these clusters were consistent with the stratification by species and within *P. cubensis* by host in the genetic distance tree (Fig. 4-5 A). F-statistics ($F_{ST} > 0.25$) and AMOVA detected significant genetic differentiation ($P = 0.01$) between pathogen species, supporting the clustering of the ordination plot (Table 4-3). Stratification by host was supported by a high level of genetic differentiation among samples collected from *Cucumis* spp. and samples collected from *C. moschata* ($F_{ST} = 0.11$, Table 4-3). AMOVA revealed that 78% of the total genetic variance was significantly associated with differences between host within *P. cubensis* ($P = 0.01$, Table 4-4).

All *P. cubensis* samples collected from *C. sativus* in the Midwest including Michigan and the reference sample from Florida clustered loosely together across all four quadrants of the ordination plot (Fig. 4-5 B). However, the reference samples from North Carolina and California clustered separately from each other and were not

contained within the 90% confidence ellipses of the other subpopulations (Fig. 4-5 B). More than 70% of the samples from the subpopulations of the central and east Michigan were contained within the 90% confidence ellipse of the Midwest-w/o-MI subpopulation (Fig. 4-5 B); however, only 40% of the samples from west Michigan were contained within the ellipse of the of the Midwest-w/o-MI subpopulation. AMOVA did not support significant genetic differentiation among the subpopulations of *P. cubensis* from *C. sativus* in Michigan and the Midwest-w/o-MI subpopulation (P = 0.21). Only 1% of the total genetic variance was associated with difference among subpopulations (or regions) (Tables 4-6 and 4-7).

The clone correction of all *P. cubensis* samples collected from *C. sativus* (N=57) resulted in 40 MLGs, 23% of which were detected in multiple subpopulations (Fig. 4-6 A, B). MLG 100 was detected in west Michigan and the Midwest-w/o-MI subpopulations (Fig. 4-6 A). The subpopulation of west Michigan also shared three MLG with the subpopulation of east Michigan (MLG 27, 36 and 46) (Fig. 4-6 A). The subpopulations of east and central Michigan shared MLG 33 and MLG 91 and two identical samples corresponding to MLG 47 were detected in two distant areas of the Midwest-w/o-MI subpopulation (i.e. Indiana and Ontario) (Fig. 4-6 A). Additionally, the MLG 29 from Florida was also detected in the east Michigan subpopulation (Fig. 4-6 A). Supporting these findings, the Mantel test did not detect a significant relationship between the genetic and physical distances of the *P. cubensis* samples collected from *C. sativus* in the Midwest (P = 0.454, Fig. 4-7 A).

The level of genetic differentiation among *P. humuli* samples from Michigan and Oregon (Fst = 0.0168) was higher when compared to the genetic differentiation

detected among *P. cubensis* samples from *C. sativus* originating in the Midwest, California, Florida and North Carolina (Fst = 0.0024). In the ordination plot of all the *P. humuli* samples, most samples from the subpopulation of west Michigan were loosely dispersed in the left quadrants while most samples from the subpopulation of north Michigan (75%) were clustered tightly in the right quadrants (Fig. 4-5 C). Only two samples from the north subpopulation were contained within the 90% confidence ellipse of the west subpopulation (Fig. 4-5 C). The samples from central and east Michigan were either contained in the ellipses from the north or west subpopulations. The reference sample from Oregon was not contained within the 90% confidence ellipse of Michigan subpopulations (Fig. 4-5 C). These patterns were supported by AMOVA in which significant genetic differentiation between the subpopulations of north and west Michigan was detected (P=0.01, Table 4-9). A total of 11.25% of the genetic variance was significantly associated with differences among subpopulations and only 2.5% of the variance was associated with differences among hop yards within a subpopulation (Table 4-10). This suggests that the geographic region has a significant effect on the structure of the *P. humuli* population in Michigan.

Clone correction of the 34 *P. humuli* samples resulted in 23 MLGs, only one of them (MLG 4) was detected in two different subpopulations (Fig. 4-6 C, D). Only two different MLGs were shared among hop yards within regions. MLG 3 was detected in two different years at the three yards in north Michigan and MLG 59 was detected once in the two hop yards sampled in west Michigan (Fig. 4-6 C). The Mantel test supported the hypothesis that the genetic distance among *P. humuli* samples collected in Michigan

was significantly associated (P= 0.0042) with the geographic distance among hop yards (Fig. 4-7 B).

Genotypic diversity. The highest level of genotypic diversity was observed among the samples of *P. humuli* followed by *P. cubensis* clade I and *P. cubensis* clade II (Table 4-5). Each species or clade consisted of different MLGs spread relatively evenly. This was reflected in the estimates of genotypic richness (eMLG= 6 to 9.54) and evenness (E_5 > 0.8) (Table 4-5). The Shannon-Wiener index, Stoddart and Taylor's index, and Simpson's index were highest among *P. cubensis* clade II samples, followed by *P. humuli* samples, and then *P. cubensis* clade I samples (Table 4-5). The greatest expected heterozygosity or proportion of heterozygous genotypes expected was observed among *P. humuli* samples followed by *P. cubensis* clade I samples, and then *P. cubensis* clade II samples (Table 4-5).

The Michigan subpopulations and the Midwest-w/o-MI subpopulation of *P. cubensis* collected from *C. sativus* exhibited similarly low levels of expected heterozygosity and genotypic diversity (Table 4-8). Expected heterozygosity ranged between 0.178 and 0.197 while genotypic richness (eMLG) ranged between 6 to 9.57. The east Michigan subpopulation had the greatest expected heterozygosity (Hexp= 0.197) followed by Midwest-w/o-MI (Hexp= 0.190), west Michigan (Hexp= 0.189), and central Michigan subpopulations (Hexp= 0.178) (Table 4-8). The east Michigan subpopulation had the highest genotypic richness (eMLG), while west Michigan and the Midwest-w/o-MI subpopulations had larger sample size and lower number of MLGs (Table 4-8). The Shannon-Wiener index, Stoddart and Taylor's index, and Simpson's index were all highest for the west Michigan subpopulation, followed by the

subpopulations of east Michigan, Midwest-w/o-MI, and then central Michigan (lowest indices) (Table 4-8). The highest evenness (E_5) was detected for the central Michigan subpopulation followed by the subpopulations of east Michigan, west Michigan and Midwest-w/o-MI (lowest E_5) (Table 4-8).

The genotypic diversity varied more widely across the *P. humuli* subpopulations of Michigan (eMLG = 5 to 11) compared to the variation detected among *P. cubensis* subpopulations (eMLG = 6 to 9.57). The expected heterozygosity among the subpopulations of *P. humuli* was higher and ranged between 0.206 to 0.220. The subpopulations of north (Hexp= 0.224) and east-central Michigan (Hexp= 0.220) had the greatest expected heterozygosity followed by the subpopulation of west Michigan (Hexp= 0.206) (Table 4-11). The subpopulation of west Michigan had the highest genotypic richness, while the north Michigan subpopulation had the largest sample size and the most MLGs. The Shannon-Wiener index, Stoddart and Taylor's index, and Simpson's index were all highest for the north Michigan subpopulation, followed by the subpopulations of west and east-central Michigan (lowest indices) (Table 4-11). The highest evenness (E5) was detected in the subpopulations of west and east-central Michigan followed by the north Michigan subpopulation (lowest E5) (Table 4-11).

Reproductive Mode. To determine whether allelic variants were randomly associated as expected in populations with a sexual mode of reproduction (low linkage), we calculated the mean index of association across loci for each species in Michigan and compared to the estimated index of association of simulated populations under strong linkage (100% linked loci), moderate linkage (75 and 50% linked loci), and low linkage (25% and 0 loci under linkage) (Fig. 4-8). Upon comparison, significant

differences were observed between the mean index of association (IA) of each species and the mean values estimated for the simulated populations (*P. cubensis*, P < 2.2e-16 and *P. humuli,* P < 2.2e-16). The IA mean value of the *P. cubensis* samples was situated between the IA mean values of the simulated data with 50 and 75% linkage (Fig. 4-8 A). This indicated that populations of *P. cubensis* have a mixed-mode of reproduction with a predominantly clonal phase. The IA mean value of the *P. humuli* samples was not significantly different to the simulated data with 25% linkage (Fig. 4-8 B), suggesting that the populations of *P. humuli* may have a mixed mode of reproduction that could be predominantly sexual.

DISCUSSION

Technological advances in genome sequencing have accelerated the cataloging of genomic variation of plant pathogens, however, extracting large amounts of high-quality DNA from obligate pathogens responsible for DM is challenging, and hampers their genotyping using next-generation sequencing. We adapted a TE method that facilitated the sequencing of 736 genes annotated as virulence factors in the genome of *P. cubensis*. We used this method to sequence *P. cubensis* and *P. humuli* DNA extracted from sporangia collected from plant tissue with signs of the pathogen. This approach facilitated the genotyping of samples that contained very low amounts of pathogen DNA mixed with other environmental contaminants (i.e. plant DNA, bacteria DNA). After aligning the sequenced DNA, we identified 2,978 SNPs and resolved the population structure of *P. cubensis* and *P. humuli* in Michigan. A significant effect of location on the genetic variation of *P. humuli* was detected and the genetic distance among samples was associated with the physical distance of the hop yards. Evidence

of location-based differentiation within Michigan was not detected for the *P. cubensis* population.

By using affinity probes and several amplification cycles, our TE protocol was designed to provide high coverage sequencing of specific loci in the *P. cubensis* and *P. humuli* genome. This facilitated the sequencing of a low amount of target (pathogen) DNA from environmental samples containing a significant amount of contaminant DNA from plant tissues and other microorganisms. Sequencing DNA directly from environmental samples reduces time, labor, and DNA input required for other sequencing approaches such as genotyping by sequencing (GBS) or WGS (Summers et al., 2015b; Thomas et al., 2017a; Gent et al., 2019). This is particularly advantageous for DM, as other sequencing approaches (GBS, WGS, Rad-Seq) rely on large amounts of high-quality DNA that can only be obtained using a laborious propagation procedure (Thomas et al., 2017a; Gent et al., 2019). Using TE, several samples with less than 50 ng of DNA were successfully genotyped. Most of the samples that failed were leaf lesions containing few or no sporangia (*P. cubensis* had been previously confirmed via qPCR). The TE protocol also enabled the genotyping of samples that were no longer viable for propagation, expanding the number of samples that could be genotyped including those collected more than ten years ago.

Using a reduced amount of DNA (2 to 100x less), the samples sequenced after TE reached similar sequencing coverage when compared to the samples sequenced using a WGS approach, at the region's target (250x). However, the enriched samples required 6 to 7 times less space for sequencing (60 to 70 samples per lane of HiSeq) compared to the space used for the sequencing of libraries using WGS (10 samples per

lane of HiSeq). This was possible because TE reduced the complexity of the *P. cubensis* genome from 88.22 MB to < 1MB (i.e. 1.13% of the genome). This reduction in the genome complexity and the enrichment of up to four samples in a single enrichment experiment (MyBaits) make TE a cost-effective alternative to WGS.

However, we did find that our TE protocol can result in a higher number of sequencing errors per sample compared to WGS. The high number of amplification cycles used for the enrichment of samples with low amounts of DNA may have led to the introduction of PCR errors and a subsequent reduction in genotyping accuracy. Typically, high-throughput sequencing (e.g. WGS and GBS) without enrichment of samples with low amounts of DNA (<250ng) requires an average of 14 PCR cycles, however, 6-14 extra cycles were used after library construction in our TE protocol (for a total of 20-28 cycles). Thus, possibly due to the high number of extra amplification cycles, the samples genotyped using TE were subject to an error rate of approximately 1%, an error rate 10 times higher than the estimated error rate for high-throughput sequencing data of >0.1% (Grünwald et al., 2017; Ma et al., 2019).

Despite an error rate of 1%, the genetic distance between samples in 95% of cases was greater than the distance generated due to PCR errors, providing confidence that our findings reflect patterns linked to the pathogen biology than an artifact of sequencing. Using TE, we detected a significant effect of host in the population structure of *P. cubensis*, and the samples collected from *C. sativus* were genetically different from the samples collected from *C. moschata*. These results support previous studies that have shown that the structure of the *P. cubensis* population is driven by host preference, with samples from *Cucumis* spp. and *C. moschata* belonging to two

distinct evolutionary clades (Thomas et al., 2017a; Wallace et al., 2020). Thomas et al. (2017) identified two *P. cubensis* clades in the U.S.; clade I occurs on *C. pepo, C. moschata, C. maxima, C. lanatus,* and clade II occurs on *Cucumis* spp. In our analyses, all *P. cubensis* samples clustered by clades according to that distribution.

Annual CDM infections in the northern U.S. are driven by an influx of airborne *P. cubensis* sporangia from overwintering sites (Bello et al., 2020; Naegele et al., 2016; Goldenhar and Hausbeck, 2019). CDM limits cucumber yield in Michigan where 15000 ha of cucumbers are planted every year (USDA, 2020). Small, yet significant genetic differences among cucumber production regions in Michigan were previously reported (Naegele et al., 2016). However, a significant effect of location in the subpopulation structure of *P. cubensis* was not detected in the current study, suggesting no differentiation within and among Michigan's regions. An exchange of migrants has a homogenizing effect on subpopulations (Milgroom, 2015) and may occur in Michigan due to the availability of susceptible crops across the state. The detection of the same multi-locus genotypes (MLG) in multiple locations supports this hypothesis and also suggests that *P. cubensis* sporangia may be disseminated unrestricted in the state as there is no geographical barrier (e.g. mountain range or water body) that may limit the homogenizing of geographically distant populations. The wide host availability in Michigan may also facilitate the establishment of incoming MLG from other subpopulations in the Midwest. The exchange of migrants may occur among Midwestern states outside of Michigan but the absence of susceptible crops between geographically distance populations may result in lower rates of exchange and

subsequently more genetically differentiated populations. Additional sampling is needed to test this hypothesis.

Significant differences were detected between the *P. humuli* populations from the north and west Michigan regions, but we did not find any evidence of genetic differentiation among hop yards within the same region. In Michigan, approximately 400 ha of hops are planted across more than 50 commercial hop yards (Michigan Department of Agriculture & Rural Development, 2018). A lack of differentiation among hop yards within regions could also be a consequence of the continuous exchange of *P. humuli* genotypes among them. However, despite the potential for airborne dispersal of hop DM (Bello et al, 2020; Gent et al., 2009) only one MLG was detected in multiple hop yards within the same region. This is consistent with the restricted pattern of dispersal suggested for this pathogen; new infections of hop plants by *P. humuli* are less likely to occur far from their inoculum source (Johnson et al., 1991). We detected a significant correlation between the genetic and geographic distance of *P. humuli* samples, providing circumstantial evidence of a higher probability for new *P. humuli* infections to occur close to their inoculum source.

In Oregon, Gent et al. (2019) found significant genetic differences between hop yards planted within 10 km of each other and a low amount of population differentiation between hop yards established from the same planting material. This suggests that infected hop plant material may be a more important source of primary inoculum than airborne migration for DM. Most of the hop yards sampled for this study were among the first yards establish from rhizomes in the mid-2000s when commercial hop production returned to Michigan and very few sources of propagation material were available

(Sirrine et al., 2014). As the hop industry matured in the state, new sources of propagation material became available, but still in limited numbers. The lack of genetic differentiation among hop yards within regions in Michigan may be a result of the introduction of a reduced number of genotypes via planting material from the same origin source into multiple hop yards. The detection of the same MLGs in multiple hop yards and relatively low genetic diversity of north Michigan partially support this hypothesis but further sampling and more information on sources of plant material are needed to verify this hypothesis in Michigan.

The restricted airborne dispersal of *P. humuli* sporangia compare to *P. cubensis* could be attributed to the cultivation practices and geographic distribution of hops. Generally, diseased basal shoots are close to the ground and during most of the season sheltered within a canopy of healthy basal shoots that hamper dispersal (Johnson et al., 1991). Additionally, the area planted with hops in the state is equivalent to only 2% of the area planted with cucumbers. This lower host availability may result in reduced *P. humuli* sporangia production compared to *P. cubensis* and lower aerial exchange of MLG among subpopulations. The restricted exchange of MLG can result in genetically differentiated subpopulations (Milgroom, 2015).

The relatively low level of genetic differentiation and genetic diversity detected within the *Pseudoperonospora* spp. populations of Michigan is consistent with the clonal reproductive mode of *P. cubensis* and inbreeding reproductive mode of *P. humuli* (Naegele et al., 2016; Gent et al., 2019). Although we estimated relatively low indices (65%) of association for both species that suggest they experience a sexual phase, especially *P. humuli*, we believe these values are an artifact of our sampling strategy.

Our samples were collected from a bulked inoculum of multiple leaf lesions (cucurbits) or diseased shoots (hops), so it is likely that our sample units may contain multiple genotypes creating an effect of random mating (no linkage-disequilibrium). An earlier study of *P. humuli* populations in the Pacific Northwest that used a similar sampling strategy compared to our study and suggested that the *P. humuli* population of Oregon was reproducing sexually (Chee et al., 2006). However, in a genetic study of *P. humuli* using more precise sample units in the same region, GBS revealed strong evidence of linkage disequilibrium (Gent et al., 2019). This is consistent with the nonrandom mating expected from species with an asexually reproducing or highly inbreed mode (Gent et al., 2019). Similarly, Wallace et al. (2020) provided evidence of non-random mating or recombination consistent with selfing or asexual reproduction for *P. cubensis* clade II.

Future studies using TE should consider the use of a single lesion as a sample unit and sequencing selectively neutral regions (Grünwald et al., 2016). We included 94 regions (genes) containing small sequence repeats (SSRs) markers among the regions targeted for sequencing, as SSRs can provide less biased estimates of population differentiation due to their neutrality. However, the sequencing of these regions was of poor quality and we could not detect SSRs within them. Instead, we found 115 SNPs within these regions that were not significantly differentiated among or within subpopulations (data not shown). Most of the signal of population differentiation was found within 66% of the HQ SNPs used, these SNPs were contained within secreted proteins or effector genes that corresponded to 10% of the genes targeted. Thus, we encourage the use of neutral polymorphic regions more evenly distributed across the genome.

We also recommend the use of a higher number of baits for enrichment when working with low concentrations of target DNA and the quantification of plant and pathogen DNA using qPCR before library preparation. More baits should increase the sequencing coverage across samples, facilitating the calling of variants. Similarly, the utilization of samples with a higher amount of pathogen DNA relative to the amount of contaminating DNA could increase the chances for the successful preparation of libraries using TE. Future studies should also include more technical replicates to assess error due to batch effects as the high number of amplification cycles resulted in lower genotyping accuracy. The introduction of technical replicates from multiple generations of clones is also advised. This is critical when working with high-throughput sequencing data due to the introduction of false mutations in the data that could create additional multi-locus genotypes (Gent et al., 2019; Potapov and Ong, 2017).

In summary, our results reveal the key strengths of TE for the genotyping of DM. This approach provides a solution for the genotyping of obligate biotrophic pathogens; for which high-throughput sequencing is typically constrained by the low amounts of target DNA and high amounts of non-target (contaminating) DNA. TE provides a cost-effective approach for the genotyping of unpurified field samples and the assessment of sequence polymorphisms across a large number of individuals. This method could be adapted to a diverse group of pathogens even without a reference genome. Future population studies using TE should carefully consider the sampling strategy and the size and complexity of the genomic regions targeted. Including technical replicates will also be important to ensure the accurate genotyping of the samples after enrichment and the reproducibility of the experiments.

APPENDIX

APPENDIX

Table 4-1. **Sequencing and alignment results from libraries sequenced using target enrichment (TE), low coverage whole genome sequencing (Lc-WGS) and whole-genome sequencing (WGS)**

Sequencing characteristics	TE set[a] 1	TE set 2	Lc-WGS	WGS[b]
Sequencing platform	HiSeq4000	HiSeq4000	MiSeq.v2.300	HiSeq
Sequencing format (bp)	2x150	2x150	2x150	2x100
Sequencing lines	1	1	2	1
Expected sequencing output per lane (Gbp)	105	105	3.6 – 4.5	105
Input amount of DNA for library preparation	5-400 ng	5-400 ng	< 50 ng	> 1 µg
Hybridization time with probes (baits)	24 h	48 h	--	--
Total number of libraries sequenced	62	72	9	10
Total number of clean reads (millions)	211	290	41	350
% Reads aligned to reference genome of *P. cubensis*	35%	54%	25%	89%
% Reads aligned to reference genome of *C. sativus*	< 5%	< 5%	> 25%	2%
Aligned reads per samples ± SD (millions) [c]	1.34 ± 1.0	2.64 ± 2.6	0.55 ± 0.37	16.6 ± 18
% Libraries with high quality SNPs [d]	61%	84%	--	100%
Average coverage among high quality SNPs ± SD [e]	262 ± 546	358 ± 546	--	180 ± 116

[a]Target enrichment set with hybridization times of 24h and 48h
[b]All the sample genotyped using whole-genome sequencing were retrieved from the bioproject PRJNA360426.
[c]Millions of reads aligned to the reference genome of *Pseudoperonospora cubensis* per sample.
[d]Libraries (%) retained containing 2,978 high quality SNPs.
[e]Average coverage among high quality SNPs within the libraries retained.

Table 4-2. **Plant hosts and the location of the 101 samples of *Pseudoperonospora* spp. samples used for the population analyses[a]**

Pathogen and host species	West Michigan	East Michigan	North Michigan	Central Michigan	Other states within the U.S	Total
***P. cubensis* clade I**						
Cucurbita spp*. and Citrullus lanatus*	1	1	0	0	6	8
***P. cubensis* clade II**						
Cucumis spp.	20	15	0	6	18	59
P. humuli						
Humulus lupulus	8	0	20	5	1	34
Total[a]	**34**	**25**	**20**	**11**	**11**	**101**

[a]The total of samples reflects the sum of the samples retained after quality filtering.

Table 4-3. **Pairwise F_{ST} comparisons among *Pseudoperonospora cubensis* (clade I and II) and *Pseudoperonospora humuli.***

Pairwise comparison	F_{ST}	P_{value}[a]
P. cubensis clade II *(Cucumis spp.)* vs *P. cubensis* clade I *(Cucurbita spp.)*	0.11	0.01
P. cubensis clade II *(Cucumis spp.)* vs *P. humuli (Humulus lupulus)*	0.27	0.01
P. cubensis clade I *(Cucurbita spp.)* vs *P. humuli (Humulus lupulus)*	0.25	0.01

[a]P_{values} were calculated using an analysis of molecular variance (AMOVA)

Table 4-4. **Analysis of molecular variance (AMOVA) for Pseudoperonospora *spp.* grouped by host. The significance of variance was tested from 999 permutations of the data[a].**

Source	df [b]	SSD [c]	MSD [d]	Sigma	Variance (%)[e]	P_{value}
Between host	5	4033.0104	806.60208	68.370171	78.720821	0.01
Between samples within host	10	301.9755	30.19755	2.353212	2.709468	
Within samples	85	1370.8853	16.12806	16.128063	18.569711	
Total	100	5705.8712	57.05871	86.851446	100	

[a]Sample sizes used in this analysis included 59, 34 and 8 samples collected from *Cucumis* spp., *Humulus lupulus* and *Cucurbita* spp., respectively.
[b]Degrees of freedom.
[c]Sum of squared differences.
[d]Mean of squared differences.
[e]Variance (%) was adjusted to zero for negative sigma values.

***Table 4-5*. Genotypic diversity estimates for *Pseudoperonospora* spp. samples grouped by host (clade).**

Clade/Host species	N [a]	MLG [b]	eMLG [c]	SE [d]	H [e]	G [f]	λ [g]	E_5 [h]	Hexp [i]
***P. cubensis* clade I**									
Cucurbita spp. and *Citrullus lanatus*	8	6	6	0	1.67	4.57	0.781	0.831	0.215
***P. cubensis* clade II**									
Cucucmis spp.	59	45	9.54	0.634	3.72	36.64	0.973	0.889	0.192
P. humuli									
Humulus lupulus	34	27	9.14	0.851	3.17	19.27	0.948	0.803	0.217
Total	101	77	9.7	0.533	4.24	59.65	0.983	0.86	0.206

[a]N is the number of individuals sampled of each region.
[b]MLG is the number of multilocus genotypes observed.
[c]eMLG is the number of expected MLGs at a sample size based on rarefaction.
[d]Standard error
[e]Shannon-Wiener Index (H)
[f]Stoddart and Taylor's Index (G)
[g]Simpson's index (lambda)
[h]Evenness (E_5)
[i]Within population gene diversity (Hexp).

Table 4-6. **Analysis of molecular variance (AMOVA) of Midwest subpopulations[a] of *Pseudoperonospora cubensis* collected from *Cucumis sativus*. The significance of variance was tested from 999 permutations of the data[a].**

Source	df[b]	SSD[c]	MSD[d]	Sigma	% variance[e]	P_{value}
Between subpopulations	3	35.30	11.76	0.012	0.125	0.21
Between samples within subpopulations	12	125.89	10.49	0.449	4.625	
Within samples	38	351.62	9.25	9.253	95.248	
Total	53	512.82	9.67	9.714	100	

[a]Sample sizes used in this analysis included 15, 19, and 6 samples collected from *Cucumis sativus* in the east, west, and central Michigan, respectively. The Midwest-w/o-MI subpopulation (17 samples) was formed by all the samples collected in the Midwest states of the U.S. and Ontario, Ca, not including Michigan
[b]Degrees of freedom.
[c]Sum of squared differences.
[d]Mean of squared differences.
[e]Variance (%) was adjusted to zero for negative sigma values.

Table 4-7. **Pairwise F_{ST} comparisons among subpopulations of *Pseudoperonospora cubensis* collected from *C. sativus* in the Midwest[a].**

Subpopulation	East Michigan	Central Michigan	West Michigan	Midwest-w/o-Michigan
East Michigan	--			
Central Michigan	0.0083*	--		
West Michigan	0.0034	0.0035	--	
Midwest-w/o-Michigan [b]	0.0025	0.0039	1E-04	--

[a]Sample sizes used in this analysis included 15, 19, and 6 samples collected from *Cucumis sativus* in the east, west, and central Michigan, respectively.
[b]The Midwest-w/o-MI subpopulation (17 samples) was formed by all the samples collected in the Midwest states of the U.S. and Ontario, Ca, not including Michigan
*Indicates a significant Fst value based on AMOVA

Table 4-8. **Genotypic diversity estimates and index of association of *Pseudoperonospora cubensis* subpopulations collected from *C. sativus* in the Midwest.**

Subpopulation	N [a]	MLG [b]	eMLG [c]	SE [d]	H [e]	G [f]	λ [g]	E_5 [h]	Hexp [i]
East Michigan	15	14	9.57	0.495	2.62	13.2	0.924	0.965	0.197
Central Michigan	6	6	6	0	1.79	6	0.833	1	0.178
West Michigan	19	16	9.07	0.772	2.7	13.4	0.925	0.893	0.189
Midwest-w/o-Michigan[j]	17	14	8.85	0.795	2.56	11.6	0.913	0.887	0.19
Total	57	44	9.54	0.638	3.69	35.7	0.972	0.886	0.192

[a]N is the number of individuals sampled of each region.
[b]MLG is the number of multilocus genotypes observed.
[c]eMLG is the number of expected MLGs at a sample size based on rarefaction.
[d]Standard error
[e]Shannon-Wiener Index (H)
[f]Stoddart and Taylor's Index (G)
[g]Simpson's index (lambda)
[h]Evenness (E_5)
[i]Within population gene diversity (Hexp).
[j]The Midwest-w/o-MI subpopulation was formed by all the samples collected in the Midwest states of the U.S. and Ontario, Ca, not including Michigan

Table 4-9. Analysis of molecular variance (AMOVA) of Michigan subpopulations of *Pseudoperonospora humuli*. The significance of variance was tested from 999 permutations of the data[a]

Source	Df [b]	SSD [c]	MSD [d]	Sigma	% variance [e]	P_{value}
Between subpopulations	1	40.187	40.18681	1.986518	11.249556	0.01
Between samples within subpopulations	3	53.042	17.68075	0.449694	2.546595	
Within samples	23	350.12	15.22243	15.22243	86.203849	
Total	27	443.34	16.42018	17.65864	100	

[a]Sample sizes used in this analysis included 8 and 20 samples from two and three hop yards in west and north Michigan, respectively.
[b]Degrees of freedom.
[c]Sum of squared differences.
[d]Mean of squared differences.
[e]Variance (%) was adjusted to zero for negative sigma values.

Table 4-10. **Pairwise F_{ST} comparisons among subpopulations *of Pseudoperonospora humuli* collected from hop yards in Michigan[a].**

Subpopulation/Yard		West		North		
		D	**E**	**B**	**A**	**C**
West	**D**	--				
	E	0.00237	--			
North	**B**	0.02269*	0.00953	--		
	A	0.03052*	0.021636*	0.002614	--	
	C	0.02879*	0.019606*	0.001831	0.002613	--

[a]Sample sizes used in this analysis included 4, 4, 6, 4 and 10 samples collected from hop yards indicated as D, E, C, B and A, respectively. The hop yards in the central region were excluded from analysis due to a low number of samples.
*Indicates a significant Fst value based on AMOVA

Table 4-11. **Genotypic diversity estimates and index of association of Michigan subpopulations of *Pseudoperonospora humuli*.**

Subpopulation	N [a]	MLG [b]	eMLG [c]	SE [d]	H [e]	G [f]	λ [g]	E_5 [h]	Hexp [i]
West	8	8	8	0	2.08	8	0.875	1	0.206
North	20	11	6.79	1.05	2.11	5.88	0.83	0.676	0.224
East-central	5	5	5	0	1.61	5	0.8	1	0.220
Total	33	22	8.33	1.08	2.86	12.52	0.92	0.701	0.217

[a]N is the number of individuals sampled of each region.
[b]MLG is the number of multilocus genotypes observed.
[c]eMLG is the number of expected MLGs at a sample size based on rarefaction.
[d]Standard error
[e]Shannon-Wiener Index (H)
[f]Stoddart and Taylor's Index (G)
[g]Simpson's index (lambda)
[h]Evenness (E_5)
[i]Within population gene diversity (Hexp).

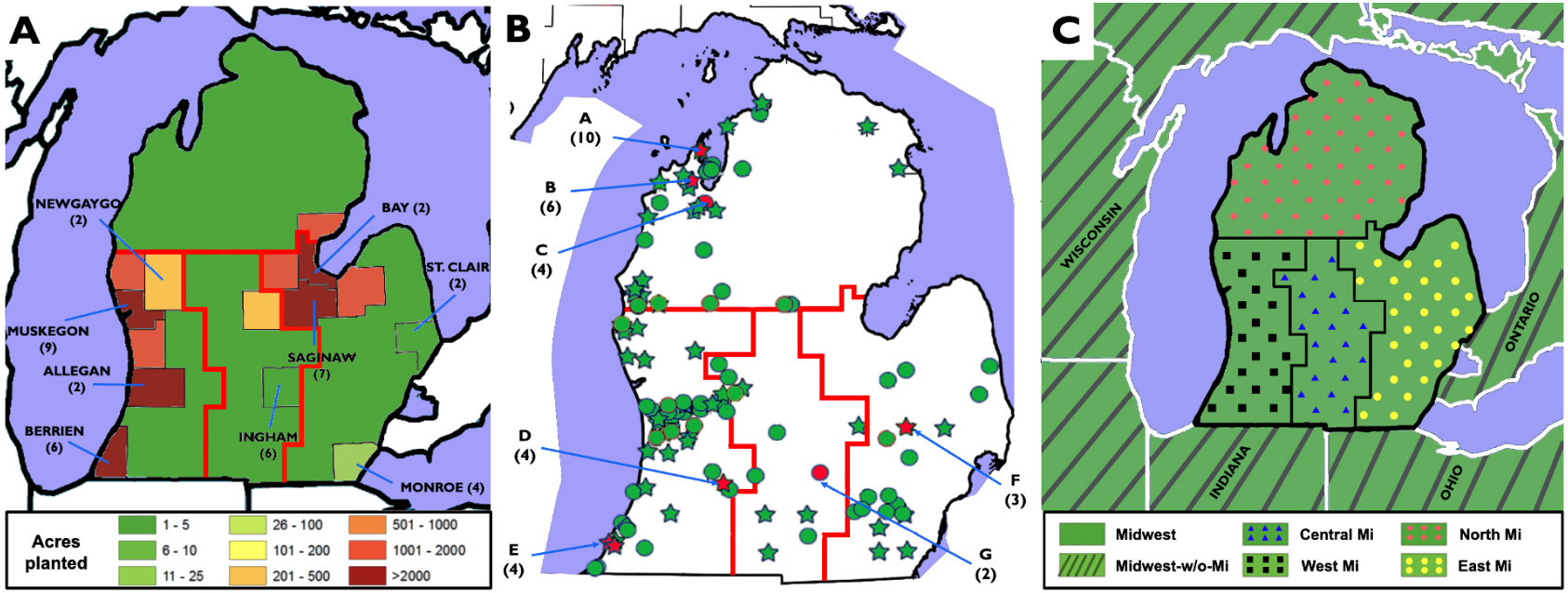

***Figure 4-1. Cucumis sativus* planted acreage and number *Humulus lupulus* planted in Michigan by county (Adapted from Neufeld, 2017).**

A) *C. sativus* planted acreage, location and number of samples collected in the Michigan (N=40). A total of 26 samples were collected outside of Michigan in Ontario Canada (N=6) and the U.S. states of Florida (N=2), Alabama (N=1), North Carolina (N=2), South Carolina (N=2), California (N=1), New York (N=1), Wisconsin (N=1), Ohio (N=3), Iowa (N=1), Indiana (N=5), Georgia (N=1). **(B)** *H. lupulus* planted, location and number of samples collected from hop yards in Michigan (N=33) and Oregon (N=1). Hop yards with more than 800 plants (*H. lupulus*) are represented by stars, those with fewer are represented by circles. Hop yard sampled (A-F) are colored in red. **(C)** Population assignment by geographic location of *Pseudoperonospora* spp. samples in the Midwest (Wisconsin, Indiana, Ohio, Michigan (Mi) and Ontario, CA).

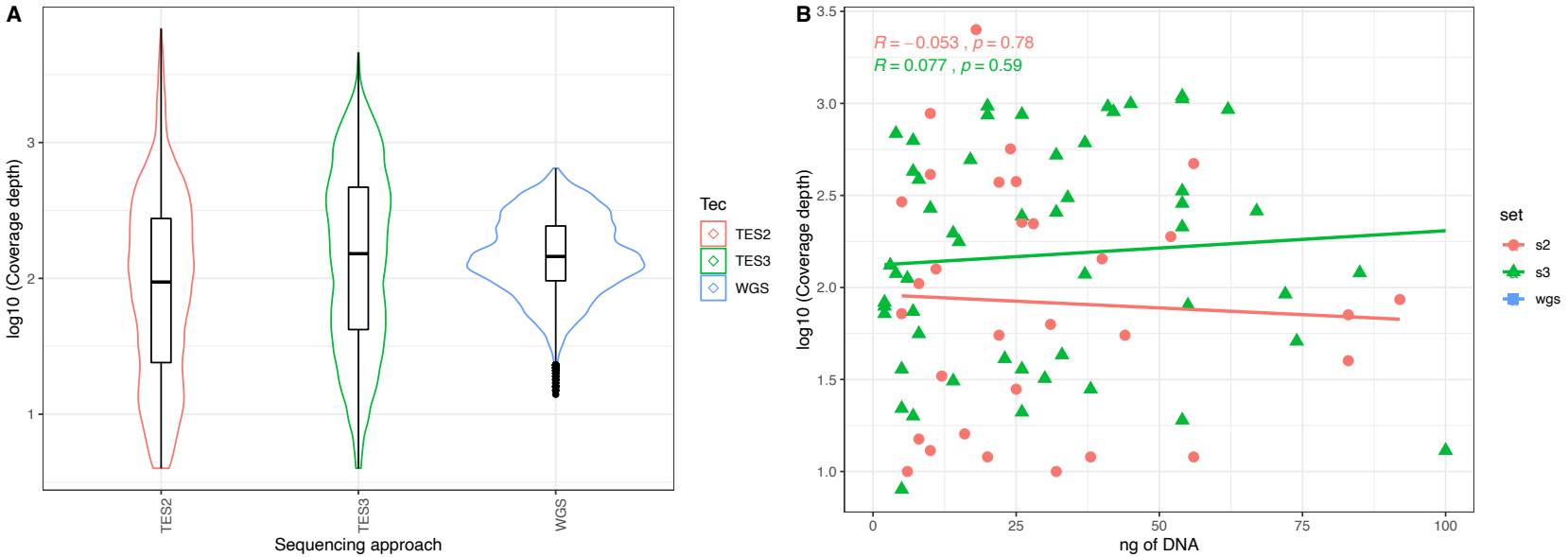

Figure 4-2. **Depth coverage of high-quality SNPs across libraries.**

(A). Depth coverage of high-quality SNPs (log_{10}) across libraries of *Pseudoperonospora cubensis* and *Pseudoperonospora humuli* sequenced using target enrichment with 24h (TES2) and 48h (TES3) of hybridization and whole genome sequencing (WGS). **(B).** Depth coverage of high-quality SNPs (log_{10}) across libraries sequenced using target enrichment with different amounts of input DNA for library preparation. Only samples that were retained after quality filtering were included in the analysis.

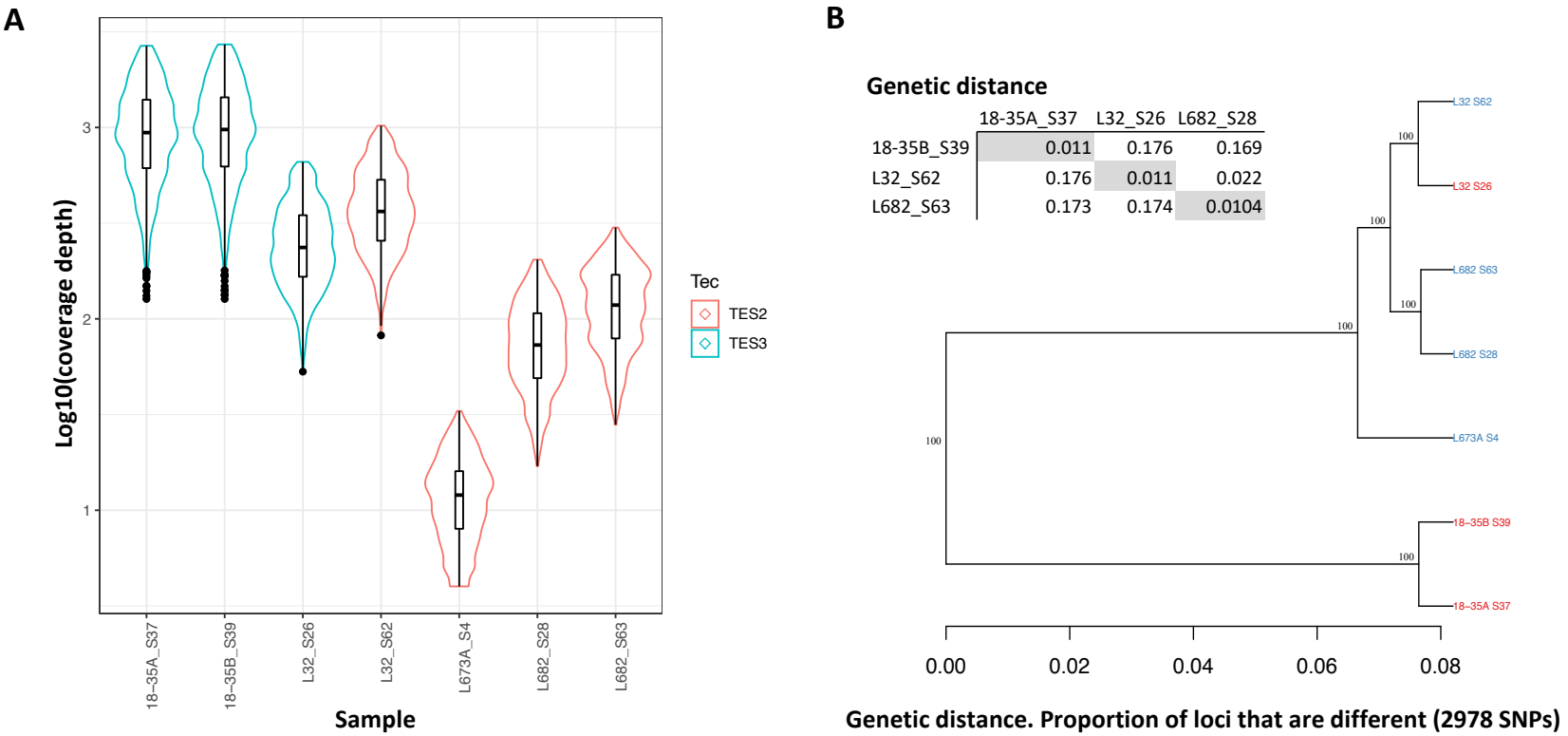

Figure 4-3. **Characterization of sequencing error among technical replicates.**

(A) Coverage distribution of the technical replicates sequenced. Violin plots are filled with 2,978 high-quality SNPs. Each sample is colored according to the sequencing batch. **(B)** Genetic differentiation among technical replicates. A UPGMA tree was reconstructed using 2,978 SNPs. The genetic distance represents the number of SNPs that are different among samples.

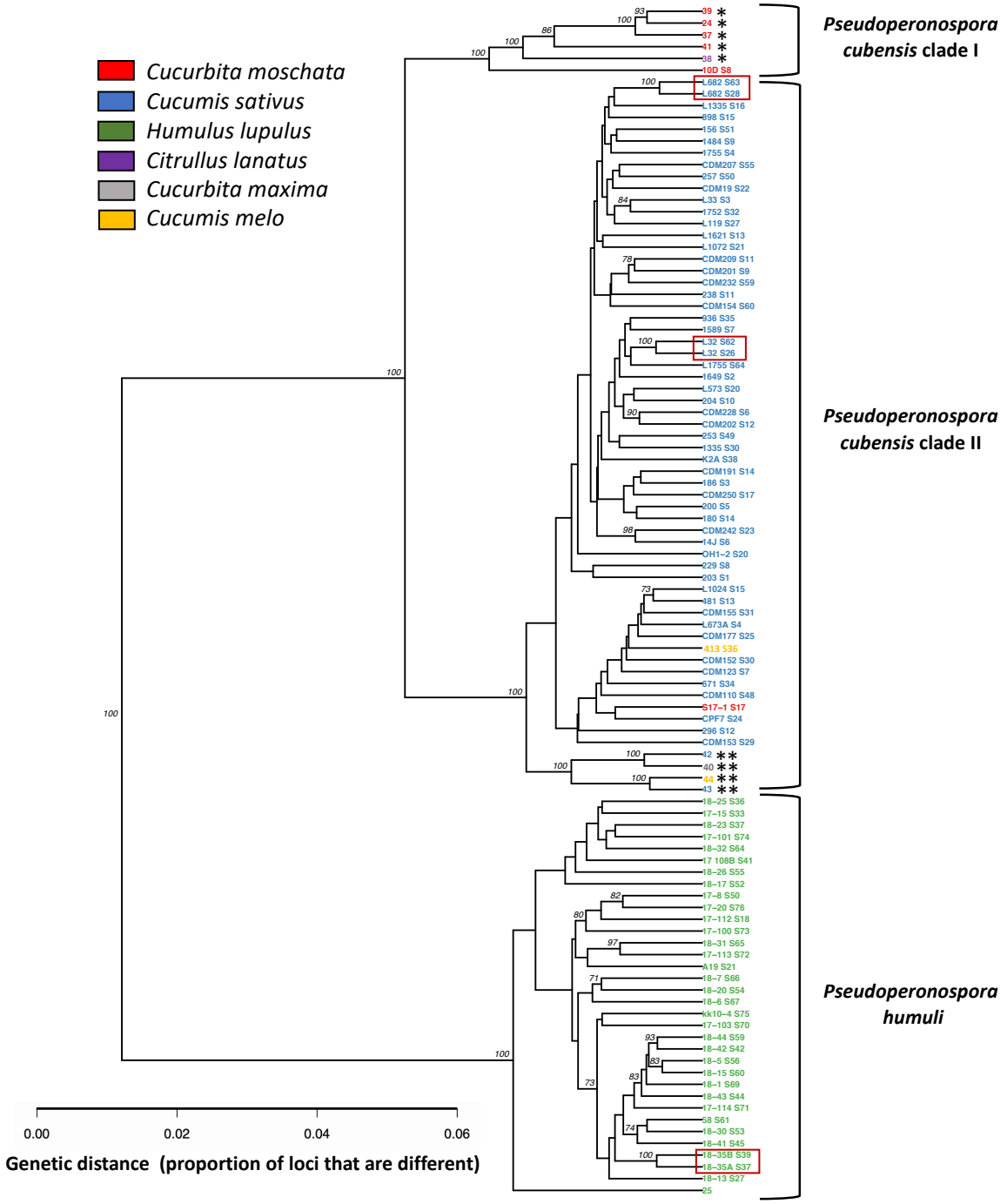

Figure 4-4. **Genetic differentiation of *Pseudoperonospora cubensis* and *Pseudoperonospora humuli* samples.**

A UPGMA tree was reconstructed using 2,978 single nucleotide polymorphism (SNP) variants. Bootstrap support values are indicated above the branches. The genetic distance represents the proportion of loci that are different between samples. * Samples previously classified as clade I members. ** Samples previously classified as clade II members. Technical replicates are enclosed in red squares.

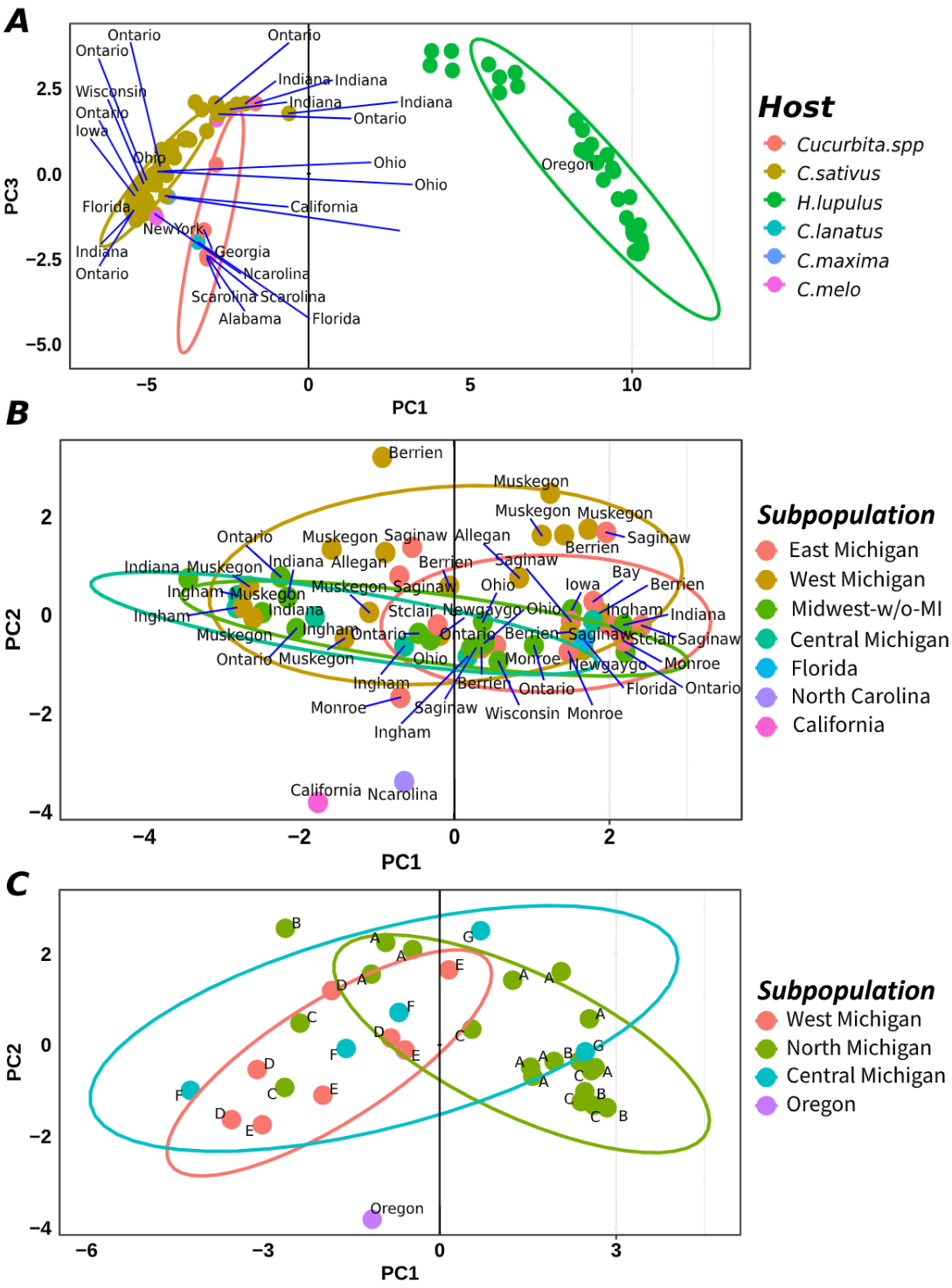

Figure 4-5. **Ordination plots of *Pseudoperonospora spp.* based on 2,978 SNPs.**

(A) Ordination plot of *Pseudoperonospora cubensis* and *P. humuli* samples according to host species. All points represent samples collected in Michigan unless indicated otherwise. **(B)** Ordination plot of *P. cubensis* samples from *Cucumis sativus* from 2007 to 2017 in the U.S. (n=57). **(C)** Ordination plot of *P. humuli* samples from hop yards of Michigan in 2017 and 2018 (n=34)

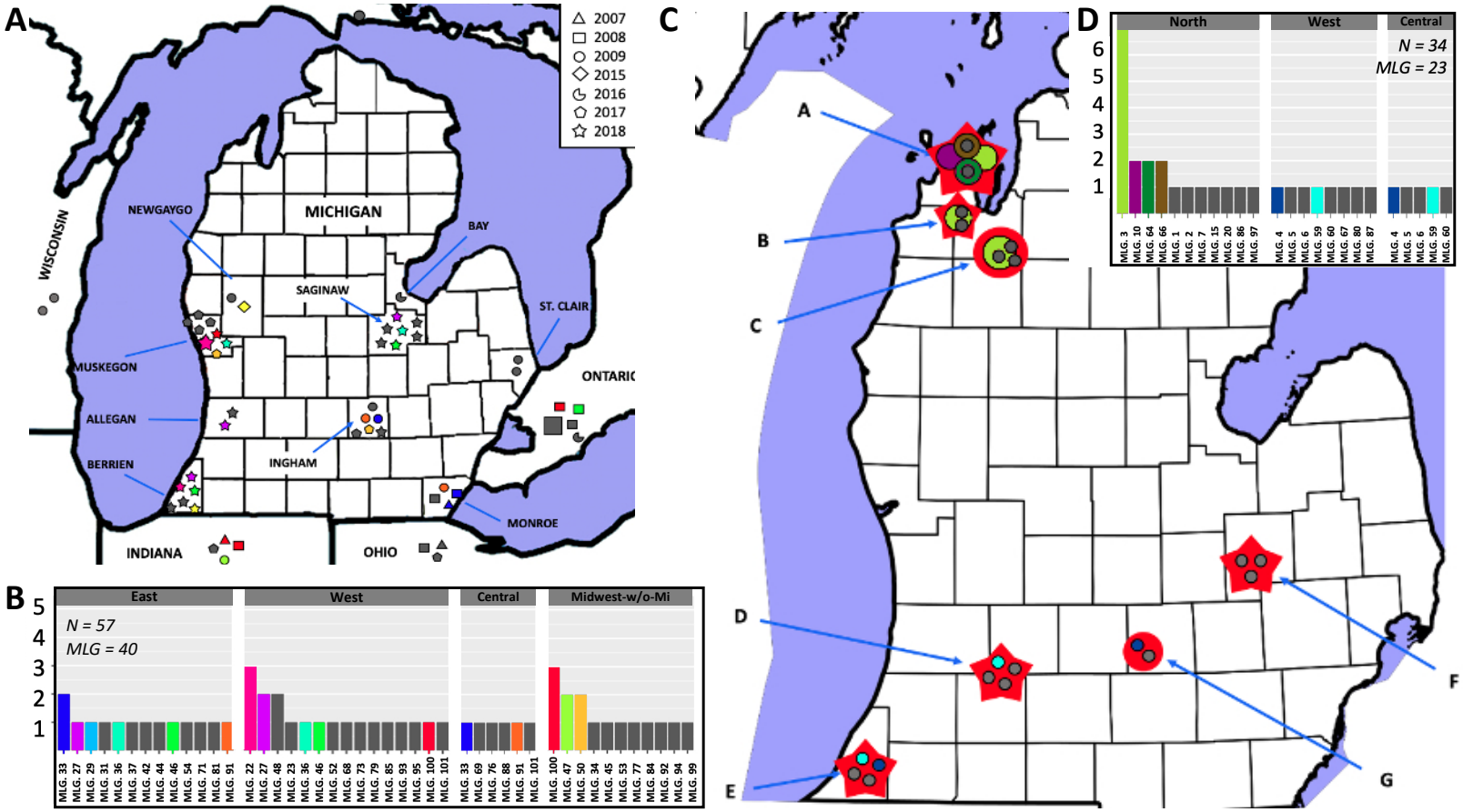

Figure 4-6. **Frequency and geographic distribution of *Pseudoperonospora cubensis* and *Pseudoperonospora humuli* genotypes (MLG).**

(A) Geographic distribution of *P. cubensis* genotypes collected from *Cucumis sativus* in the Midwest. Unique genotypes are colored in gray. **(B)** Frequency of *P. cubensis* genotypes collected from *C. sativus* in the Midwest. Unique genotypes are colored in gray. **(C)** Geographic distribution of *P. humuli* genotypes collected from *Humulus lupulus* in Michigan. Unique genotypes are color coded in gray. The circles and stars colored in red represent

different hop yards. **(D)** Frequency of *P. humuli* genotypes collected from *H. lupulus* in Michigan. Unique genotypes are colored in gray.

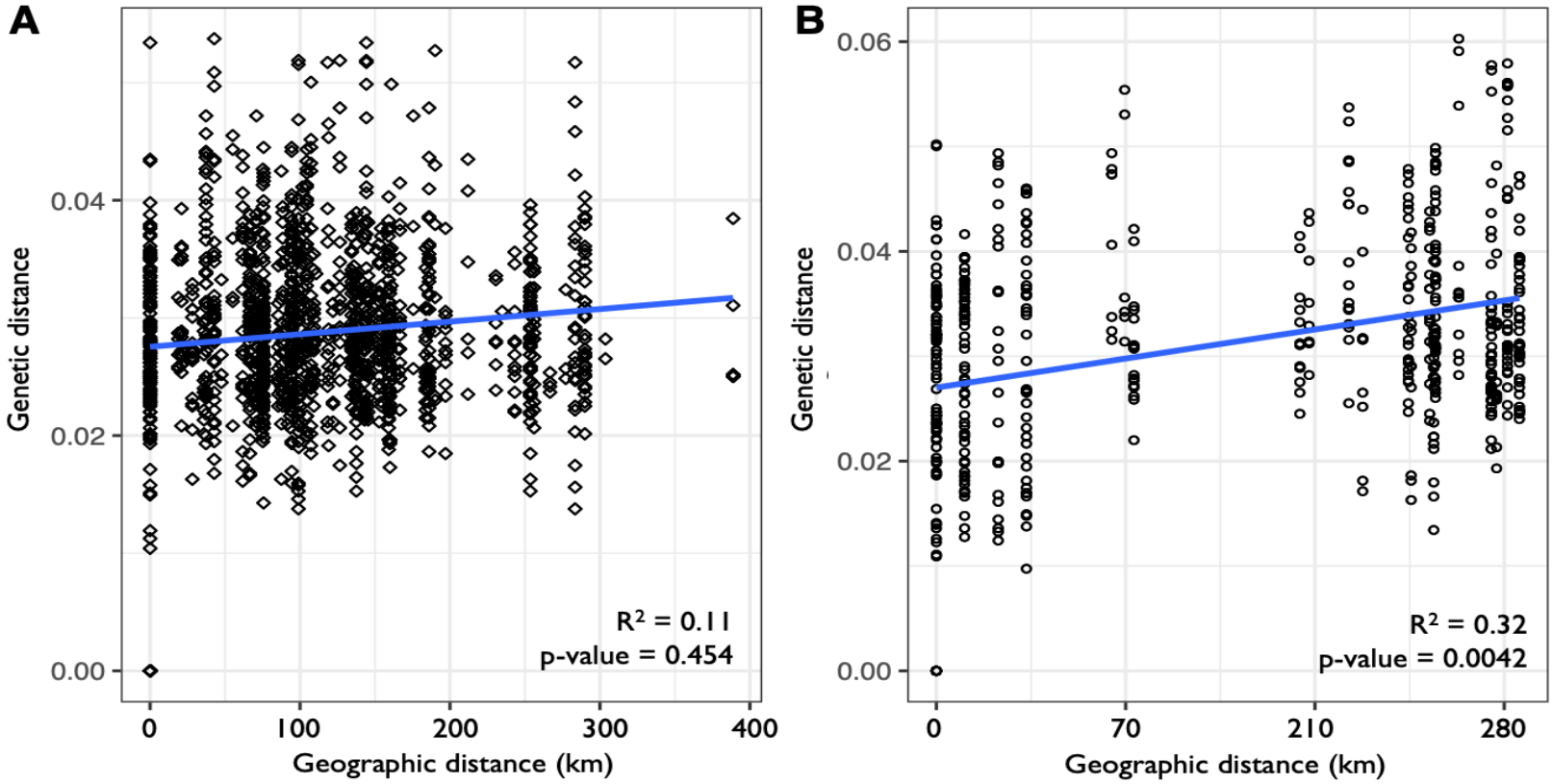

***Figure 4-7*. The relationship between genetic differences among samples and geographic distances of the locations from which samples originated.**

(A) *P. cubensis* samples from *Cucumis sativus* and **(B)** *P. humuli* samples from *Humulus lupulus* in Michigan.

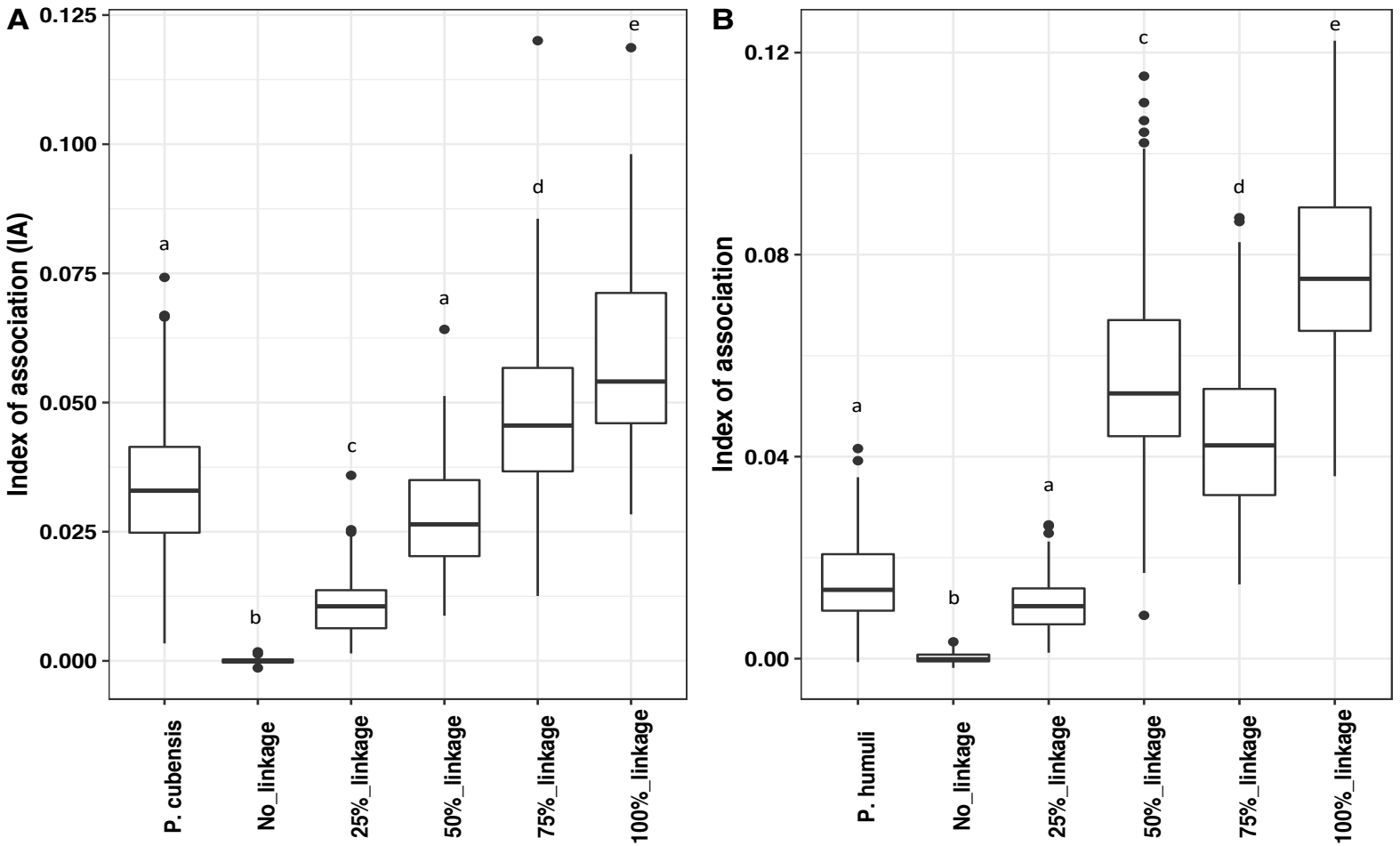

Figure 4-8. **Estimation of the degree of linkage disequilibrium within *Pseudoperonospora cubensis* and *Pseudoperonospora humuli* of Michigan.**

(A) Observed index of association (IA) distribution of *P. cubensis* samples compared with the IA distribution values of 0, 25, 50, 75, and 100% linkage. **(B)** Observed IA distribution of *P. humuli* samples compared with the IA distribution values of 0, 25, 50, 75, and 100% linkage. Groupings based on the Kruskal-Wallis rank-sum test are noted by the letters over the boxplots, in which the *P. cubensis* and the *P. humuli* population datasets are grouped with the simulated 50% and 25% linkage data, respectively

SUPPLEMENTARY TABLES

Supplementary Table 4-1: Samples sequenced using target enrichment (TE), whole genome sequencing (WGS) or low coverage whole genome sequencing (Lc-WGS)

Sample	*Input DNA (ng)*	*Hybr. Time*[a]	*Enri. set*[b]	*Log10 Depth*	*State*	*County / Yard*	*Region*	*Year*	*Host Species*	*Collector*
10D_S8	2	48 h	ES3	1.9	Michigan	Newaygo	Eastern	2015	*C. moschata*	J. Bello
1335_S30	83	24 h	ES2	1.6	Michigan	St. Clair	Eastern	2009	*C. sativus*	L, Quesada-Ocampo,
1484_S9	8	48 h	ES3	1.75	Michigan	Newaygo	Western	2009	*C. sativus*	L, Quesada-Ocampo,
14J_S6	4	48 h	ES3	2.08	Michigan	Newaygo	Western	2015	*C. sativus*	J, Bello
156_S51	14	48 h	ES3	1.49	Michigan	Muskegon	Western	2017	*C. sativus*	J, Bello
1589_S7	17	48 h	ES3	2.69	Indiana	-	Midwest	2009	*C. sativus*	L, Quesada-Ocampo,
1649_S2	54	48 h	ES3	2.46	Iowa	-	Midwest	2009	*C. sativus*	L, Quesada-Ocampo,
17-100_S73	6	48 h	ES3	2.05	Michigan	Barry (D)	Western	2017	*H. lupulus*	D, Higgins
17-101_S74	5	48 h	ES3	1.34	Michigan	Leelanau (B)	Northern	2017	*H. lupulus*	D, Higgins
17-103_S70	54	48 h	ES3	2.52	Michigan	Leelanau (A)	Northern	2017	*H. lupulus*	D, Higgins

[a]Hybridization time. [b]Enrichment set (ES2 = 24h, ES3=48h)

Supplementary Table 4-1. ***(cont'd)***

Sample	*Input DNA (ng)*	*Hybr. Time*[a]	*Enri. set*[b]	*Log10 Depth*	*State*	*County / Yard*	*Region*	*Year*	*Host Species*	*Collector*
17_108B_S41	54	48 h	ES3	1.28	Michigan	Genesee (F)	Central	2017	*H. lupulus*	D, Higgins
17-112_S18	85	48 h	ES3	2.08	Michigan	Leelanau (A)	Northern	2017	*H. lupulus*	D, Higgins
17-113_S72	54	48 h	ES3	2.33	Michigan	Leelanau (A)	Northern	2017	*H. lupulus*	D, Higgins
17-114_S71	34	48 h	ES3	2.49	Michigan	Leelanau (A)	Northern	2017	*H. lupulus*	D, Higgins
17-15_S33	38	48 h	ES3	1.45	Michigan	Leelanau (B)	Northern	2017	*H. lupulus*	D, Higgins
17-20_S76	5	24 h	ES2	1.86	Michigan	Berrien (E)	Western	2017	*H. lupulus*	D, Higgins
1752_S32	72	48 h	ES3	1.96	Michigan	Ingham	Central	2009	*C. sativus*	L, Quesada-Ocampo,
1755_S4	23	48 h	ES3	1.61	Michigan	Ingham	Central	2009	*C. sativus*	L, Quesada-Ocampo,
17-8_S50	25	24 h	ES2	1.45	Michigan	Genesee (F)	Central	2017	*H. lupulus*	D, Higgins
180_S14	4	48 h	ES3	2.84	Michigan	Muskegon	Western	2018	*C. sativus*	J, Bello

[a]Hybridization time. [b]Enrichment set (ES2 = 24h, ES3=48h)

Supplementary Table 4-1. ***(cont'd)***

Sample	*Input DNA (ng)*	*Hybr. Time*[a]	*Enri. set*[b]	*Log10 Depth*	*State*	*County / Yard*	*Region*	*Year*	*Host Species*	*Collector*
18-13_S27	32	48 h	ES3	2.72	Michigan	Grand Traverse (C)	Northern	2018	*H. lupulus*	J, Bello
18-15_S60	136	48 h	ES3	2.84	Michigan	Grand Traverse (C)	Northern	2017	*H. lupulus*	D, Higgins
18-17_S52	33	48 h	ES3	1.63	Michigan	Grand Traverse (C)	Northern	2017	*H. lupulus*	D, Higgins
18-1_S69	45	48 h	ES3	3	Michigan	Grand Traverse (C)	Northern	2018	*H. lupulus*	J, Bello
18-20_S54	26	48 h	ES3	1.56	Michigan	Genesee (F)	Central	2017	*H. lupulus*	D, Higgins
18-23_S37	56	24 h	ES2	1.08	Michigan	Berrien (E)	Western	2018	*H. lupulus*	J, Bello
18-25_S36	145	24 h	ES2	1.43	Michigan	Berrien (E)	Western	2018	*H. lupulus*	J, Bello
18-26_S55	30	48 h	ES3	1.51	Michigan	Barry (D)	Western	2018	*H. lupulus*	J, Bello
18-30_S53	42	48 h	ES3	2.95	Michigan	Leelanau (A)	Northern	2018	*H. lupulus*	J, Bello
18-31_S65	205	48 h	ES3	2.28	Michigan	Leelanau (A)	Northern	2018	*H. lupulus*	J, Bello

[a]Hybridization time. [b]Enrichment set (ES2 = 24h, ES3=48h)

Supplementary Table 4-1. ***(cont'd)***

Sample	*Input DNA (ng)*	*Hybr. Time*[a]	*Enri. set*[b]	*Log10 Depth*	*State*	*County / Yard*	*Region*	*Year*	*Host Species*	*Collector*
18-32_S64	342	48 h	ES3	1.3	Michigan	Barry (D)	Western	2018	*H. lupulus*	J, Bello
18-35A_S37	54	48 h	ES3	3.02	Michigan	Leelanau (A)	Northern	2018	*H. lupulus*	J, Bello
18-35B_S39	54	48 h	ES3	3.04	Michigan	Leelanau (A)	Northern	2018	*H. lupulus*	J, Bello
18-41_S45	37	48 h	ES3	2.79	Michigan	Leelanau (A)	Northern	2018	*H. lupulus*	J, Bello
18-42_S42	62	48 h	ES3	2.97	Michigan	Leelanau (B)	Northern	2018	*H. lupulus*	J, Bello
18-43_S44	26	48 h	ES3	2.94	Michigan	Leelanau (B)	Northern	2018	*H. lupulus*	J, Bello
18-44_S59	20	48 h	ES3	2.99	Michigan	Leelanau (B)	Northern	2018	*H. lupulus*	J, Bello
18-5_S56	41	48 h	ES3	2.98	Michigan	Leelanau (A)	Northern	2018	*H. lupulus*	J, Bello
186_S3	26	48 h	ES3	2.39	Michigan	Muskegon	Western	2018	*C. sativus*	J, Bello
18-6_S67	37	48 h	ES3	2.07	Michigan	Berrien (E)	Western	2018	*H. lupulus*	J, Bello

[a]Hybridization time. [b]Enrichment set (ES2 = 24h, ES3=48h)

Supplementary Table 4-1. ***(cont'd)***

Sample	*Input DNA (ng)*	*Hybr. Time*[a]	*Enri. set*[b]	*Log10 Depth*	*State*	*County / Yard*	*Region*	*Year*	*Host Species*	*Collector*
18-7_S66	392	48 h	ES3	1.76	Michigan	Barry (D)	Western	2018	*H. lupulus*	J, Bello
200_S5	20	48 h	ES3	2.94	Michigan	Saginaw	Eastern	2018	*C. sativus*	J, Bello
203_S1	74	48 h	ES3	1.71	Michigan	Saginaw	Eastern	2018	*C. sativus*	J, Bello
204_S10	8	48 h	ES3	2.59	Michigan	Saginaw	Eastern	2018	*C. sativus*	J, Bello
229_S8	14	48 h	ES3	2.29	Michigan	Berrien	Western	2018	*C. sativus*	J, Bello
238_S11	7	48 h	ES3	1.87	Michigan	Allegan	Western	2018	*C. sativus*	J, Bello
24	NA	wgs	wgs	2.33	Alabama	-	Alabama	2013	*C. moschata*	Thomas, A
253_S49	7	48 h	ES3	2.8	Michigan	Saginaw	Eastern	2018	*C. sativus*	J, Bello
257_S50	3	48 h	ES3	2.12	Michigan	Saginaw	Eastern	2018	*C. sativus*	J, Bello
25	NA	wgs	wgs	2.11	Oregon	-	Oregon	2012	*H. lupulus*	Thomas, A

[a]Hybridization time. [b]Enrichment set (ES2 = 24h, ES3=48h)

Supplementary Table 4-1. ***(cont'd)***

Sample		*Input DNA (ng)*	*Hybr. Time*[a]	*Enri. set*[b]	*Log10 Depth*	*State*	*County / Yard*	*Region*	*Year*	*Host Species*	*Collector*
296_S12		5	48 h	ES3	1.56	Michigan	Ingham	Central	2018	*C. sativus*	J, Bello
	37	NA	wgs	wgs	2.38	South Carolina	-	South Carolina	2013	*C. moschata*	Thomas, A
	38	NA	wgs	wgs	2.43	Florida	-	Florida	2013	*C. lanatus*	Thomas, A
	39	NA	wgs	wgs	2.3	South Carolina	-	South Carolina	2012	*C. moschata*	Thomas, A
	40	NA	wgs	wgs	1.97	North Carolina	-	North Carolina	2013	*C. maxima*	Thomas, A
413_S36		26	48 h	ES3	1.32	Michigan	Clinton	Eastern	2007	*C. melo*	L, Quesada-Ocampo,
	41	NA	wgs	wgs	1.93	Georgia	-	Georgia	2008	*C. moschata*	Thomas, A
	42	NA	wgs	wgs	1.97	California	-	California	2008	*C. sativus*	L, Quesada-Ocampo,
	43	NA	wgs	wgs	2.33	North Carolina	-	Ncarolina	2012	*C. sativus*	Thomas, A
	44	NA	wgs	wgs	2.42	New York	-	New York	2013	*C. melo*	Thomas, A

[a]Hybridization time. [b]Enrichment set (ES2 = 24h, ES3=48h)

Supplementary Table 4-1. ***(cont'd)***

Sample	*Input DNA (ng)*	*Hybr. Time*[a]	*Enri. set*[b]	*Log10 Depth*	*State*	*County / Yard*	*Region*	*Year*	*Host Species*	*Collector*
481_S13	5	48 h	ES3	0.9	Indiana	-	Midwest	2007	*C. sativus*	L, Quesada-Ocampo,
58_S61	197	48 h	ES3	3.07	Michigan	Ingham (G)	Central	2017	*H. lupulus*	D, Higgins
671_S34	7	48 h	ES3	1.3	Ontario	-	Midwest	2008	*C. sativus*	L, Quesada-Ocampo,
898_S15	2	48 h	ES3	1.92	Ohio	-	Midwest	2008	*C. sativus*	L, Quesada-Ocampo,
936_S35	7	48 h	ES3	2.63	Ontario	-	Midwest	2008	*C. sativus*	L, Quesada-Ocampo,
A19_S21	67	48 h	ES3	2.41	Michigan	Ingham	Central	2019	*H. lupulus*	J, Bello
CDM110_S48	16	24 h	ES2	1.2	Michigan	Ingham	Central	2017	*C. sativus*	J, Bello
CDM123_S7	10	24 h	ES2	1.11	Michigan	Ingham	Central	2017	*C. sativus*	J, Bello
CDM152_S30	8	24 h	ES2	1.18	Michigan	Muskegon	Western	2017	*C. sativus*	J, Bello
CDM153_S29	12	24 h	ES2	1.52	Michigan	Muskegon	Western	2017	*C. sativus*	J, Bello

[a]Hybridization time. [b]Enrichment set (ES2 = 24h, ES3=48h)

Supplementary Table 4-1. ***(cont'd)***

Sample	*Input DNA (ng)*	*Hybr. Time*[a]	*Enri. set*[b]	*Log10 Depth*	*State*	*County / Yard*	*Region*	*Year*	*Host Species*	*Collector*
L32_S26	10	48 h	ES3	2.43	Michigan	Monroe	Eastern	2007	*C. sativus*	L, Quesada-Ocampo,
L32_S62	10	24 h	ES2	2.61	Michigan	Monroe	Eastern	2008	*C. sativus*	L, Quesada-Ocampo,
L33_S3	31	24 h	ES2	1.8	Michigan	Monroe	Eastern	2007	*C. sativus*	L, Quesada-Ocampo,
L573_S20	5	24 h	ES2	2.47	Florida	-	Florida	2008	*C. sativus*	L, Quesada-Ocampo,
L673A_S4	20	24 h	ES2	1.08	Ontario	-	Midwest	2008	*C. sativus*	L, Quesada-Ocampo,
L682_S28	22	24 h	ES2	NA	Ontario	-	Midwest	2008	*C. sativus*	L, Quesada-Ocampo,
L682_S63	11	24 h	ES2	2.1	Ontario	-	Midwest	2008	*C. sativus*	L, Quesada-Ocampo,
OH1-2_S20	55	48 h	ES3	1.9	Ohio	-	Midwest	2017	*C. sativus*	J, Bello
S17-1_S17	100	48 h	ES3	1.11	Indiana	-	Western	2017	*C. moschata*	J, Bello

[a]Hybridization time. [b]Enrichment set (ES2 = 24h, ES3=48h)

Supplementary Table 4-1. ***(cont'd)***

Sample	*Input DNA (ng)*	*Hybr. Time*[a]	*Enri. set*[b]	*Log10 Depth*	*State*	*County / Yard*	*Region*	*Year*	*Host Species*	*Collector*
CDM232_S59	26	24 h	ES2	2.35	Michigan	Allegan	Western	2018	*C. sativus*	J, Bello
CDM242_S23	18	24 h	ES2	3.4	Michigan	Berrien	Western	2018	*C. sativus*	J, Bello
CDM250_S17	10	24 h	ES2	2.95	Michigan	Berrien	Western	2018	*C. sativus*	J, Bello
CPF7_S24	162	48 h	ES3	1.11	Indiana	-	Midwest	2017	*C. sativus*	J, Bello
K2A_S38	32	48 h	ES3	2.41	Michigan	Bay	Eastern	2016	*C. sativus*	J, Bello
kk10-4_S75	15	48 h	ES3	2.25	Michigan	Leelanau (B)	Northern	2018	*H. lupulus*	J, Bello
L1024_S15	6	24 h	ES2	1	Indiana	-	Midwest	2008	*C. sativus*	L, Quesada-Ocampo,
L1072_S21	8	24 h	ES2	2.02	Michigan	Monroe	Eastern	2008	*C. sativus*	L, Quesada-Ocampo,
L119_S27	22	24 h	ES2	1.74	Ohio	-	Midwest	2007	*C. sativus*	L, Quesada-Ocampo,
L1335_S16	2	48 h	ES3	1.86	Michigan	St. Clair	Eastern	2009	*C. sativus*	L, Quesada-Ocampo,

[a]Hybridization time. [b]Enrichment set (ES2 = 24h, ES3=48h)

Supplementary Table 4-1. ***(cont'd)***

Sample	*Input DNA (ng)*	*Hybr. Time*[a]	*Enri. set*[b]	*Log10 Depth*	*State*	*County / Yard*	*Region*	*Year*	*Host Species*	*Collector*
CDM154_S60	44	24 h	ES2	1.74	Michigan	Muskegon	Western	2017	*C. sativus*	J, Bello
CDM155_S31	32	24 h	ES2	1	Michigan	Muskegon	Western	2017	*C. sativus*	J, Bello
CDM191_S14	24	24 h	ES2	2.75	Michigan	Muskegon	Western	2018	*C. sativus*	J, Bello
CDM19_S22	83	24 h	ES2	1.85	Ontario	-	Midwest	2016	*C. sativus*	J, Bello
CDM201_S9	52	24 h	ES2	2.28	Michigan	Saginaw	Eastern	2018	*C. sativus*	J, Bello
CDM202_S12	56	24 h	ES2	2.67	Michigan	Saginaw	Eastern	2018	*C. sativus*	J, Bello
CDM207_S55	92	24 h	ES2	1.93	Michigan	Berrien	Western	2018	*C. sativus*	J, Bello
CDM209_S11	28	24 h	ES2	2.35	Michigan	Berrien	Western	2018	*C. sativus*	J, Bello
CDM228_S6	25	24 h	ES2	2.58	Michigan	Berrien	Western	2018	*C. sativus*	J, Bello
L1621_S13	40	24 h	ES2	2.16	Wisconsin	-	Midwest	2009	*C. sativus*	L, Quesada-Ocampo,
L1755_S64	22	24 h	ES2	2.57	Michigan	Ingham	Central	2009	*C. sativus*	L, Quesada-Ocampo,

[a]Hybridization time. [b]Enrichment set (ES2 = 24h, ES3=48h)

LITERATURE CITED

LITERATURE CITED

Ali, S., Gautier, A., Leconte, M., Enjalbert, J., de Vallavieille-Pope, C. (2011) A rapid genotyping method for an obligate fungal pathogen, *Puccinia striiformis f.sp. tritici*, based on DNA extraction from infected leaf and multiplex PCR genotyping. BMC Res Notes 4: 240

Baxter, L., Tripathy, S., Ishaque, N., Boot, N., Cabral, A., Kemen, E., Thines, M., Ah-Fong, A., Anderson, R., Badejoko, W., et al (2010) Signatures of adaptation to obligate biotrophy in the *Hyaloperonospora arabidopsidis* genome. Science (80) 330: 1549 LP – 1551

Bello, J.C., Sakalidis, M.L., Perla, D.E., Hausbeck, M.K. (2020) Detection of airborne sporangia of *Pseudoperonospora cubensis* in Michigan using Burkard spore traps coupled to qPCR. Plant Dis. - Manuscript in review

Blum, M., Waldner, M., Olaya, G., Cohen, Y., Gisi, U., Sierotzki, H. (2011) Resistance mechanism to carboxylic acid amide fungicides in the cucurbit downy mildew pathogen *Pseudoperonospora cubensis.* Pest Manag Sci 67: 1211–1214

Bolger, A.M., Lohse, M., Usadel, B. (2014) Trimmomatic: a flexible trimmer for Illumina sequence data. Bioinformatics 30: 2114–2120

Bourret, T.B., Choudhury, R.A., Mehl, H.K., Blomquist, C.L., McRoberts, N., Rizzo, D.M. (2018) Multiple origins of downy mildews and mito-nuclear discordance within the paraphyletic genus Phytophthora. PLoS One 13: e0192502

Brown, A.H.D., Feldman, M.W., Nevo, E. (1980) Multilocus structure of natural populations of *Hordeum spontaneum*. Genetics 96: 523-536.

Burkhardt, A., Buchanan, A., Cumbie, J..S, Savory, E.A., Chang, J.H., Day, B. (2014) Alternative splicing in the obligate biotrophic oomycete pathogen *Pseudoperonospora cubensis*. Mol Plant-Microbe Interact 28: 298–309

Burkhardt, A., Day, B. (2016) Transcriptome and small RNAome dynamics during a resistant and susceptible interaction between cucumber and downy mildew. Plant Genome. doi: 10.3835/plantgenome2015.08.0069

Carleson, N.C., Fieland, V.J., Scagel, C.F., Weiland, J.E., Grünwald, N.J. (2019) Population structure of *Phytophthora plurivora* on rhododendron in Oregon nurseries. Plant Dis 103: 1923–1930

Chee, H.Y., Nelson, M.E., Grov,e G.G., Eastwell, K.C., Kenny, S.T., Klein, R.E. (2006) Population biology of *Pseudoperonospora humuli* in Oregon and Washington. Plant Dis 90: 1283–1286

Choi, Y-J., Hong, S-B., Shin, H-D. (2005) A re-consideration of *Pseudoperonospora cubensis* and *P. humuli* based on molecular and morphological data. Mycol Res 109: 841–848

Choi, Y-J., Thines, M. (2015) Host jumps and radiation, not co-divergence drives diversification of obligate pathogens. A case study in Downy mildews and Asteraceae. PLoS One 10: e0133655

Clark, M.J., Chen, R, Lam, H.Y.K., Karczewski, K.J., Chen, R., Euskirchen, G., Butte, A.J., Snyder, M. (2011) Performance comparison of exome DNA sequencing technologies. Nat Biotechnol 29: 908–914

Cruz-Dávalos, D.I., Llamas, B., Gaunitz, C., Fages, A., Gamba, C., Soubrier, J., Librado, P., Seguin-Orlando, A., Pruvost, M., Alfarhan, A.H., et al (2017) Experimental conditions improving in-solution target enrichment for ancient DNA. Mol Ecol Resour 17: 508–522

Cui, C., Herlihy, J.H., Bombarely, A., McDowell, J.M., Haak, D.C. (2019) Draft assembly of *Phytophthora capsici* from long-read sequencing uncovers complexity. Mol Plant-Microbe Interact 32: 1559–1563

Dray, S., Dufour, A. (2007) The ade4 package: implementing the duality diagram for ecologists. J Stat Softw 22(4): 1–20

Faircloth, B.C., Branstetter, M.G., White, N.D., Brady, S.G. (2015) Target enrichment of ultraconserved elements from arthropods provides a genomic perspective on relationships among Hymenoptera. Mol Ecol Resour 15: 489–501

Fletcher, K., Gil, J., Bertier, L.D., Kenefick, A., Wood, K.J., Zhang, L., Reyes-Chin-Wo, S., Cavanaugh, K., Tsuchida, C., Wong, J., et al (2019) Genomic signatures of heterokaryosis in the oomycete pathogen *Bremia lactucae*. Nat Commun 10: 2645

Gent, D.H., Adair, N., Knaus, B.J., Grünwald, N.J. (2019) Genotyping-by-sequencing reveals fine-scale population differentiation in populations of *Pseudoperonospora humuli*. Phytopathology. doi: 10.1094/PHYTO-12-18-0485-R

Gent, D.H., Nelson, M.E., Farnsworth, J.L., Grove, G.G. (2009) PCR detection of *Pseudoperonospora humuli* in air samples from hop yards. Plant Pathol 58: 1081–1091

Gent, D.H., Ocamb, C.M., Farnsworth, J.L. (2010) Forecasting and management of hop downy mildew. Plant Dis 94: 425–431

Gisi, U., Sierotzki, H. (2008) Fungicide modes of action and resistance in downy mildews. Eur J Plant Pathol 122: 157–167

Gnirke, A., Melnikov, A., Maguire, J., Rogov, P., LeProust., E. M., Brockman, W., Fennell, T., Giannoukos, G., Fisher, S., Russ, C., et al (2009) Solution hybrid selection with ultra-long oligonucleotides for massively parallel targeted sequencing. Nat Biotechnol 27: 182–189

Goldenhar, K.E., Hausbeck, M.K. (2019) Fungicides for control of downy mildew on pickling cucumber in Michigan. Plant Heal Prog **20**: 165–169

Goudet, J. (2005) Hierfstat, a package for r to compute and test hierarchical F-statistics. Mol Ecol Notes 5: 184–186

Grünwald, N.J., Everhart, S.E., Knaus, B.J., Kamvar, Z.N. (2017) Best practices for population genetic analyses. Phytopathology 107: 1000–1010

Grünwald, N.J., McDonald, B.A., Milgroom, M.G. (2016) Population genomics of fungal and oomycete pathogens. Annu Rev Phytopathol 54: 323–346

Holdsworth, W.L., Summers, C.F., Glos, M., Smart, C.D., Mazourek, M. (2014) Development of downy mildew-resistant cucumbers for late-season production in the Northeastern United States. HortScience horts 49: 10–17

Johnson, D.A, Alldredge, J.R, Allen, J.R, Allwine, R. (1991) Spatial pattern of downy mildew in hop yards during severe and mild disease epidemics. Phytopathology 81: 1369–1374

Jombart, T., and Ahmed, I. (2011) adegenet 1.3-1: new tools for the analysis of genome-wide SNP data. Bioinformatics 27: 3070–3071

Jones, L., Riaz, S., Morales-Cruz, A., Amrine, K.C.H., McGuire, B., Gubler, W.D., Walker, M.A., Cantu, D. (2014) Adaptive genomic structural variation in the grape powdery mildew pathogen, *Erysiphe necator*. BMC Genomics 15: 1081

Jouet, A., Saunders, D.G.O., McMullan, M., Ward, B., Furzer, O., Jupe, F., Cevik, V., Hein, I., Thilliez, G.J.A., Holub, E., van Oosterhout, C. and Jones, J.D.G. (2019), *Albugo candida* race diversity, ploidy, and host-associated microbes revealed using DNA sequence capture on diseased plants in the field. New Phytol, 221: 1529-1543

Kamvar, Z.N., Brooks, J.C., Grünwald, N.J. (2015) Novel R tools for analysis of genome-wide population genetic data with emphasis on clonality. Front Genet 6: 208

Kamvar, Z.N., Tabima, J.F., Grünwald, N.J. (2014) Poppr: an R package for genetic analysis of populations with clonal, partially clonal, and/or sexual reproduction. PeerJ 2: e281

Kanetis, L., Vasiliou, A., Neophytou, G., Samouel, S., Tsaltas, D. (2013) First report of downy mildew caused by *Peronospora belbahrii* on sweet basil (Ocimum basilicum) in Cyprus. Plant Dis 98: 283

Kitner, M., Lebeda, A., Sharma, R., Runge, F., Dvořák, P., Tahir, A., Choi, Y-J., Sedláková, B., Thines, M. (2015) Coincidence of virulence shifts and population genetic changes of *Pseudoperonospora cubensis* in the Czech Republic. Plant Pathol 64: 1461–1470

Knaus, B.J., Grünwald, N.J. (2017) vcfr: a package to manipulate and visualize variant call format data in R. Mol Ecol Resour 17: 44–53

Kozarewa, I., Armisen, J., Gardner, A.F., Slatko, B.E., Hendrickson, C.L. (2015) Overview of target enrichment strategies. Curr Protoc Mol Biol 112: 7.21.1-7.21.23

Kunjeti, S.G., Anchieta, A., Martin, F.N., Choi, Y-J., Thines, M., Michelmore, R.W., Koike, S.T., Tsuchida, C., Mahaffee, W., Subbarao, K.V., et al (2016) Detection and quantification of *Bremia lactucae* by spore trapping and quantitative PCR. Phytopathology 106: 1426–1437

Lane, C.R., Beales, P.A., O'Neill, T.M., McPherson, G.M., Finlay, A.R., David, J., Constantinescu, O., Henricot, B. (2005) First report of Impatiens downy mildew (Plasmopara obducens) in the UK. Plant Pathol 54: 243

Li, H., Durbin, R. (2009) Fast and accurate short read alignment with Burrows-Wheeler transform. Bioinformatics. doi: 10.1093/bioinformatics/btp324

Li, H., Handsaker, B., Wysoker, A., Fennell, T., Ruan J., Homer, N., Marth, G., Abecasis, G., Durbin, R., Subgroup 1000 genome project data processing (2009) The sequence alignment/map format and SAMtools. Bioinformatics 25: 2078–2079

Lim, H.C., Braun, M.J. (2016) High-throughput SNP genotyping of historical and modern samples of five bird species via sequence capture of ultraconserved elements. Mol Ecol Resour 16: 1204–1223

Ma, X., Shao, Y., Tian, L., Flasch, D.A., Mulder, H.L., Edmonson, M.N., Liu, Y., Chen, X., Newman, S., Nakitandwe, J., et al (2019) Analysis of error profiles in deep next-generation sequencing data. Genome Biol 20: 50

Mantel, N. (1967) The detection of disease clustering and a generalized regression approach. Cancer Res **27**: 209–220

McCormack, J.E., Tsai, W.L.E., Faircloth, B.C. (2016) Sequence capture of ultraconserved elements from bird museum specimens. Mol Ecol Resour 16: 1189–1203

Milgroom, M.G. (2015) Population biology of plant pathogens : genetics, ecology, and evolution. The American Phytopathological Society, St. Paul, Minnesota

Milgroom, M.G. (1996) Recombination and the multilocus structure of fungal populations. Annu Rev Phytopathol 34: 457–477

Mitchell, M.N., Ocamb, C.M., Grünwald, N.J., Mancino, L.E., Gent, D.H. (2011) Genetic and pathogenic relatedness of *Pseudoperonospora cubensis* and *P. humuli.* Phytopathology 101: 805–818

Naegele, R.P., Quesada-Ocampo, L.M., Kurjan, J.D., Saude, C., Hausbeck, M.K. (2016) Regional and temporal population structure of *Pseudoperonospora cubensis* in Michigan and Ontario. Phytopathology 106: 372–379

Nei, M (1972) Genetic distance between populations. Am Nat 106: 283–292

Neufeld, K. N. (2017) Epidemiology of cucurbit downy mildew: predicting risk of disease infection and validation of the CDM ipmPIPE forecasting system. (Doctoral dissertation thesis, North Carolina State University, Raleigh, USA). Retrieved from https://repository.lib.ncsu.edu/bitstream/handle/1840.20/33592/etd.pdf?sequence=1&isAllowed=y

Perea, C., De La Hoz, J.F., Cruz, D.F., Lobaton, J.D., Izquierdo, P., Quintero, J.C., Raatz, B., Duitama, J. (2016) Bioinformatic analysis of genotype by sequencing (GBS) data with NGSEP. BMC Genomics 17: 498

Potapov, V., Ong, J.L. (2017) Examining sources of error in PCR by single-molecule sequencing. PLoS One 12: e0169774

Purayannur, S., Cano, L.M., Bowman, M.J., Childs, K.L., Gent, D.H., Quesada-Ocampo, L.M. (2020) The effector repertoire of the hop downy mildew pathogen *Pseudoperonospora humuli*. Front Genet 11: 910

Quesada-Ocampo, L.M., Granke, L.L., Olsen, J., Gutting, H.C., Runge, F., Thines, M., Lebeda, A., Hausbeck, M.K. (2012) The genetic structure of *Pseudoperonospora cubensis* populations. Plant Dis 96: 1459–1470

Quinlan, AR, Hall, IM (2010) BEDTools: a flexible suite of utilities for comparing genomic features. Bioinformatics 26: 841–842

Rahman, A., Góngora-Castillo, E., Bowman, M.J., Childs, K.L., Gent, D.H., Martin, F.N., Quesada-Ocampo, L.M. (2019) Genome sequencing and transcriptome analysis of the hop downy mildew pathogen *Pseudoperonospora humuli* reveal species-specific genes for molecular detection. Phytopathology 109: 1354–1366

Rivera, Y., Salgado-Salazar, C., Gulya, T.J., Crouch, J.A. (2016) Newly emerged populations of *Plasmopara halstedii* infecting rudbeckia exhibit unique genotypic profiles and are distinct from sunflower-infecting strains. Phytopathology 106: 752–761

Savory, E.A., Adhikari, B.N., Hamilton, J.P., Vaillancourt, B., Buell, C.R., Day, B. (2012a) mRNA-Seq Analysis of the *Pseudoperonospora cubensis* transcriptome during cucumber (*Cucumis sativus L.*) infection. PLoS One 7: e35796

Savory, E.A., Zou, C., Adhikari, B.N., Hamilton, J.P., Buell, C.R., Shiu, S-H., Day, B. (2012b) Alternative splicing of a multi-drug transporter from *Pseudoperonospora cubensis* generates an RXLR effector protein that elicits a rapid cell death. PLoS One 7: e34701

Simpson, E. H. (1949) Measurement of diversity. Nature 163: 688

Sirrine, R., Lizotte, E., Brown, D., O'Brien, T., and Leach, A. 2014. Estimated costs of producing hops in Michigan. Michigan State University Extension E3236. Online publication.

Shannon, C. E. (1948). A mathematical theory of communication. Bell System Technical Journal 27:379-423

Sharma, R., Xia, X., Cano, L.M., Evangelisti, E., Kemen, E., Judelson, H., Oome, S., Sambles, C., van den Hoogen, D.J., Kitner, M., et al (2015) Genome analyses of the sunflower pathogen *Plasmopara halstedii* provide insights into effector evolution in downy mildews and *Phytophthora*. BMC Genomics 16: 741

Starrett, J., Derkarabetian, S., Hedin, M., Bryson, Jr. R.W., McCormack, J.E., Faircloth, B.C. (2017) High phylogenetic utility of an ultraconserved element probe set designed for Arachnida. Mol Ecol Resour 17: 812–823

Stassen, J., Seidl, M., Vergeer, P., Nijman, I., Snel, B., Cuppen, E., Van den ackerveken, G. (2012) Effector identification in the lettuce downy mildew *Bremia lactucae* by massively parallel transcriptome sequencing. Mol Plant Pathol 13: 719–731

Stoddart, J.A., Taylor, J.F. (1988) Genotypic diversity: estimation and prediction in samples. Genetics 118: 705 LP – 711

Summers C.F., Gulliford C.M., Carlson C.H., Lillis J.A., Carlson M.O., Cadle-Davidson L., Gent, D.H., Smart, C.D. (2015) Identification of genetic variation between obligate plant pathogens *Pseudoperonospora cubensis* and *P. humuli* using RNA sequencing and genotyping-by-sequencing. PLoS One 10: e0143665

Tabima, J.F., Coffey, M.D., Zazada, I.A., Grünwald, N.J. (2018) Populations of *Phytophthora rubi* show little differentiation and high rates of migration among states in the western United States. Mol Plant-Microbe Interact 31: 614–622

Thines, M. (2014) Phylogeny and evolution of plant pathogenic oomycetes—a global overview. Eur J Plant Pathol 138: 431–447

Thilliez, G.J.A., Armstrong, M.R., Lim, T.-Y., Baker, K., Jouet, A., Ward, B., van Oosterhout, C., Jones, J.D.G., Huitema, E., Birch, P.R.J. and Hein, I. (2019), Pathogen enrichment sequencing (PenSeq) enables population genomic studies in oomycetes. New Phytol, 221: 1634.-1648

Thomas, A., Carbone, I., Choe, K., Quesada-Ocampo, L.M., Ojiambo, P.S. (2017) Resurgence of cucurbit downy mildew in the United States: Insights from comparative genomic analysis of *Pseudoperonospora cubensis*. Ecol Evol 7: 6231–6246

USDA (2020) United States Department of Agriculture. 2019. Vegetables Annual Summary.

Wallace, E.C., D'Arcangelo, K.N., Quesada-Ocampo, L.M. (2020) Population analyses reveal two host-adapted clades of *Pseudoperonospora cubensis*, the causal agent of cucurbit downy mildew, on commercial and wild cucurbits. Phytopathology. doi: 10.1094/PHYTO-01-20-0009-R

Wallace, E.C., Quesada-Ocampo, L.M. (2017) Analysis of microsatellites from the transcriptome of downy mildew pathogens and their application for characterization of *Pseudoperonospora* populations. PeerJ 5: e3266

Withers, S., Gongora-Castillo, E., Gent, D., Thomas, A., Ojiambo, P.S., Quesada-Ocampo, L.M. (2016) Using next-generation sequencing to develop molecular diagnostics for *Pseudoperonospora cubensis,* the cucurbit downy mildew pathogen. Phytopathology 106: 1105–1116

Wong, F.P, and Wilcox, W.F (2001) Comparative physical modes of action of azoxystrobin, mancozeb, and metalaxyl against *Plasmopara viticola* (Grapevine Downy Mildew). Plant Dis 85: 649–656

CHAPTER V

CONCLUSIONS

The research reported in this dissertation provides an assessment of the population structure of *Pseudoperonospora cubensis*, the causal agent of cucurbit downy mildew (CDM) in Michigan and evaluates the performance of spore traps coupled to qPCR for the monitoring of airborne *Pseudoperonospora* spp. sporangia. The population structure of *P. cubensis* was investigated using a target enrichment protocol that allowed the genotyping of environmental samples with low concentrations of a mix of plant and pathogen DNA. A significant effect of the host type on the population structure of *P. cubensis* was observed while no evidence of location-based differentiation was detected within the *P. cubensis* population of Michigan. In addition, this study identified an improved detection system for the monitoring of *P. cubensis* sporangia that allowed the differentiation between *Pseudoperonospora* spp. and the detection of *P. cubensis* DNA before symptoms were observed in commercial cucumber fields.

This study provided evidence of significant genetic differentiation among the *P. cubensis* population from squash (clade I) and cucumber (clade II) but there was insufficient evidence to conclude that location (region) within Michigan has a significant effect on the distribution of the genetic variation of the *P. cubensis* population. Contrasting evidence was found for the population of *Pseudoperonospora humuli* (the causal agent of hop downy mildew), and a significant effect of location on the genetic variation of the population was detected in the state. The differences in the distribution of genetic variation between the population of each species could be explained by differences in the dispersion patterns between them. Although both pathogens

propagate via asexual sporangia that are aerially dispersed, empirical evidence indicates that only *P. cubensis* sporangia may spread unrestricted over long distances. The isolation and divergence of geographically distant populations of Michigan may be limited by the exchange of migrants between them. This was supported by the detection of the same multilocus genotypes of *P. cubensis* in multiple geographically distant populations. On the other hand, despite the potential for airborne dispersal of hop downy mildew, only one MLG was detected in two geographically distant populations which is consistent with the restricted pattern of dispersion suggested for this pathogen. This was also supported by a significant correlation between the genetic and geographic distance among *P. humuli* samples, that was not detected for the *P. cubensis* population.

In Michigan, CDM occurs annually due to an influx of aerially dispersed *P. cubensis* sporangia from overwinter sources. Thus, timely alerts of an influx of the airborne inoculum of *P. cubensis* can assist Michigan growers in assessing the need to initiate fungicide sprays. In the current study, we reported the use of a highly specific and sensitive qPCR assay that allows the differentiation between *P. humuli*, and each host-adapted clade of *P. cubensis* (clade I and II) on spore trap samples. A distinction that was not possible using light microscopy only. After two years of monitoring using a Burkard and impaction spore traps coupled with qPCR in cucumber fields, *P. humuli* DNA was detected more frequently than *P. cubensis* early during the growing season from May to June. *P. cubensis* clade II DNA was detected in spore trap samples approximately 2-7 days before CDM symptoms were observed in commercial cucumber fields in July or August, while *P. cubensis* clade I DNA was never detected. The

differences in the airborne inoculum of each clade documented here are likely the result of differences in the total area planted of the susceptible hosts to each clade in Michigan.

In addition, this study sheds light on the utilization of Burkard and impaction spore traps for the airborne monitoring or Pseudoperonospora spp. sporangia. In agreement with theoretical expectations, our results suggest that the Burkard spore traps are a more efficient instrument for the detection of airborne sporangia at low concentrations (<100 sporangia/day) than impaction spore traps. Adjustments can be made to increase the efficiency of the detection of *P. cubensis* using impaction spore traps. This includes the utilization of multiple impaction spore traps per location and increasing the sampling surface width and the exposition time of the impaction rods. The use of spore traps couple with qPCR could be used as part of a CDM risk advisory system to time fungicide applications that protect cucurbit crops in Michigan.